Lisa Krug, BSc

Microalgae in an industrial-scale process: analyzing the co-microbiome dynamics

MASTER'S THESIS

to achieve the university degree of

Diplom-Ingenieurin

Master's degree programme: Biotechnology

submitted to

Graz University of Technology

Supervisor

Univ.-Prof. Dipl.-Biol. Dr.rer.nat. Gabriele Berg

Institute of Environmental Biotechnology

Graz, August, 2016

AFFIDAVIT

I declare that I have authored this thesis independently, that I have not used other than the declared sources/resources, and that I have explicitly indicated all material which has been quoted either literally or by content from the sources used. The text document uploaded to TUGRAZonline is identical to the present master‘s thesis.

Date

Signature

Acknowledgements

First of all, I would like to thank my supervisor at the Institute of Environmental Biotechnology, Univ.-Prof. Dipl.-Biol. Dr.rer.nat. Gabriele Berg, who allowed me to get insight into fascinating fields of environmental biotechnology and microbial diversity. I want to thank her for the outstanding intellectual support during all steps of my Master Thesis. Furthermore Dipl.-Ing. Dr.techn. BSc Armin Erlacher deserves special thanks for his patience, motivation, enthusiasm and immense knowledge. The door to his office was always open whenever I ran into troubles or had questions about my research or writing.

I am very grateful to my colleagues at the Institute of Environmental Biotechnology of the University of Technology Graz for inspiring discussions and for the great time we spent together.

Special thanks to BioEnergy International (BDI) for enabling this outstanding project with funding and providing the samples.

Finally I would like to show my gratitude to my family, and especially my parents for their absolute confidence in me. They provided me with unfailing support and continuous encouragement throughout my years of study and through the process of researching and writing this thesis. This accomplishment would not have been possible without them.

Thank you.

Abstract

Haematococcus pluvialis is a unicellular freshwater algae belonging to the phylum *Chlorophyta*, which can accumulate large amounts of astaxanthin under stressful environmental conditions in their cell. Due to their industrial relevance, they are cultivated in large scale production processes. Axenic production cannot be carried out, thus microbiological shares are natural constituents of the algae-biomass cultivation. Contrary, such shares can include candidates, which have potential to cause complete production stops, and need therefore to be controlled. The *Haematococcus pluvialis*-associated microbiome during an industrial-scale mass cultivation was studied in depth by targeting specific taxonomic marker (16S rRNA, 18S rRNA and ITS) in combination with a cultivation-dependent approach to investigate the co-occurring microbiome and to identify synergistic and antagonistic organisms. Microbial fingerprints (single-strand conformation polymorphism) and 16S rRNA gene sequencing (Illumina MiSeq/HiSeq) revealed that random driven community assembly of high abundant taxa was prevalent. *Runella, Sediminibacterium* and *Sphingobacteriales* belonging to the phylum *Bacteriodetes* and *Prosthecobacter* (*Verrucomicrobia*) were most abundant in the first analyzed mass cultivation, *Comamonadaceae* (*Proteobacteria*) and *Flavobacteria* (*Bacteriodetes*) dominated the second analyzed approach. Minor taxa including *Flectobacillus* and *Fimbriimonas* formed a small core microbiome across all reactor types in one cultivation process, were only 46 OTUs of total 2,538 OTUs were shared. OTU-networks confirmed stochastic cluster formation of predominant bacterial taxa within the scale-up process. A stable microbial structure was only found in a time course sampling of the DEMO reactors with 3,000 L capacity where a general high biodiversity was observed. Microalgae including *Chlorella*, *Scenedesmus* and *Ochrophyta* (*Poterioochromonas*) were detected as contaminants already in starting inoculums and could be linked to substantial reduction of *H. pluvialis* biomass production. In particular, these contaminations accounted in the latter for more than 40 % relative to the total eukaryotic biomass in the DEMO reactors. Except of *Poterioochromonas,* which could only be detected in cultivation-independent approaches, all unwanted algae could be isolated from the process allowing further *in vitro* analysis. The obtained results suggest that eukaryotic shares,

mainly other algae species, have predominant impact on biomass and astaxanthin yield of *H. pluvialis* in large scale production. Although diverse bacterial taxa in high abundances were found, no negative interactions with *H. pluvialis* could be directly linked. Moreover, microscopic analysis revealed that bacteria tended to colonize the microalgae and might fulfill important interactions with their host as already reported for higher plants.

Kurzfassung

Die einzellige Süßwasseralge *Haematococcus pluvialis* aus dem Phylum *Chlorophyta* ist in der Lage unter ungünstigen Umweltbedingungen große Mengen Astaxanthin zu produzieren. Aufgrund ihrer Bedeutung wird sie industriell in großem Maßstab kultiviert. Weil eine gänzlich sterile Produktion kaum durchführbar und nicht wirtschaftlich ist, haben einzelne Organismen aus dem Begleitmikrobiom das Potential vollständige Produktionsstopps zu verursachen und müssen daher möglichst vermieden oder kontrolliert werden. Das Mikrobiom einer *Haematococcus pluvialis* Kultivierung in industriellen Anlagen wurde detailliert analysiert. Fokus lag dabei auf der Untersuchung spezifischer taxonomischer Marker (16S rRNA, 18S rRNA und ITS) mit molekularen Nachweisverfahren (mikrobielle Fingerprints, Illumina MiSeq/HiSeq Amplikon Sequenzierung), in Kombination mit kultivierungsabhängigen Methoden. Bei der Untersuchung zweier Kultivierungsansätze zeigte sich keine regelmäßige Zusammensetzung des bakteriellen Mikrobioms. In einem Kultivierungsansatz traten mit größter Häufigkeit *Runella*, *Sediminibacterium* und *Sphingobacteriales* des Phylums *Bacteriodetes* und *Prosthecobacter* (*Verrucomicrobia*) auf. Unterschiedliche Reaktortypen zeigten eine große Diversität, nur 46 OTUs von insgesamt 2,538 OTUs wurden in allen Typen gefunden. Als dominante Taxa des anderen Kultivierungsansatzes wurden *Comamonadaceae* (*Proteobacteria*) und *Flavobacteria* (*Bacteriodetes*) identifiziert. OTU-Netzwerke bestätigten das zufällige Auftreten der Bakterien, unabhängig von der Größe der untersuchten Reaktoren. Nur Probenentnahmen des 3,000 L DEMO Reaktors im zeitlichen Verlauf einer Kultivierung konnten ein stabiles, wenn auch stark diverses Mikrobiom nachweisen. Mikroalgen wie *Chlorella*, *Scenedesmus* und *Ochrophyta* (*Poterioochromonas*) wurden bereits im Startinokulum gefunden. Deren Vorkommnis konnte mit verminderter Biomassenausbeute von *H. pluvialis* in Verbindung gebracht werden. Ihr Anteil an der gesamten eukaryotischen Biomasse des DEMO Reaktors erreichte über 40 %. Alle Algen mit Ausnahme von *Poterioochromonas*, die nur mittels kultivierungsunabhängiger Verfahren nachgewiesen werden konnte, wurden isoliert, wodurch weitere *in vitro* Analysen möglich wurden. Die Ergebnisse lassen darauf schließen, dass unerwünschte eukaryotische Mikroorganismen - Großteils andere Algenarten - einen starken Einfluss auf die Ausbeute an Biomasse von *H. pluvialis* in Großanlagen nehmen.

Obwohl sehr viele verschiedene bakterielle Taxa im Prozess gefunden wurden, konnte kein direkter negativer Effekt auf das Wachstum von *H. pluvialis* gezeigt werden. Mikroskopische Analysen ließen eine Besiedelung der Algen durch Bakterien erkennen. Die Interaktion zwischen Algen und Bakterien könnte von Wichtigkeit sein, wie auch bereits für höher entwickelte Pflanzen beschrieben wurde.

Content

I. Introduction

1.1 Industrial relevance of large scale algae cultivation

The optimization of industrial cultivation of microalgae has gained more and more attention over the last few decades since the potential of the unicellular organisms as feedstock for the production of bio-energy and bio-fuel was realized (Christi, 2007). Besides the ability to produce lipids and hydrocarbons in a high amount, which are raw materials for bioethanol and biodiesel production, algae have a high protein content which makes them attractive as a source of animal feed (Banerjee *et al.*, 2002). Some algae produce high valuable compounds used in pharmaceutical and cosmetic industry (Skjånes *et al.*, 2013, Tominaga *et al.*, 2012). Additionally, the ability of microalgae to remove phosphorus and nitrogen from aquatic environments makes them interesting candidates for wastewater treatment (Chevalier and Noüe, 1985; Allen *et al.*, 2011). Co-cultivation of unwanted microorganisms is a problem in large scale cultivation approaches but mostly unavoidable. To date very little is known about the associated microbiome of an artificial algae-cultivation process. Potential interactions between algae and co-cultivated microorganisms influencing the growth behavior of microalgae still have to be investigated to unravel synergistic or antagonistic effects.

1.2 The unicellular freshwater microalgae

Haematococcus pluvialis

Haematococcus pluvialis FLOT. EMEND. WILLE (Flotow, 1844) is a green unicellular freshwater algae belonging to the phylum *Chlorophyta*. The organism is worldwide distributed and inhabits temporary water bodies such as rain pools, ponds and birdbaths. The ability of *Haematococcus pluvialis* to encyst allows the microalgae to survive under harsh conditions such as extreme temperatures, salt concentrations, exposure to strong light or lack of nutrients. In response to non-favorable environmental conditions, the green algae accumulate large amounts of the high-value carotenoid astaxanthin (Tjahjono *et al.*, 1994; Sarada *et al.*, 2002; Kobayashi *et*

al., 1992; Kakizono *et al*., 1992*)*. The production of the antioxidant astaxanthin is associated with a change in morphology of the cells. The life cycle of *Haematococcus pluvialis* consists of four stages. The macrozooids or zoospores are predominant in the early vegetative growing stage. Their morphology is spherical, ellipsoidal or pear-shaped. Characteristic for this cell-type is its motility with two flagella. The extracellular matrix in this stage consists of an inner, an outer and an intermediate tripartite crystalline layer. The inner layer is nearly transparent and of variable thickness, consisting of a loose network of granules and fibers. Under favorable conditions those cells can divide into two to eight daughter cells (Hagen *et al.*, 2002). Stressful environmental conditions cause the algae to encyst and change into spherical, non-motile cells – so called palmella. Changes in the cell extracellular matrix are observable as a primary cell wall is formed. From the inner of the cells vesicles transport granules into the inner layer of the extracellular matrix leading to the formation of two-layered cell wall. The outer layer and parts of the intermediate tripartite crystalline layer peels off. As soon as this stage is reached calcofluor-white staining results positive, indicating the presence of β-1,4-glycosidic linkages (cellulose; Hagen *et al.*, 2002). When stressful conditions persist, algae cells change their cell form again. They form mature, asexual aplanospores with a characteristic thick cell wall (maturation). Additionally to the primary cell wall a trilaminar sheath is formed. The separation of this trilaminar sheath from the plasmalemma generates an interspace which is filled with granules, forming the secondary cell wall (Hagen *et al.*, 2002). During the maturation the accumulation of astaxanthin in cytosolic lipid bodies takes place. When then the growth conditions for *Haematococcus pluvialis* return to optimal, non-motile aplanospores germinate to start a new life cycle. Flagellated macrozooids form until the next stressful situation forces the cells to encyst (Hazen, 1899). In some cases, aplanospores are able to reproduce themselves sexually by performing gametogenesis after exposure to extreme adverse conditions such as freezing dehydration or the complete lack of nutrients. When again favorable conditions for reproduction are given, up to 32 daughter-flagellates form within a mother cell after cytokinesis (Figure 1). The newly formed cells are so called microzooids as their diameter is less than 10 µm, in contrast to the macrozooids which reach a diameter ranging from 20 to 50 µm (Triki *et al.*, 1997; Wayama *et al.*, 2013). While in the vegetative cells of *H. pluvialis* the chlorophyll and protein content is high, the level of carotenes is low. The encystment is associated with the

degradation of chlorophyll and proteins (Kobayashi *et al.*, 1997). During maturation the level of protein degradation is accelerated while the amount of astaxanthin increases rapidly. A reverse process occurs during germination – protein and chlorophyll are synthesized while the carotene is degraded (Kobayashi *et al.*, 1997). While in non-encysted cell-form the carotenes lutein and β-carotene dominate, carotenes in the aplanospores consist to 98 % of astaxanthin (Boussiba *et al.*, 1999).

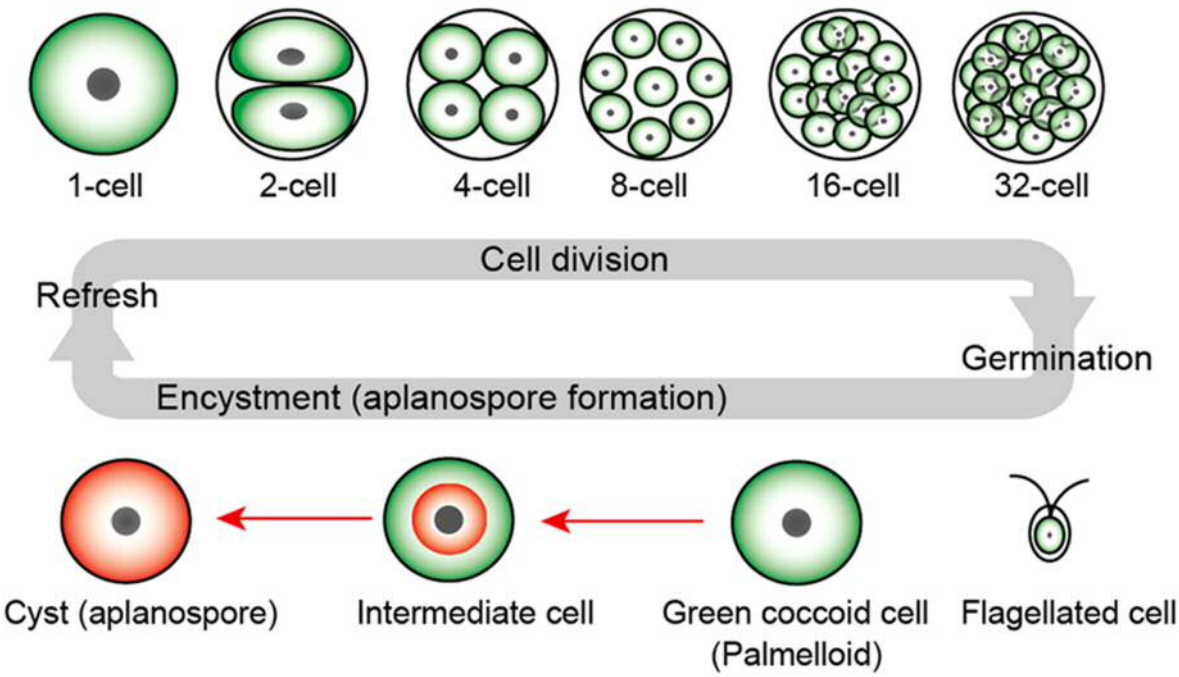

Figure 1: Schematic representation of the life cycle of *Haematococcus pluvialis*. When transferring old cultures on new, fresh media, flagellated cells form after cell division (refresh). Motile cells are able to settle and form non-flagellated coccoid cells (germination). Exposure to extreme light or other stressful environmental conditions like lacking nutrients lead to the accumulation of astaxanthin within the cell during encystment (red arrows). Figure reproduced from Wayama *et al*. (2013).

1.3 Astaxanthin

1.3.1 Antioxidative role of astaxanthin produced by *Haematococcus pluvialis*

Reactive oxygen species (ROS) are an unavoidable consequence in photosynthetic organisms of the electron transport chain. Light energy in form of photons is absorbed by chromophores and converted into chemical energy (ATP and NADH) which can be stored in form of starch or sugars by CO_2 fixation through the Calvin cycle. When the photosynthetic energy balance between the absorbed light energy and the carbon dioxide fixation is not equated, reactive oxygen species are produced (i.e.: superoxide anion O_2•-; hydrogen peroxide H_2O_2; hydroxyl radical HO•, singlet oxygen $^1O_2$). Excessive exposure to light can cause an over-reduction of photosystem 1 resulting in the formation of superoxide anions (O_2•-). In addition triplet chlorophyll (3Chl) is formed which generates the reactive oxygen species $^1O_2$ when interacting with molecular oxygen.

Three mechanisms how carotenes protect organisms from photo oxidative damage are described. The first method – described by Krinsky (1979) – suggests that the carotenes prevent the cells from damage by directly quenching the triplet chlorophyll or singlet oxygen. To make this mechanism possible, the immediate proximity between the carotene and the chlorophyll is required. Ben-Amotz *et al.* (1989) revealed that a large amount of β-carotenes accumulated in the algae *Dunallella bardawil* acts as a screen, absorbing the blue light. The protection against extreme exposure is attributed to the fact that carotenes and chlorophyll possess similar absorption spectra, resulting in a filter effect of β-carotenes. As the astaxanthin in *H. pluvialis* cells is accumulated in the cytoplasm (Santos and Mesquita, 1984), a direct interaction between the ROS and the carotene is unlikely due to the distance between astaxanthin and the chlorophyll. Additionally, the absorbance spectrum from astaxanthin and the chlorophyll is mostly different, suggesting that astaxanthin does not serve as filter for blue light. Fan *et al.* (1998) revealed that not astaxanthin itself serves as a protecting agent, but the synthesis thereof prevents the cells from photo oxidation. Cells which are supplemented with astaxanthin suffer as well from photo oxidation as cells in which the astaxanthin synthesis is blocked. Protection only can be provided when astaxanthin biosynthesis is not interrupted.

1.3.2 Applications as dietary supplements and for human health

Astaxanthin does not only protect algae cells from photo oxidation but has many applications for human health and nutrition. Tso and Lam (1996) found out that astaxanthin is able to pass the blood-brain barrier and then accumulate in the retina of mammals. During their studies they revealed the protective effect of astaxanthin on the photoreceptors in rats. Tanaka *et al.* (1995) showed that the development of cancer cells in the urinary bladder in mice as well as the growth of tongue neoplasm in rats is depressed after oral administration of the carotene astaxanthin. The study of Palozza *et al.* (2009) described a growth inhibiting effect of astaxanthin in several colon cancer cell lines, suggesting its application as chemo preventive agent. Bennedsen *et al.* (2000) assumed anti-inflammatory activity of astaxanthin as bacterial load and mucosal inflammation was reduced in mice suffering from a *Helicobacter pylori* infection. Additionally, astaxanthin prevents LDL-cholesterol (low-density lipoprotein) from oxidation reducing the risk of arteriosclerosis (Iwamoto *et al.*, 2000). During the study of Tominaga *et al*. (2012) the effect of astaxanthin on human skin was tested considering skin texture, skin wrinkles and moist content, and an improvement of skin conditions was revealed.

1.4 Industrial mass cultivation of H. pluvialis

The carotene contains two chiral centers and therefore can occur in three isomers (3S, 3'S), (3R, 3'S) and (3R, 3'R), two of them are enantiomers (3S, 3'S), (3R, 3'R) and one mesomer (3R, 3'S). By chemical synthesis all three isomers are produced in a ratio 1:2:1 while *Haematococcus pluvialis* synthesizes only the most valuable isomer – (3S, 3'S). To date 95 % of the astaxanthin available worldwide is produced synthetically. Therefore the optimization of algae-cultivation gains more and more attention. For large scale algae production different cultivation systems are used. Either they are naturally illuminated by solar light (open ponds, flat-plate photobioreactor, tubular photobioreactor, vertical-column photobioreactor) or by artificial light sources such as fluorescent lamps.

The sufficient supply with CO_2 is achieved by surface driven aeration, microporous hollow-fiber membranes, airlift loops, bubble columns, stirrer blade bubbling or gas exchanger (reviewed by Ugwu *et al.*, 2008; Carvalho *et al.*, 2006).

1.5 Algae-associated microorganisms and their potential interactions

Most microalgae are auxotrophic for vitamin B_{12}, which can only be synthesized by prokaryotes. Therefore, some algae species in nature are dependent from the co-occurrence of bacteria, as they supply them with vitamins such as cobalamin, thiamin and biotin which influence the nutrient exchange, signal transduction and gene transfer (Croft *et al*., 2006; Grant *et al*., 2014). Phototrophic algae produce a large amount of organic compounds, which can be recycled and degraded from heterotrophic organisms. Furthermore, chemicals operate as signal transmitter activating or inhibiting the expression of certain genes (Kouzuma and Watanabe, 2015). Mackiewicz *et al.* (2013) suggest that gene transfer happens from bacteria of the phylum *Bacteriodetes* (*Algoriphagus, Cytophaga*) to dinoflagellate minicircles. It is assumed, that horizontally transferred genes result in a better adaptability to changes in the surrounding environment (Brembu *et al.*, 2014). Bashan *et al.* (2002) and Gonzalez and Bashan (2000) revealed that the growth of *Chlorella vulgaris* can be significantly enhanced when co-immobilizing the freshwater algae and the plant-growth-promoting bacterium *Azospirillum brasilense* in alginate. *Azospirillum brasilense* is – as a member of the group plant rhizosphere bacteria – known to be a plant-growth-promoting bacterium which produces indole-3-acetic acid to enhance the nitrogen cycle in microalgae (Bashan and Holguin, 1998; Glick, 1995; Kloepper *et al*., 1980). Kim *et al*. (2014) revealed the positive effect of *Rhizobium* as plant growth promoting bacteria on green algae such as *Chlorella vulgaris*, *Scenedesmus sp*. and *Batryoccus brauniia*s by fixing nitrogen (Bloemberg and Lugtenberg, 2001). Furthermore, the enhanced growth behavior of *Chlorella vulgaris* in presence of the nitrogen-fixing bacterium *Bacillus pumilus* was confirmed by Hernandez *et al*. (2009). Cho *et al.* (2015) investigated the effect of co-cultivation of *Flavobacterium, Hyphomonas, Rhizobium, Sphingomonas, Microbacterium* and *Exophilia* on the growth of *C. vulgaris.* They revealed that, compared to axenic cultivation, cultivating

the algae in combination with the first four mentioned bacteria resulted in enhanced growth. The presence of *Microbacterium* decreased the growth rate and *Exophilia* led to growth inhibition. A co-cultivation of a combination of all four growth enhancing bacteria resulted in a significantly higher algae growth compared to the presence of only one bacterial strain.

The cyanobacterium *Microcystis aeruginosa* can be harmful for human and animal as they can produce toxins (cyanotoxins). Bacteria can also play a role when combating cyanobacteria (Carmichael, 2001). Su *et al.* (2016) examined the negative effect of the denitrifying bacterium *Acinetobacter sp.* (*Gammaproteobacteria*) on the growth of the *Microcystis aeruginosa*. Furthermore the denitrifying algicidal bacterium *Raoultella* (*Gammaproteobacteria*) was identified to have a negative influence on growth behavior of *Microcystis* (Su *et al*., 2016).

When focusing on the harmful bloom forming freshwater diatom *Stephanodiscus hantzschii* and the dinoflagellate *Peridinium bipes*, algicidal bacteria were identified to be *Acidovorax delafieldii, Variovorax paradoxus*, *Hydrogenophaga palleronii* and *Pseudomonas plecoglossicida* by Kang *et al*. (2008).

1.6 Objectives of the study

To date, little is known about the *Haematococcus pluvialis*-associated microbiome under mass-cultivation conditions. In particular, impact of antagonistic, synergistic or commensal organisms on *H. pluvialis* are poorly understood, but were reported to have decisive influence on both, biomass yield and quality.

Principle aims of this study were (I) to investigate the co-occurring microbiome of industrial-scale cultivation of *H. pluvialis*, (II) to determine possible antagonists or synergists, (III) to unravel the distribution of bacterial and eukaryotic taxa along an artificial algae cultivation process and (IV) to identify potential inhibitors or contaminants in the biomass production. Among those (V) a procedure to optimize and handle axenic pure *H. pluvialis* cultures was developed.

II. Materials and Methods

2.1 Experimental design and *H. pluvialis* industrial mass-cultivation

The company BioEnergy International (BDI) located in Styria, Austria, is specialized on the production of the super-antioxidant Astaxanthin (3,3'-dihydroxy-β,β-carotene-4,4'-dione) for food supplementation. The production is mainly based on the metabolism of *Haematococcus pluvialis*, an algae species which is known for its ability to accumulate a large amount of the carotene when exposed to stressful environmental conditions (Goodwin and Jamikorn, 1954; Boussiba and Vonshak, 1991). Proliferation of algae cells takes place in internally-illuminated photobioreactors with different capacities. The cultures are supplied with air and CO_2 through dynamic gas spargers. The cultivation process of the company is constructed as follows: Algae cultures – provided by "Culture Collection of Algae" (SAG, Göttingen, Germany) – serve as inoculum for a 500 mL Erlenmeyer flask. When a high cell density is reached the algae suspension is transferred into photobioreactors with a capacity of 5 L and 25 L (labor-plant). Thereof at least 25 L are needed for the inoculation of the pilot-plant, consisting of a photobioreactor with a capacity of 150 L and another with 300 L. The last step of the scale-up procedure is the transfer of 300 to 400 L of algae suspension from the pilot-plant into 4 DEMO-plants - three photobioreactors with a capacity of 3,000 L and one of 6,700 L. Schematic overviewindustrial-scale is shown in Figure 2. For harvesting, cells are dried and subsequently disrupted by high-pressure homogenization.

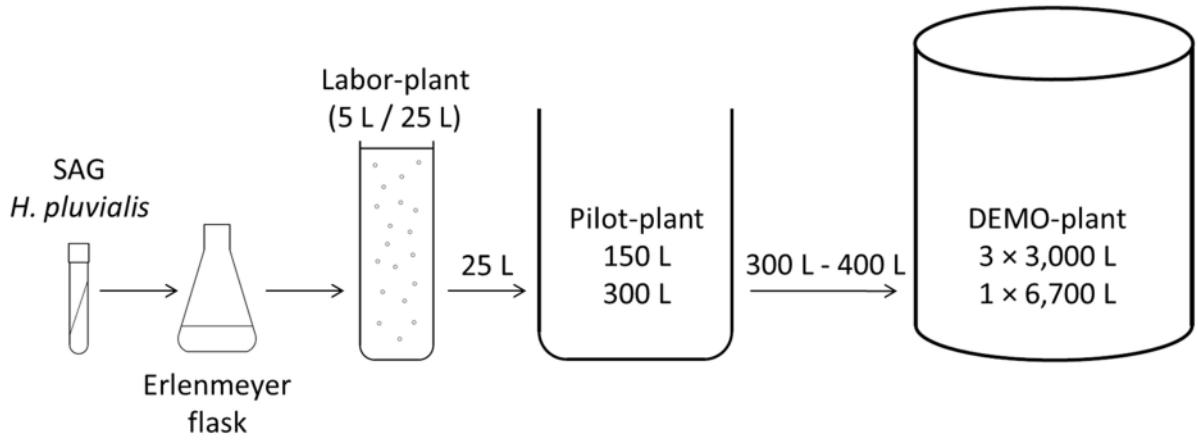

Figure 2: Schematic representation of *Haematococcus pluvialis* cultivation in an industrial-scale operation.

During cultivation a loss in the yield of *Haematococcus pluvialis* is detectable. After microscopic observation the possibility of contamination cannot be excluded. Generally, contamination – accompanied by the loss of biomass – increases with reactor size. In order to find reasons for the loss of algae biomass the co-occurring microbiome was investigated. To identify unwanted co-cultivated algae or bacteria but also beneficial organisms for algal-growth four complementary approaches were used (Figure 3).

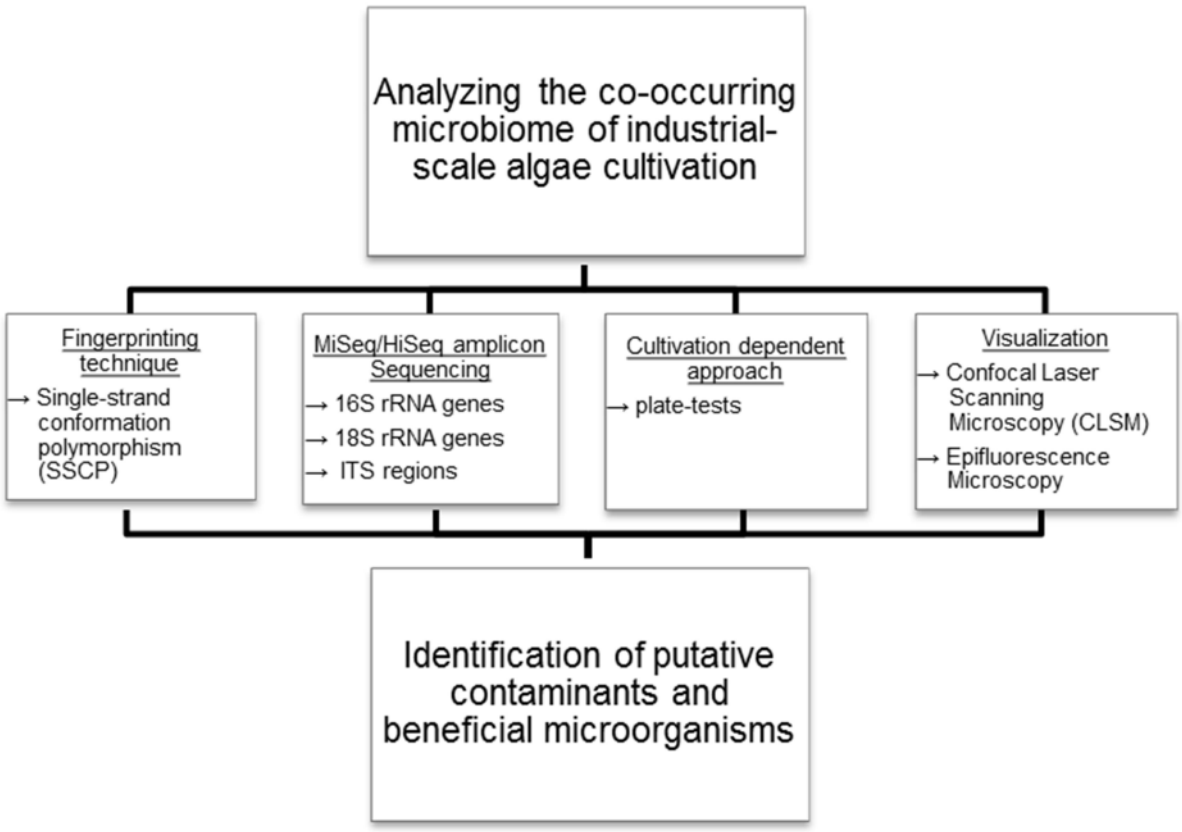

Figure 3: Workflow scheme.

Samples from bioreactors with different capacities (flask, 5 L photobioreactor (PBS), 300 L photobioreactor and 3,000 L, respectively 6,700 L photobioreactor (DEMO)) were provided. According to microscopic analysis by BDI, the samples were classified as weak, moderate and strong contaminated. In the present study the co-occurring microbiome was examined. Bacterial colony forming units (CFU) were determined (photobioreaction A). Two individually started cultivation approaches were partially studied (photobioreaction B, photobioreaction C) by doing cultivation-dependent and cultivation-independent analyzes.

2.2 Sampling of *H. pluvialis* from industrial-scale photobioreactors

Samples were taken sequentially and provided by BioEnergy International (BDI). Three separately run biomass cultivations (photobioreaction A, B, C) were partially examined. Samples from photobioreaction A were plated on different cultivation media to determine the viable bacterial cell count.

Samples of photobioreaction B were provided in form of frozen cell pellets for microbiological analyzes. The putative pure cultures of *Haematococcus pluvialis* and the contamination isolated from the DEMO 10300 photobioreactor were provided in form of fresh samples. Additionally to microbiological analyzes these two samples were observed microscopically.

All samples of photobioreaction C were analyzed microbiologically. Except “DEMO 17.03.2016” which was considered to be strongly contaminated, all samples were provided in form of frozen cell pellets.

An overview of the analyzed samples is given in Table 1. Photobioreaction B was inoculated with *Haematococcus pluvialis* strain 192.80, while approach A and approach C were inoculated with *H. pluvialis* strain 34-1e.

Table 1: Sample overview.

PBR	ID[1]	Sampling[2]	Source[3]	Medium[4]	Cont[5]	Extract[6]	CD[7]	CI[8]	Viz[9]
A	**Flask**	04.09.2015	Flask	BBM	I	-	**X**		
	5L PBR	04.09.2015	5 L PBR	BBM	II	-	**X**		
	DEMO 10100	04.09.2015	DEMO 10100	BBM	III	-	**X**		
B	**Flask**	15.09.2015	Flask	BBM	I	MoBio		**X**	
	Flask	15.09.2015	Flask	BBM	I	MP		**X**	
	5 L PBR	15.09.2015	5 L PBR	BBM	II	MoBio		**X**	
	5 L PBR	15.09.2015	5 L PBR	BBM	II	MP		**X**	
	DEMO 10100	15.09.2015	DEMO 10100	BBM	III	MoBio		**X**	
	DEMO 10100	15.09.2015	DEMO 10100	BBM	III	MP		**X**	
	Contamination	17.11.2015	DEMO 10300	BBM	-	EtOH		**X**	**X**
	***H. pluvialis* strain 192.80 preculture**	17.11.2015	Flask preculture	CBM	-	EtOH		**X**	**X**
C	**Flask**	05.02.2016	Flask	CBM	ND	MP		**X**	
	5 L PBR	05.02.2016	5 L PBR	CBM	ND	MP		**X**	
	DEMO 10100	02.02.2016	DEMO 10100	CBM	I	MP		**X**	
	DEMO 10100	05.02.2016	DEMO 10100	CBM	I	MP		**X**	
	DEMO 10100	08.02.2016	DEMO 10100	CBM	I	MP		**X**	
	DEMO 10100	19.02.2016	DEMO 10100	CBM	I	MP		**X**	
	DEMO 10100	17.03.2016	DEMO 10100	CBM	III	MP	**X**	**X**	**X**
	300 L PBR	19.02.2016	300 L PBR	CBM	I	MP		**X**	
	***H. pluvialis* strain 34-1e**	-	SAG Göttingen	CBM agar	-	MP		**X**	

PBR = Photobioreaction; [1] Sample identifier; [2] Date of sampling; [3] Source of sampling along the reaction concept, [4] BBM = Bold's basal medium, CBM = Courtney Boyd Myers; [5] Severity of contamination according BDI rating: I = little, II = moderate, III = strong contamination; [6] DNA extraction method: MP = MP FastDNA SPIN kit for soil, MoBio = MoBio PowerSoil isolation kit, EtOH = ethanol precipitation; [7] CD = Cultivation dependent analysis; [8] CI = Cultivation independent analysis; [9] Vis = Visualization; X = Analyzes were carried out.

2.3 Cultivation-dependent analyzes

Different cultivation media (NA, SNA, PDA, CBM, BBM, BBM I, Rice-Agar, Plant Agar) were used to find the favorable nutrient media for algae cultivation under lab conditions. Detailed information about the media composition can be found in the appendix 7.1.

2.3.1 Viable cell counts of bacteria in the algae cultivation process

Provided algae suspensions of photobioreaction A were diluted up to 10^{-7} in 0.85% NaCl. Dilution series were plated (100 µL) on different growth media (NA, SNA, PDA, CBM, BBM I) to get an overview of the cultivable compositions in the different bioreactors. Plates were incubated at room temperature. Colony forming units (CFU) of respective samples were counted after 24, 48, 122 and 144 hours. When calculating the CFU per mL, plates with less than five CFU and more than 300 CFU were not taken into account.

2.3.2 Isolation of co-cultivated algae

To get insight in the algal diversity in the reactor 100 µL of the strongly contaminated sample “DEMO 10100 17.03.16” were plated on different solid cultivation media (plant agar, rice agar, BBM + ampicillin [50 µg × mL^{-1}], [50 µg × mL^{-1}], CBM, CBM + ampicillin [50µg × mL^{-1}]). A mineral media according to Tarayre *et al.* (2014) was used to isolate *Poterioochromonas* (identified by cultivation-independent analysis). Ampicillin was added on respective plates to prevent bacteria from overgrowing the plates. In a second approach, 100 µL of respective samples were suspended in 20 mL still liquid but cooled agar (plant agar, BBM, rice agar) before pouring in Petri dishes (in-agar method).

First attempt in cultivating algae species was done by plating dilution series up to 10^{-2} of the algae suspension onto BBM dosed with ampicillin and by doing the in-agar method. Same procedure was done using plant agar and rice agar. To obtain pure cultures of the co-cultivated algae and *H. pluvialis* strain 34-1e, single colonies were transferred onto new respective plates by using a heat sterilized inoculation loop. Finally, pure cultures of *H. pluvialis* 34-1e were cultured on CBM plates with and without ampicillin.

2.3.3 Identification of co-cultivated algae

To reveal the species of the co-cultivated algae, cells were resuspended in 300 µL 0.85 % NaCl and subsequently mechanically disrupted. Therefore the suspension was transferred in sterile Eppendorf tubes filled with glass beads and processed in a FastPrep FP120 instrument. Partial 18S rRNA gene sequence was amplified by using primer pair TAReuk454FWD1 and TAReukREV3P (Stoeck *et al*., 2010) covering the variable region 4 (V4). The PCR reaction mix (30 µL) contained 16.2 µL ultrapure water (Roth, Karlsruhe, Germany), 6 µL Taq&Go (5 ×), 2.4 µL $MgCl_2$ [25mM], 1.2 µL of each primer [10 µM] and 3 µL template DNA. (98 °C, 30 sec; 10 cycles of 98 °C, 10 sec; 53 °C, 10 sec; 72 °C, 30 sec, followed by 20 cycles of 98 °C., 10 sec; 48 °C, 30 sec; 72 °C, 30 sec; final extension at 72 °C, 10 min). PCR products were purified using Wizard SV Gel and PCR clean-up system (Promega, Fitchburg, USA). Samples were treated according to manufacturer's protocol. 18S rRNA genes were sequenced by LGC genomics (Berlin, Germany) and subsequently aligned against the NCBI nucleotide collection database excluding uncultured and environmental sample sequences using the BLAST algorithm (Altschul *et al.*, 1997).

2.3.4 Quality control of axenic *H. pluvialis* cultures

Algae culture of *Haematococcus pluvialis* strain 192.80 provided from the SAG Göttingen, was analyzed by cultivation-dependent techniques to verify their purity. For that purpose algae colonies were transferred onto CBM plates with and without ampicillin and processed further.

2.4 Visualization of *H. pluvialis* and its co-occurring microorganisms

For *in vivo* and *in situ* visualization a confocal laser scanning microscope (CLSM) and an epifluorescence microscope were used. For specific and histochemical staining LIVE/DEAD cell viability assays (Thermo Fisher Scientific; Waltham, Massachusetts, USA) combined with calcofluor-white staining was done.

2.4.1 Confocal laser scanning microscopy (CLSM)

Confocal laser scanning microscopy allows *in situ* visualization and examination of biological samples like plant tissues or single cells. A confocal laser scanning microscope is an optical system which can be used for transmitted light-, fluorescent- and confocal-microscopy. It has three different light sources: a white lamp – to observe specimen using transmitted light, a wide-spectrum mercury lamp – to observe under fluorescent light, and lasers – to observe in confocal mode. Micrographs were acquired with a Leica TCS SPE confocal laser scanning microscope (Leica Microsystems GmbH, Mannheim, Germany) using the oil immersion objectives Leica ACS APO 40.0 × 1.15 (183.33 µm × 183.33 µm) and ACS APO 63 × 1.30 (116.40 µm × 116.40 µm). Solid state lasers were used with 405 nm, 488 nm, 532 nm, 635 nm excitation.

2.4.2 Epifluorescence microscopy

Micrographs of algae cells from solid media were observed using an epifluorescence microscope (Motic, Hongkong, Japan) which is equipped with a high-intensity light source that emits light in a broad spectrum from visible to ultraviolet. Samples were illuminated from above allowing the objective lens to be both the illuminator condenser and the fluorescent light. This microscope allows observation in bright field and phase contrast mode. Furthermore samples can be excited at 488 nm and 532 nm.

2.4.3 LIVE/DEAD bacterial viability kit (BacLight)

Staining with the LIVE/DEAD bacterial viability kit (Thermo Fisher Scientific, Massachusetts, USA) allows differentiation between viable and dead cells. For staining, two different fluorophores are applied to the respective samples (3 µL × mL^{-1}) and then incubated in the dark for at least 15 minutes. SYTO 9 green fluorescent nucleic-acid stains both living and dead cells, while the red fluorescent propidium iodide nucleic-acid dyes cells with compromised cell membranes that are considered to be dead. By using CLSM and epifluorescence microscopy the samples can be excited at different wavelengths, SYTO 9 has an excitation maximum at 480 nm and propidium iodide at 490 nm. The detectable emission maxima are at 530 nm for SYTO 9 and at 630 nm for propidium iodide. For better visibility of the algal cell wall, samples were additionally stained with calcofluor-white (0.15% in H_2O, 15 min incubation).

2.4.4 Microscopic analysis of reactor samples

The preculture of *H. pluvialis* and the reference sample of the putative contamination, isolated from the DEMO 10300 reactor within photobioreaction B, were visualized using confocal laser scanning microscopy (CLSM) after staining with LIVE/DEAD bacterial viability kit and calcofluor-white (0.15%). Cells were fixed on polysine microscope adhesion slides (Thermo Fisher Scientific, Massachusetts, USA). Additionally sample “DEMO 10100 17.03.2016” of photobioreaction C which was considered strongly contaminated was visualized using CLSM and epifluorescence microscopy after staining with LIVE/DEAD bacterial viability kit. The sample was fixed on polysine microscope adhesion slides (Thermo Fisher Scientific, Massachusetts, USA) to keep the algae in place for imaging. In addition un-coated slides were used. As non-encapsulated cells do not withstand the pressure of the cover slip, a provisional spacer was created by applying adhesive tape on the object slide. In addition, cultivated algae isolates were observed microscopically under bright field, at 532 nm and at 488 nm.

2.5 Cultivation-independent analyzes

2.5.1 Total community DNA extraction

For each sample 2 mL of algae suspension were centrifuged at 13,000 rpm for 20 minutes at 4 °C. The supernatant was discarded and the pellets were used for DNA extraction. Initially, samples of photobioreaction B were treated with two different DNA-extraction kits, while DNA from references (*Haematococcus pluvialis* and putative contamination) was extracted by doing ethanol precipitation. DNA extraction from samples of photobioreaction C was performed using FastDNA SPIN kit for soil (MP Biomedicals, Eschenberg, Germany) only.

2.5.1.1 PowerSoil DNA isolation kit

Obtained pellets were used for isolation of the total community DNA with the PowerSoil DNA isolation kit (Mo Bio Laboratories, Carlsbad, USA). Briefly, the pellet was resuspended in 60 µL of solution C1 containing SDS (sodium dodecyl sulfate). For mechanical lysis, the cells were homogenized three times in a FastPrep FP120 instrument for 30 seconds at a speed of 5.5 m s^{-1}. 250 µL solution C2 containing a reagent to precipitate non-DNA organic and inorganic material including humic substances, cell debris, and proteins were added to the supernatant. After centrifugation at 10,000 × g for one minute, 200 µL solution C3 were added and briefly vortexed to again precipitate non-DNA organic and inorganic material. Suspension was incubated at 4 °C for five minutes. Avoiding the pellet, supernatant was transferred into a new tube. Adding 1200 µL of high a concentration salt solution (C4) leads to a tight DNA binding to the silica matrix. After several centrifugation steps, 500 µL of C5, an ethanol based wash solution, were added onto the spin filter. After centrifugation at 10,000 × g for 30 seconds, the flow through was discarded. Another centrifugation step (10,000 × g) was done before adding 56 µL ultrapure water onto the spin filter. At last, centrifugation at 10,000 × g for 30 seconds eluted the DNA for any downstream processes. Extracted DNA was stored at -20 °C.

2.5.1.2 FastDNA SPIN kit for soil

In a complementary approach, total community DNA was extracted using the FastDNA SPIN kit for soil (MP Biomedicals, Eschenberg, Germany). Pellets were

treated according to manufacturer's protocol. Briefly, 978 µL sodium phosphate buffer and 122 µL MT buffer were added to respective pellets. For mechanical lysis, the cells were homogenized in a FastPrep FP120 instrument for 30 seconds at a speed of 5.5 m s^{-1}. After 15 minutes centrifugation at 14,000 × g, 250 µL protein precipitation solution (PPS) were added to the supernatant. After another five minutes centrifugation (14,000 × g), one mL binding matrix solution was added to the supernatant. After inverting the tube for two minutes by hand the tubes were placed in a rack for ten minutes to allow settling of silica matrix. Approximately 800 µL supernatant were discarded. Resuspended binding matrix was transferred to a spin filter with subsequent centrifugation at 14,000 × g for one minute. After resuspending the pellet in 500 µL SEWS-M the suspension was again centrifuged (14,000 × g, one minute). The catch tube was discarded and replaced by a new, clean catch tube. After air drying the spin filter for five minutes the binding matrix was resuspended in 56 µL ultrapure water. For better binding, the matrix was incubated for five minutes at 55 °C. After another centrifugation step (14,000 × g, one minute), DNA was ready for further processing and stored at -20 °C until further use.

2.5.1.3 Ethanol precipitation

Extracting the DNA from single organisms by ethanol precipitation was done according to Anderson *et al.* (1983), modified by Berg *et al.* (2002). Briefly, 300 µL of the respective samples was transferred into Eppendorf tubes filled with glass beads. Mechanical disruption was done by homogenizing the suspension twice in a FastPrep FP120 instrument for 30 seconds at a speed of 6.5 m s^{-1}. After centrifugation for three minutes at 4,000 rpm, 500 µL lysis-buffer, containing 1.4 % cetrimonium bromide (CTAB; Merck, Darmstadt, Germany), 1 M; NaCl (Roth, Karlsruhe, Germany), 7 mM Tris (Roth, Karlsruhe, Germany), 30 mM ethylenediaminetetraacetic acid (EDTA; Roth, Karlsruhe, Germany) were added to the supernatant. After incubation at 65 °C for one hour, 500 µL chlorophorm/Isoamylalcohol in a 1:24 ratio (C/I) were added and mixed. This procedure was repeated twice before 1 1 mL precipitation-buffer containing 0.5 % cetrimonium bromide (CTAB; Merck, Darmastadt, Germany) and 40 mM NaCl was added. 15 minutes centrifugation at 12,000 rpm were followed by the addition of 210 µL ice-cold isopropanol to the supernatant. Suspension was incubated at -20 °C over night before it was centrifuged for 20 minutes at 12,500 rpm. Supernatant was

discarded and the pellet was resuspended in 200 µL ice-cold ethanol (80%). After another centrifugation step (12,500 rpm, nine minutes), the supernatant was discarded. Pellet was air-dried to remove any residual ethanol. Resuspending the pellet in 50 µL ultrapure water makes the DNA ready for downstream processing. DNA was stored at -20 °C.

2.5.2 Analysis of the community structure by single-strand conformation polymorphism (SSCP)

In order to unravel the co-occurring microbiome along the sequential cultivation steps and to compare the different DNA extraction methods single-strand conformation polymorphism done with samples of photobioreaction B and photobioreaction C were performed. Detailed information of the samples and primers used for the SSCP analysis are given in Tables 2, 3 and 4.

Table 2: Sample overview of photobioreaction B.

Sample ID	Source	Cont.	DNA Isolation
Flask 15.09.15 (MoBio)	Flask	Little	MoBio PowerSoil isolation kit
Flask 15.09.15 (MP)	Flask		MP FastDNA SPIN kit for soil
5 L PBR 15.09.15 (MoBio)	5 L PBR	Moderate	MoBio PowerSoil isolation kit
5 L PBR 15.09.15 (MP)	5 L PBR		MP FastDNA SPIN kit for Soil
DEMO 10100 15.09.15 (MoBio)	DEMO 10100	Strong	MoBio PowerSoil isolation kit
DEMO 10100 15.09.15 (MP)	DEMO 10100		MP FastDNA SPIN kit for soil
Contamination 17.11.15	DEMO 10300		Ethanol precipitation
Contamination 17.11.15	DEMO 10300		Ethanol precipitation
H. pluvialis preculture 17.11.15	Flask-preculture		Ethanol precipitation
H. pluvialis preculture 17.11.15	Flask-preculture		Ethanol precipitation

MoBio = MoBioPowerSoil isolation kit

MP = MP FastDNA SPIN kit for soil

Cont. = Contamination

Table 3: Sample overview of photobioreaction C.

Sample ID	Source	Cont.	DNA Isolation
Flask 05.02.16	Flask	None	MP FastDNA SPIN kit for soil
5 L PBR 05.02.16	5 L PBR	None	MP FastDNA SPIN kit for soil
DEMO 10100 02.02.16	DEMO 10100	Little	MP FastDNA SPIN kit for soil
DEMO 10100 05.02.16	DEMO 10100	Little	MP FastDNA SPIN kit for soil
DEMO 10100 08.02.16	DEMO 10100	Little	MP FastDNA SPIN kit for soil
DEMO10100 19.02.16	DEMO 10100	Little	MP FastDNA SPIN kit for soil
DEMO 10100 17.03.16	DEMO 10100	Strong	MP FastDNA SPIN kit for soil
300 L PBR 19.02.16	300 L PBR	Little	MP FastDNA SPIN kit for soil
H. pluvialis strain 34-1e	SAG Göttingen	None	MP FastDNA SPIN kit for soil

MoBio = MoBio PowerSoil isolation kit

MP = MP FastDNA SPIN kit for soil

Cont. = Contamination

Table 4: Primers used for amplification of 16S rRNA genes, 18S rRNA genes and ITS regions for SSCP analyzes.

Primer	Sequence (5' - 3')	Target	References
515f 806rP	GTGYCAGCMGCCGCGGTAA GGACTACHVGGGTWTCTAAT	16S rRNA	Caporaso *et al*., 2012
1391f EukBrP	AATGATACGGCGACCACCGA GATCTACAC CAAGCAGAAGACGGCATACG AGAT	18S rRNA (V9)	Vestheim *et al*., 2008; Caporaso *et al*., 2012; Amaral *et al*., 2009
TAReuk454FWD1 TAReukREV3P	CCAGCASCYGCGGTAATTCC ACTTTCGTTCTTGATRA	18S rRNA (V4)	Stoeck *et a*l., 2010
ITS1f ITS4r ITS2rP	TCCGTAGGTGAACCTGCGG TCCTCCGCTTATTGATATGC GCTGCGTTCTTCATCGATGC	ITS regions	White *et al*., 1990

2.5.2.1 Polymerase chain reaction (PCR) using taxonomic markers for SSCP analysis

Community pattern analysis was performed by using three complementary approaches. For SSCP analysis 18S rRNA genes, 16S rRNA genes and ITS regions were amplified by using specific primers.

For amplifying the bacterial rRNA gene sequence, universal primers 515f and 806rP were used (Caporaso *et al.,* 2012). The PCR was performed by using a total volume of 60 µL containing 36.3 µL ultrapure water, 12 µL Taq&Go (5 ×), 2.4 µL of each primer [10 µM], 0.45 µL pPNA [100 µM], 0.45 µL mPNA [100 µM] (Lundberg *et al*., 2013), and 6 µL template (96 °C, 5 min; 30 cycles of 96 °C, 1 min; 78 °C, 5 sec; 54 °C, 1 min; 74 °C, 1 min; final extension at 74 °C, 10 min).

For amplifying the 18S rRNA gene sequences of the eukaryotic microbiome of photobioreaction B, the primers 1391f and EukBrP covering the variable region 9 (V9) were used (Vestheim *et al*., 2008; Caporaso *et al*., 2012; Amaral *et al*., 2009). The PCR was performed by using a total volume of 60 µL containing 40.8 µL ultrapure water, 12 µL Taq&Go (5 ×), 0.6 µL of each primer [10 µM] and 6 µL template. (98 °C, 5 min; 10 cycles of 98 °C, 10 sec; 53 °C, 10 s; 72 °C, 30 sec; 20 cycles of 98 °C., 10 sec; 48 °C, 30 sec; 72 °C, 30 sec; final extension at 72 °C, 10 min). In addition primer pair TAReuk454FWD1 and TAReukREV3P (Stoeck *et al*., 2010) covering the variable region 4 (V4) were used for comparing the two photobioreactions. The PCR was performed by using a total volume of 60 µL containing 35 µL ultrapure water, 12 µL Taq&Go (5 ×), 4.8 µL $MgCl_2$ [25 mM], 2.4 µL of each primer [10 µM] and 3 µL template DNA.(98 °C, 30 sec; 10 cycles of 98 °C, 10 sec; 53 °C, 10 s; 72 °C, 30 sec, followed by 20 cycles of 98 °C., 10 sec; 48 °C, 30 sec; 72 °C, 30 sec; final extension at 72 °C for 10 min)

ITS regions of the different samples were amplified in a nested PCR approach with the primers ITS1f, ITS4r and ITS2r (White *et al.*, 1990). The first PCR reaction mixture (10 µl) contained 5.6 µL ultrapure water, 2 µL 5× Taq&Go ready-to-use PCR mix, 0.1 µl of each primer [10 µM], 1.2 µL $MgCl_2$ [25 mM] and 1 µL1 µl of template DNA (94°C, 5 min; 36 cycles of 94°C, 30 sec; 54°C, 35 sec; 72°C, 40 sec; final extension at 72°C, 10 min). In a second PCR, 1 µL of the PCR product was used as template. For the amplification primers ITS1f and ITS2rP were used. The reaction mixture for the second PCR (60 µl) contained 38.6 µL ultrapure water, 12 µL 5 × Taq&Go ready-to-use PCR mix, 7.2 µL $MgCl_2$ [25 mM] 0.6 µL of each

primer [10 µM] (94 °C, 5 min; 30 cycles of 94 °C, 30 sec; 58 °C, 35 sec; 72 °C, 140 sec; final extension at 72 °C, 10 min).

2.5.2.2 SSCP analysis of bacterial and eukaryotic communities

PCR products were purified by the Wizard SV Gel and PCR clean-up system before a λ-exonuclease digestion and DNA single-strand folding according to Schwieger and Tebbe (1998). 12 µL of each DNA product, amplified with 515f/806rP, 1391f/EukBrP, TAReuk454FWD1/TAReukREV3P and ITS1f/ITS2rP were applied on the gel. The polyacrylamide gel electrophoresis was performed on a TGGE apparatus (Biometra, Göttingen, Germany). 16S rRNA genes, 18S rRNA genes amplified with TAReuk454FWD1 and TAReukREV3P, and ITS regions were analyzed on an 8 % (wt vol^{-1}) acrylamide gel which run at 26 °C and 400 V for 26 hours. 18S rRNA genes amplified with 1391f and EukBrP were analyzed on a 9.5 % (wt vol^{-1}) acrylamide gel at 26 °C and 400 V run for 15 hours. The procedure of single-strand conformation polymorphism analysis (SSCP) was performed according to Schwieger and Tebbe (1998). Afterwards, the gels were silver-stained according to the procedure of Bassam *et al.* (1991).

2.5.2.3 SSCP band-identification and GelComparII analysis

Computer-assisted evaluation of bacterial and eukaryotic communities obtained by SSCP was performed by using the GelComparII software (Applied Math, Kortrijk, Belgium). The silver-stained SSCP gels were scanned using a transmitted light scanner (Epson perfection 4990 Photo, Nagano, Japan) to obtain digitized gel images. After normalizing the gels and subtracting the background, cluster analysis was performed by using “Dice” as similarity coefficient. Selected DNA bands of the fingerprint profiles were excised using a scalpel and subsequently eluted by suspending the gel slice in 150 µL elution buffer, containing 0.5 M ammonium acetate 10 mM magnesium acetate tetrahydrate, 1 mM EDTA (pH 8.0) and 0.1 % (wt vol^{-1}) SDS for 3 days at 4 °C, following DNA ethanol precipitation, centrifugation and resuspension in 10 mM Tris-HCl (pH 8.0). Gel-extracted DNA was reamplified. PCR products were purified by using the Wizard SV Gel and PCR clean-up system according to manufacturer’s protocol. DNA concentration was measured using UV-Vis spectrophotometer (NanoDrop, Thermo Fisher Scientific, Massachusetts,

USA). For Sanger-Sequencing, samples were pooled equimolar and processed by LGC Genomics GmbH (Berlin, Germany). 16S rRNA genes, 18S rRNA genes and ITS regions were sequenced and subsequently aligned against the 16S ribosomal RNA sequences database and the NCBI nucleotide collection database excluding uncultured and environmental sample sequences, respectively, using the BLAST algorithm (Altschul *et al.*, 1997).

2.5.3 Illumina MiSeq/HiSeq sequencing of 16S rRNA gene, 18S rRNA gene and ITS region amplicons

The 16S rRNA gene sequences, 18S rRNA gene sequences and ITS regions were each amplified by doing four technical replicates. The products of four independent PCR reactions from independent samples with four different primer pairs were pooled and purified using the Wizard SV Gel and PCR clean-up system (Promega, Madison, USA). Samples were treated according to manufacturer's protocol. Detailed overview of samples used for amplification analysis is provided in Table 5 and Table 6. Primers used in this study are provided in Table 7. Detailed information about the primer constructs can be found in the appendix 7.4.

Table 5: Sample overview of photobioreaction B.

Sample ID	Source	Cont.	DNA Isolation
Flask 15.09.15 (MoBio)	Flask	Little	MoBio PowerSoil isolation kit
Flask 15.09.15 (MP)	Flask		MP FastDNA SPIN kit for soil
5 L PBR 15.09.15 (MoBio)	5 L PBR	Moderate	MoBio PowerSoil isolation kit
5 L PBR 15.09.15 (MP)	5 L PBR		MP FastDNA SPIN kit for soil
DEMO 10100 15.09.15 (MoBio)	DEMO 10100	Strong	MoBio PowerSoil isolation kit
DEMO 10100 15.09.15 (MP)	DEMO 10100		MP FastDNA SPIN kit for soil
Contamination 17.11.15	DEMO 10300		Ethanol precipitation
Contamination 17.11.15	DEMO 10300		Ethanol precipitation
H. pluvialis strain 192.80 17.11.15	Flask-preculture		Ethanol precipitation
H. pluvialis strain 192.80 17.11.15	Flask-preculture		Ethanol precipitation

MoBio = MoBio PowerSoil isolation kit

MP = MP FastDNA SPIN kit for soil

Cont. = Contamination

Table 6: Sample overview of photobioreaction C.

Sample ID	Source	Cont.	DNA Isolation
Flask 05.02.16	Flask	None	MP FastDNA SPIN kit for soil
5 L PBR 05.02.16	5 L PBR	None	MP FastDNA SPIN kit for soil
300 L PBR 19.02.16	300 L PBR	Little	MP FastDNA SPIN kit for soil
DEMO 10100 02.02.16	DEMO 10100	Little	MP FastDNA SPIN kit for soil
DEMO 10100 08.02.16	DEMO 10100	Little	MP FastDNA SPIN kit for soil
DEMO 10100 19.02.16	DEMO 10100	Little	MP FastDNA SPIN kit for soil
DEMO 10100 17.03.16	DEMO 10100	Strong	MP FastDNA SPIN kit for soil
H. pluvialis strain 34-1e	SAG Göttingen	None	MP FastDNA SPIN kit for soil

MoBio = MoBioPowerSoil isolation kit

MP = MP FastDNA SPIN kit for soil

Cont. = Contamination

Table 7: Primers used for amplification of 16S rRNA genes, 18S rRNA genes and ITS regions for Illumina sequencing.

Primer	Sequence (5' to 3')	Target	References
515f	GTGYCAGCMGCCGCGGTAA	16S rRNA	Caporaso *et al*., 2012
806rP	GGACTACHVGGGTWTCTAAT		
golay_515f	TATGGTAATTGTGTGYCAGCMGC		Hamady *et al*., 2008
golay_926r	AGTCAGCCAGGGCCGYCAATTYM		
golay_1391f	ATGGTAATTGTGTACACACCGCC CGTC	18S rRNA	Vestheim *et al.*, 2008; Caporaso *et al.,* 2012; Amaral *et al*., 2009
golay_EukBr	AGTCAGCCAGGGTGATCCTTCTGC AGGTTCACCTAC		Hamady *et al*., 2008
ITS1f	TCCGTAGGTGAACCTGCGG	ITS region	White *et al.*, 1990
ITS2r	GCTGCGTTCTTCATCGATGC		

2.5.3.1 Amplification of 16S rRNA, 18S rRNA gene and ITS fragments for Illumina sequencing

The 16S rRNA fragments in the algae suspension were amplified for Illumina sequencing using eubacterial barcoded-primers 515f and 806r (Caporaso *et al*., 2012; further described as barcode construct 1). The seven base long barcode sequences are part of the primer. Peptide nucleic acid (PNA) was added to the PCR mix to prevent the amplification of unwanted sequences such as mitochondrial (mPNA) or plastidial (pPNA) RNA from eukaryotes (Lundberg *et al*., 2013). The PCR was performed by using a total volume of 30 0 µL containing 20.15 5 µL ultrapure water, 6 6 µL Taq&Go (5 ×) 1.2 2 µL of each primer (5µM), 0.225 µL pPNA [100 µM], 0.225 µl mPNA [100 µM] and1 µL template. The cycling program was adjusted to an initial denaturation at 96°C for 5 min, followed by 30 cycles of 96 °C for 1 min, 78 °C for 5 sec, 54 °C for 1 min, and 74 °C for 1 min. Final extension was done at 74°C for 10 min. Additionally a second attempt in amplifying bacterial rRNA genes was done using golay_515f_primer_pad and golay_926r_primer_pad (further described as barcode construct 2). Primers which contain a two base long linker sequence on which in an additional PCR the 12-base long golay barcode had to be amplified were used (Hamady *et al*., 2008). Therefore a PCR reaction with a total volume of 20 µL containing 13.1 µL ultrapure water, 4 µL Taq&Go (5 ×), 0.15 µL pPNA [100 µM], 0.15 µL mPNA [100 µM], 0.8 µL of each primer (10 µM) and 1 µL template was carried out (95 °C, 55 min; 30 cycles of 95 °C, 20 sec; 78 °C 5 sec; 54 °C, 20 sec; 74 °C 1 min; final extension at 74°C for 10 min). To apply the barcodes for sequencing an additional PCR had to be carried out. Each PCR-product served as template for a PCR-reaction containing 18.6 µL ultrapure water, 6 µL Taq&Go (5 ×), 1.2 µL of each barcode-primer (10 µM) and 3 µL template (95 °C, 5 min; 10 cycles of 95 °C, 30 sec; 56 °C, 30 s; 72 °C, 30 sec; 72 °C, min; and final extension at 72 °C for 10 min).

18S rRNA gene fragments of eukaryotic compartments were amplified using universal eukaryotic primers golay_1391f_primer_pad and golay_EukBr_primer_pad (Vestheim et al., 2008; Caporaso *et al.*, 2012; Amaral *et al.*, 2009). The PCR was performed by using a total volume of 20 µL containing 14.6 µL ultrapure water, 4 µL Taq&Go (5 ×), 0.2 µL of each primer (10 µM) and 1 µL template (98 °C, 5 min; 10 cycles of 98 °C, 10 sec; 53 °C, 10 s; 72 °C, 30 sec; 20 cycles of 98 °C, 10 sec; 48 °C, 30 sec; 72 °C, 30 sec; and final extension at 72 °C for 10 min). To apply the

barcodes for sequencing an additional PCR was done. Each PCR-product served as template for a PCR-reaction containing 20.6 µL ultrapure water, 6 µL Taq&Go (5 ×), 1.2 µL of each barcode-primer (10 µM) and 1 µL template (95 °C, 5 min; 10 cycles of 95 °C, 30 sec; 56 °C, 30 s; 72 °C, 30 sec; 72 °C, min; and final extension at 72 °C for 10 min).

ITS regions of the different samples for sequencing were amplified in a nested PCR approach with t primers ITS1f and ITS2r (White *et al.*, 1990). The PCR reaction mixture (10 µL) contained 5.6 µL ultrapure water, 2 µL 5 × Taq&Go ready-to-use PCR mix, 0.1 µL of 1 µL of each primer [10 µM], 1.2 µL $MgCl_2$ [25mM] and 1 µL of template DNA (94 °C, 5 min; 30 cycles of 94 °C, 30 sec; 58 °C, 35 sec; 72 °C, 40 sec; and final extension at 72 °C, 10 min). In a second PCR, 1 µL of the PCR-product was used as template. Therefore barcode-primer ITS1f and ITS2r were used. The reaction mixture for the second PCR (30 µL) contained 19.7 µL ultrapure water, 6 µL 55 × Taq&Go ready-to-use PCR mix, 0.9 µL $MgCl_2$ [25 mM] 1.2 µL of each barcode-primer [5 µM] (94°C, 5 min; 15 cycles of 94°C, 30 sec; 58°C, 35 sec; 72°C, 40 sec; and final extension at 72°C, 10 min).

Analysis of 18S rRNA genes, 16S rRNA genes and ITS regions was done on all provided samples of photobioreaction B. Bacterial community within photobioreaction C was investigated by amplifying the 16S rRNA gene sequence from the respective DEMO 10100 samples and the 300 L PBR-sample using barcoded primers (primer construct 1). 18S gene and ITS region analysis were performed for all samples listed in Table 6.

2.5.3.2 Bioinformatics and statistical analysis

Sequences were analyzed with the QIIME (quantitative insights into microbial ecology) software developed by Caporaso *et al.* (2010). Barcodes, primer and adapter sequences were removed and the sequences were quality filtered (maximum unacceptable phred quality score: 19; phred offset: 33). Chimeras were removed from the 16S rRNA gene sequences by using usearch61 to perform both *de novo* (abundance based) chimera and reference based detection. OTU (operational taxonomic unit) tables were created by an open reference method with UCLUST at a 97% cut-off level for the amplified 16S rRNA gene, 18S rRNA gene and ITS regions. OTU tables for 16S rRNA gene sequences were aligned to the latest green genes release (v 13.8), 18S rRNA gene sequences were aligned to SILVA release 119.

Taxonomic assignment of ITS region was carried out using SILVA release 111. Representative sequences of the 16S rRNA gene, 18S rRNA gene and ITS regions - clusters with less than 1% of relative abundance were not considered - were selected for further analyzes.

Furthermore 18S rRNA gene sequences and ITS region sequences were identified by performing a standard nucleotide BLAST with the NCBI nucleotide collection database excluding uncultured and environmental sample sequences (Altschul *et al.*, 1997). OTU table obtained for 18S was subsequently filtered at domain level for Eukaryotes. When analyzing 18S rRNA gene and ITS region sequences using the BLAST algorithm, OTUs with at least 100 reads in total were aligned. Output sequences were classified as domain, phylum, family, and genus depending on the depth of reliable classifier assignments.

Core diversity analysis was performed to reveal alpha and beta diversity. Furthermore core microbiome analysis was done to expose the bacterial, eukaryotic and fungal communities which persist over the whole process. For core microbiome analysis and OTU network profile analysis the sample “Contamination” from photobioreaction B was excluded, as the provided sample is not part of the scale-up process and did not serve as inoculate.

The profile network was constructed using Cytoscape version 3.4.0 (Shannon *et al*., 2003). Datasets for 16S rRNA gene analysis were not reduced. All abundant taxa were taken into consideration when computing the OTU-networks.

To unravel the interactions of the bacterial communities in the algae cultivation process, a co-occurrence network was computed using the Cytoscape add-on “CoNet” (a co-occurrence network inference-tool). The sample “Contamination” was also here not taken into account as it is not part of the scale-up process.

For network analysis a reduced dataset was used. Taxa with a relative abundance lower than 1% were not considered. Analysis was done by using Spearman and Kendall correlation measurements, Bray Curtis and Kullback-Leibler dissimilarity measurements and “mutual information” for similarity calculation. The false discovery rate was adjusted by applying the Benjamini-Hochberg method. P-values were merged based on the Brown-method. Significant interactions were calculated (p-value ≤ 0.05) and displayed.

III. Results

3.1 Cultivation-dependent analyzes

3.1.1 In vitro cultivation of reactor samples revealed an abundant bacterial share

Colony forming units (CFU) were determined of photobioreaction A after different periods of incubation at room temperature. Three samples with different contamination severities according to the BDI rating were investigated. Overview of the obtained results can be found in the appendix 7.3

After 24 hours no CFU of sample “Flask 02.09.2015” were determined after 24 hours of cultivation at room temperature (Figure 4). A total number of 130 CFU × mL^{-1} were countable on NA solid medium after 48 hours. No growth was observable on SNA, PDA, CBM and BBM I. After 144 hours of incubation at room temperature CFU were only countable for dilutions 10^{-3} and 10^{-4} on NA solid medium. More than 300 colonies grew on other plates. A number of approximately 3.6 × 105 CFU × mL^{-1} on NA solid medium was determined. Approximately 4.7 × 106 CFU × mL^{-1} were determined on CBM after 120 hour of incubation and 1.4 × 104 CFU × mL^{-1} on BBM I. On SNA solid media 104 CFU × mL^{-1} were observed and 104 CFU × mL^{-1} on PDA plates after 144 hours of incubation (Table 14). Additionally, sample “5 L PBR 04.09.2015” was investigated. After 24 hours of incubation at room temperature 260 CFU × mL^{-1} were counted on NA solid medium (Table 15, Figure 4). On PDA plates 6 × 10^2 CFU were observed after 24 hours of incubation. 48 hours of incubation resulted in growth of 1.3 × 10^3 CFU/mL on NA solid medium and 2.7 × 10^3 CFU × mL^{-1} on PDA plates. Colonies on CBM were too little to count. No growth was detected on SNA and BBM I. Number of CFU increased to 1.85 × 10^5 CFU × mL^{-1} after 144 hours on NA medium and 2.74 × 10^4 CFU × mL^{-1} on PDA plates. Still no growth was observable on SNA and BBM I. Colonies on CBM were too small to count after 120 hours of incubation. Sample “DEMO 10100 04.09.2015” was also investigated to unravel the viable bacterial communities within the algae cultivation. After 24 hours of incubation, growth was observable on NA (>400 CFU × mL^{-1}) and on PDA (1.8 × 10^3 CFU × mL^{-1}; Figure 4). Cell density was determined after 48 hours of

incubation. Growth was seen on NA (1.36×10^4 CFU mL^{-1}) and on PDA (3.82×10^4 CFU $\times$ mL^{-1}). Determination of colony forming units on SNA and CBM was not feasible as the number of observed CFU per plate was outside the evaluable range. On BBM I no growth was detectable (Table 16).

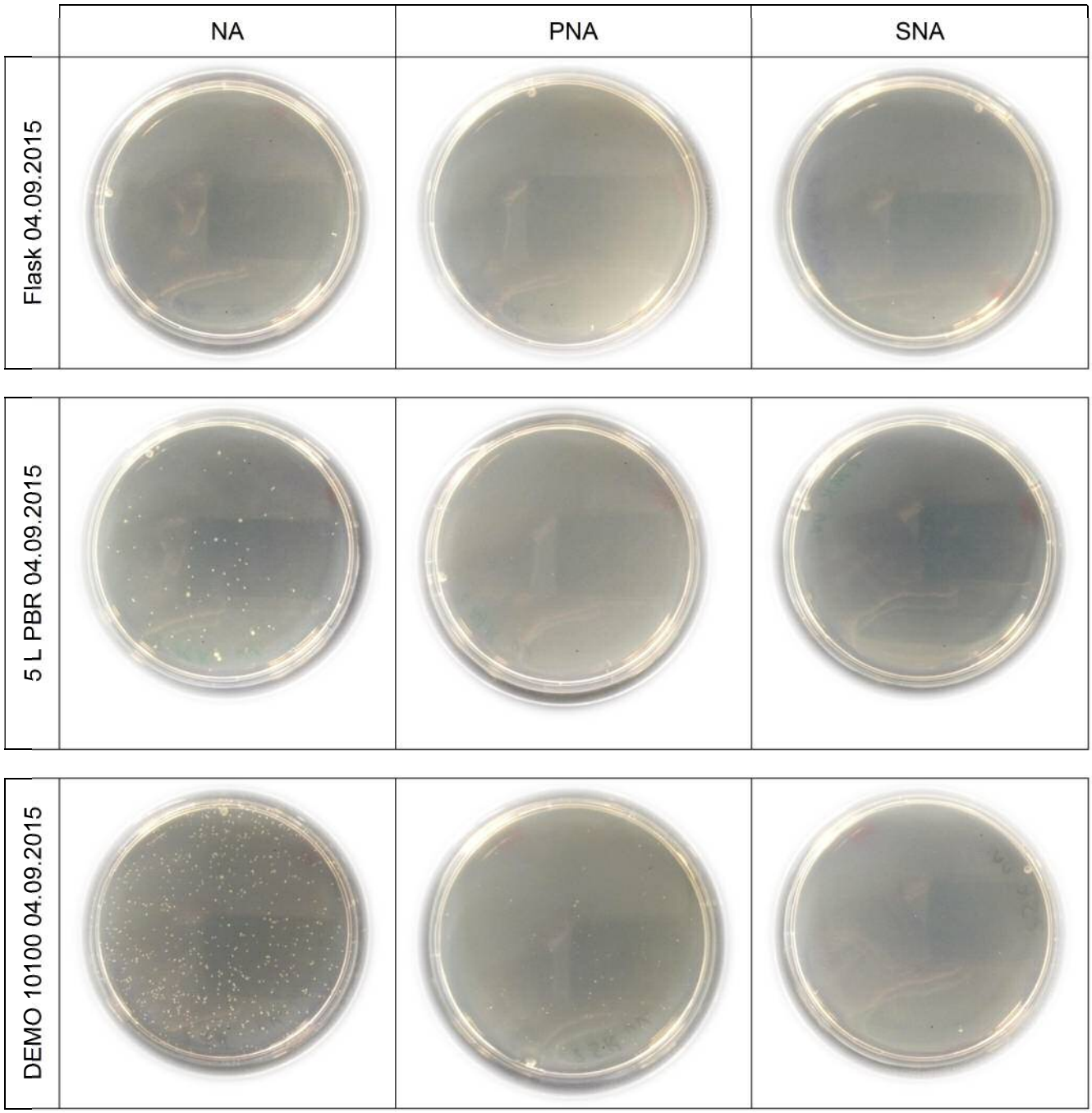

Figure 4: Cultivation pattern of differently contaminated samples after 24 hours of incubation at room temperature. Undiluted algae suspensions were plated. No growth was observable for sample "Flask" on any medium. In sample "5 L PBR" few colonies (26 CFU × 100 μL^{-1}) grew on NA solid medium. 60 CFU × 100 μL^{-1} were determined on PDA plates. No growth was observable on SNA plates. Sample "DEMO 10100 04.09.2015" showed growth on NA (<400 CFU × 100 μL^{-1}) and on PDA (264 CFU × 100 μL^{-1})

3.1.2 Isolation and identification of *H. pluvialis* and co-cultivated algae species revealed unwanted algae in the industrial process

After screening a variety of different culture media and conditions, best results were achieved when plating sample “DEMO 10100 17.03.16” on BBM and CBM. After one week of incubation at 25°C at a light/dark cycle (L: 16h, D: 8h), first algae cells were detectable. On BBM plates with ampicillin and plant agar red and green algae cells were detected both by using an in-agar method and by plating the suspension onto solid media but not on rice agar. Growth of algae was regularly inspected microscopically under bright field using an epifluorescence microscope. Differences in morphology suggested the abundance of at least two co-cultivated algae species (Figure 5.A).

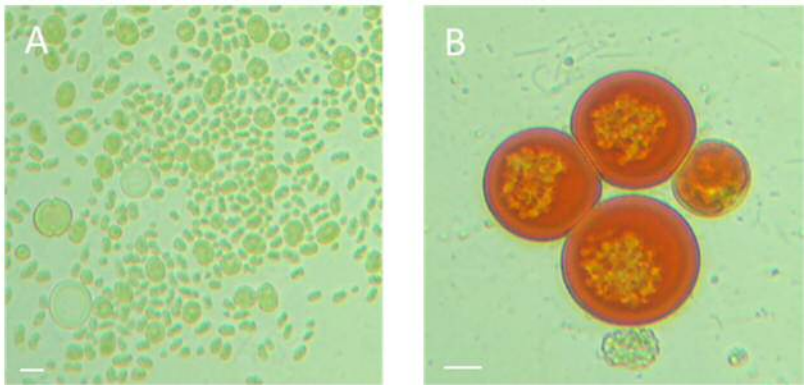

Figure 5: Microscopic analysis of algae colonies from solid media (BBM + ampicillin). A: Co-cultivated, unwanted algae. B: *Haematococcus pluvialis*. Scale bar: 10 µm.

After several transfers of single colonies onto new plates, putative pure cultures of *H. pluvialis* strain 34-1e and four co-cultivated algae species were isolated (Figure 6). After Sanger-sequencing, these were identified as member of the phylogenetic family of *Scenedesmaceae* (Figure 6.B and C) and of the genus *Chlorella* (Figure 6.A and D).

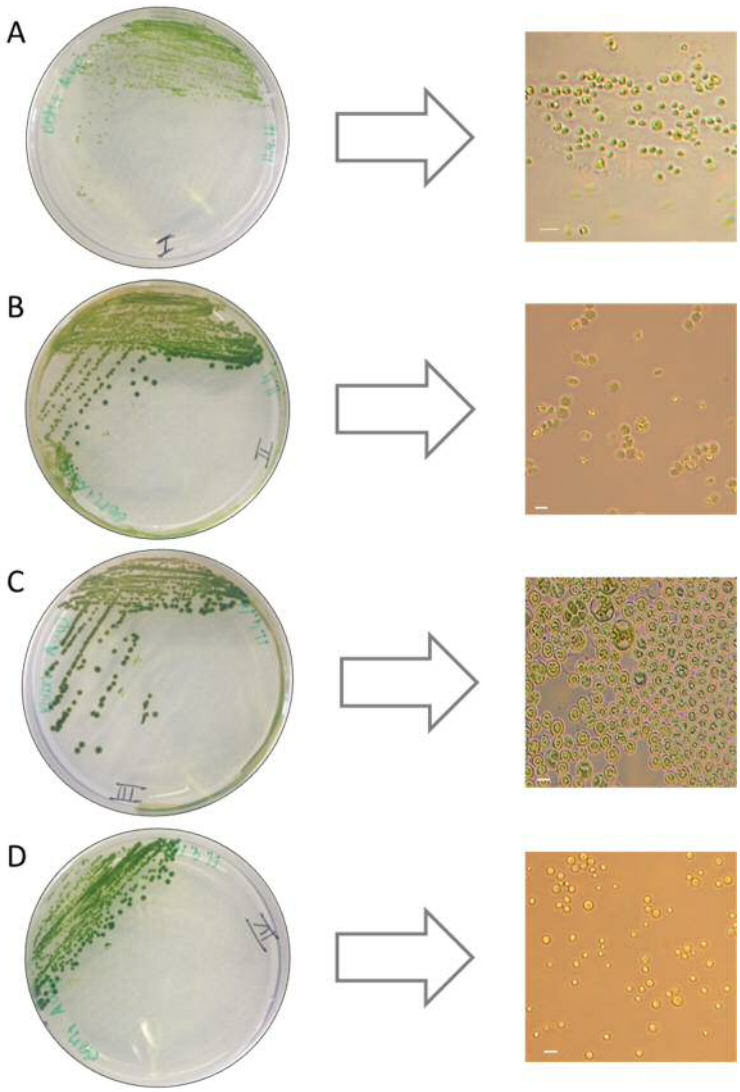

Figure 6: Microscopic observation of co-cultivated algae cultures using phase contrast. Scale bar: 10 µm

Isolates of co-cultivated, unwanted algae were transferred on BBM, *H. pluvialis* on CBM with and without ampicillin. *H. pluvialis* cells showed green growth at first while they changed their color to red when nutrient availability depleted. Furthermore, it was clearly observable that colonies growing close to each other on CBM changed their color more quickly than more separately grown colonies. No differences of the growth behavior between CBM plates with or without ampicillin were detected. A color-shift of co-cultivated algae from green to orange was noticed after days of incubation at 25°C and subjected a light-dark circle (L: 16h, D: 8h; Figure 7). Microscopic observations revealed phototrophic cells with a diameter of 5 µm to

10 µm. Sanger-sequencing identified the co-cultivated algae species as *Scenedesmus*.

Figure 7: Co-cultivated algae on BBM (in agar). Left: After eight days incubation at 25°C at a light/dark cycle (L: 16h, D: 8h), green colonies form. Middle: Color shift to orange after 39 days of incubation. Right: Observation of the orange colonies using an epifluorescence microscope under phase contrast conditions. After Sanger-sequencing the 18S rRNA gene sequence and subsequent alignment algae were identified as *Scenedesmus* sp. Scalebar = 10 µm

3.1.3 Phenotype based visual control of *H. pluvialis* pure cultures

After sequential transfers of single colonies onto new BBM I plates, pure culture of *H. pluvialis* strain 192.80 were obtained. Green algae colonies formed after seven days of incubation at 25°C and at a light/dark cycle (L: 16, D: 18). After another 40 days their color turned red (Figure 8).

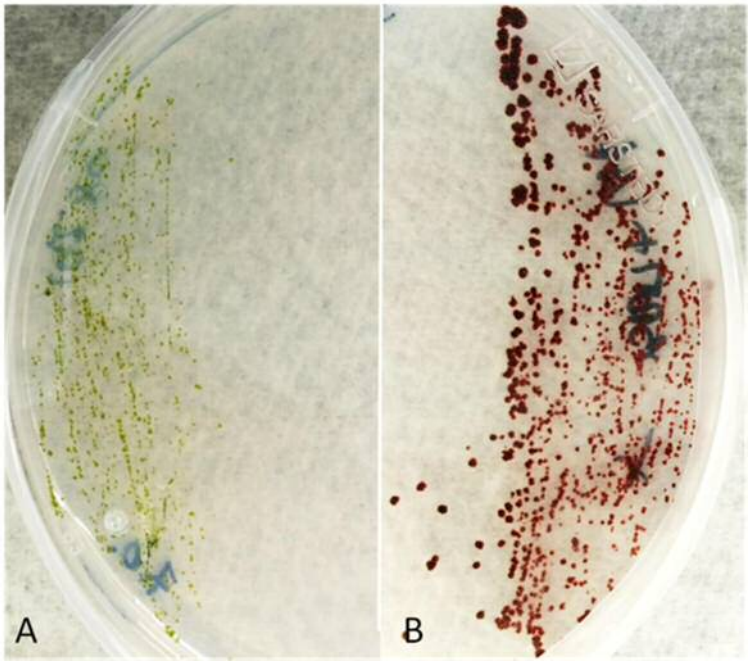

Figure 8: *H. pluvialis* strain 192.80 on BBM I. A: Growth pattern after seven days of incubation. B: *H. pluvialis* strain 192.80 cells after 47 days.

3.2 Visualization of co-occurring microorganisms in industrial-scale microalgae cultivation

3.2.1 CLSM coupled with BacLight allowed detailed visualization of *H. pluvialis* and its associated microbiota

Confocal laser scanning microscopy of the putative contamination and the *H. pluvialis* preculture (photobioreaction B; see Table 1) revealed high abundance of bacterial cells within the samples. The colors red, blue and green were assigned to the fluorophores SYTO 9, propidium iodide and to auto fluorescence, respectively. Excitation of calcofluor-white is between 365 nm and 395 nm while its emission is at 420 nm. Observed algae cells (*H. pluvialis*) had a diameter between 15 µm and 20 µm. Dead bacterial cells aggregated into clusters (grey marks 9.C). CLSM observations of the preculture of *H. pluvialis* showed already a high bacterial percentage. Again, interactions between algae and bacteria were assumed. Dead and vital bacteria cells surrounded the algae cells, predominantly dead cells (Figure 9.A). When analyzing the micrographs, only encapsulated *H. pluvialis* cells with calcofluor-white stained cell walls were detectable. Reason thereof may be that

the non-encapsulated cells do not bind on the polysinslides and were washed off while encapsulated cells stick to the slide. Observed algae cells (*H. pluvialis*) had a diameter between 15 µm and 20 µm. Dead bacterial cells aggregated into clusters (grey marks in Figure 9.C).

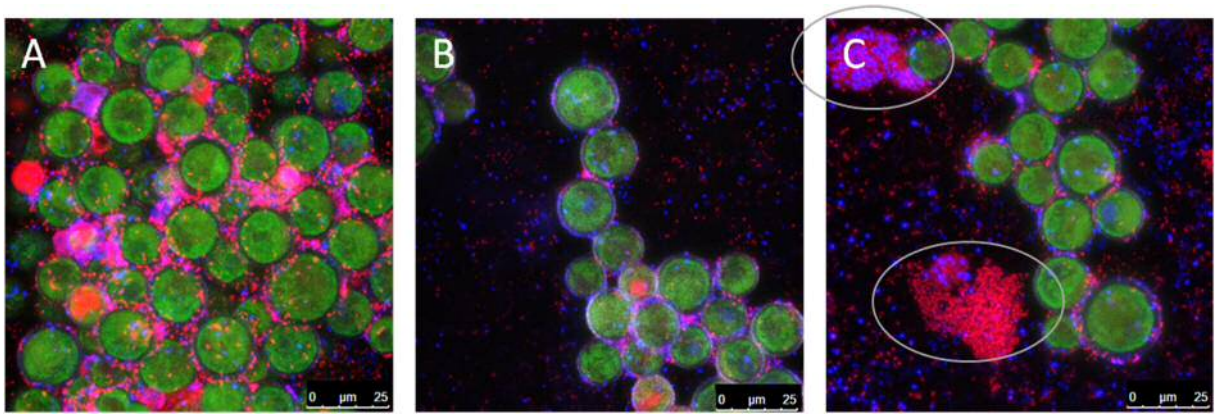

Figure 9: Confocal laser scanning microscopy of putative contamination. The colors red and blue indicate the fluorophores SYTO 9 and propidiumiodide, respectively. The green color stems from the autofluorescence of chlorophyll. Red: dead bacteria; blue: vital bacteria; green: algae; white: cell membrane. Grey marks indicate clusters of dead cell aggregates (C). Scale bar: 25 µm.

Visualization of putative contamination within photobioreaction B using CLSM after LIVE/DEAD staining in combination with calcofluor-white showed cluster-forming algae cells with a diameter of approximately 5 µm (Figure 10).

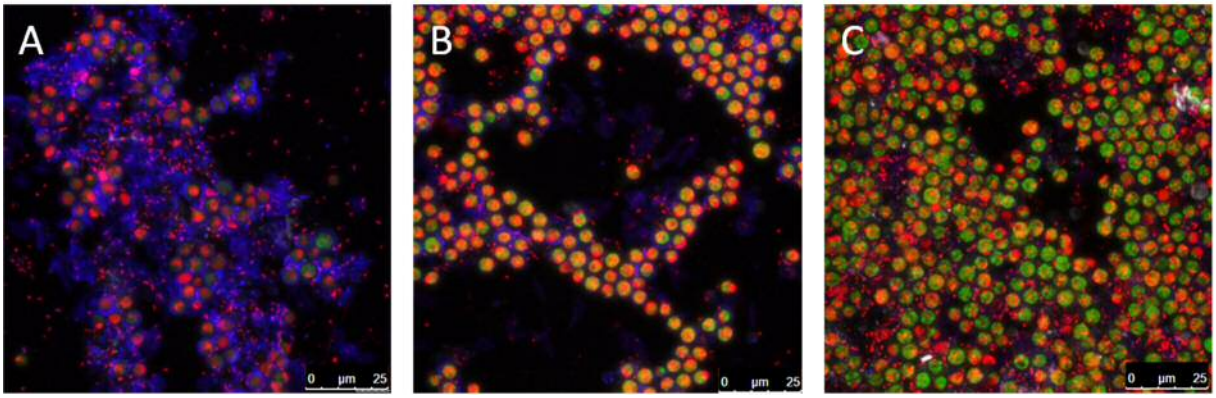

Figure 10: Confocal laser scanning microscopy of putative contamination. The colors red and blue indicate the fluorophores SYTO 9 and propidium iodide, respectively. The green color stems from the autofluorescence of chlorophyll. Red: dead bacteria; blue: vital bacteria; green: algae; white: cell membrane. Scale bar: 25 µm.

In addition samples of photobioreaction C were investigated. After staining viable and dead cells using the LIVE/DEAD bacterial viability kit the sample “DEMO 10100 17.03.2016” was observed using CLSM. A high bacterial community was observable. Rod-shaped bacteria were detectable forming chains (Figure 11.A). Life and dead bacteria seem to form clusters around algae cells (Figure 11.C).

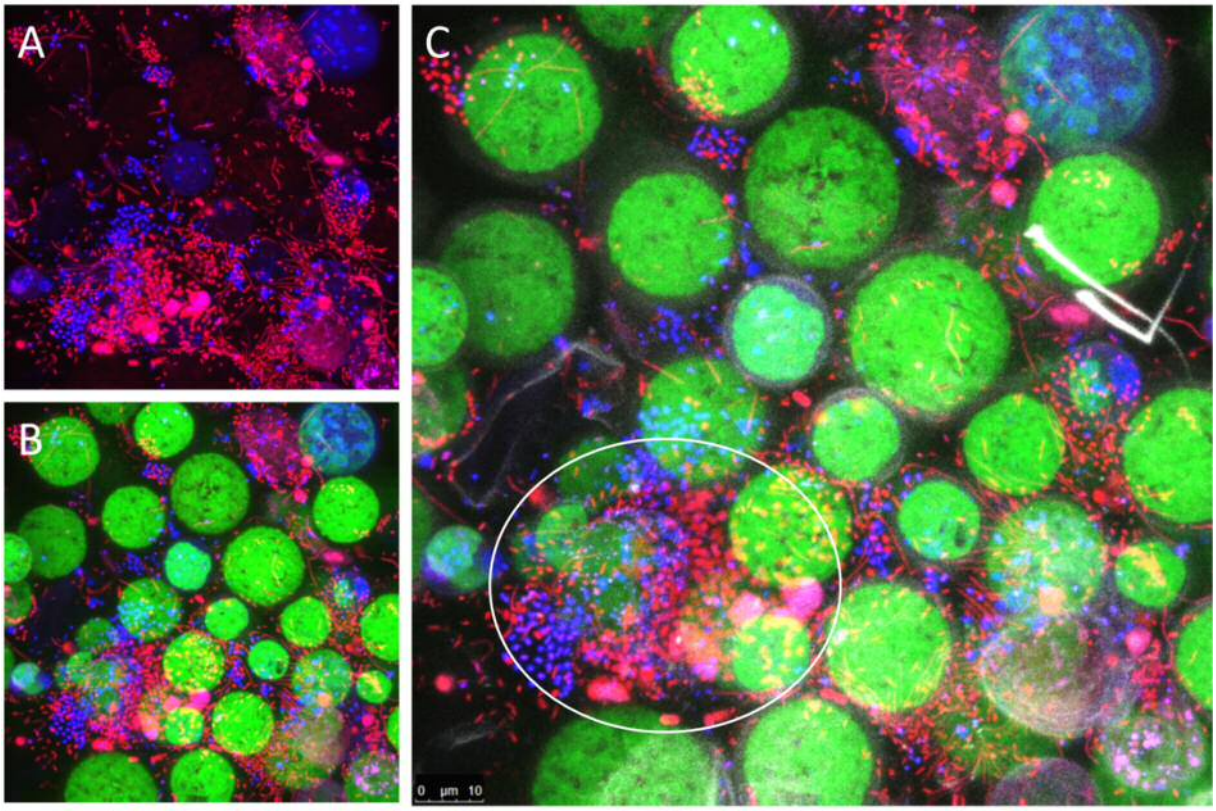

Figure 11: Confocal laser scanning microscopy (CLSM) micrographs showing the bacterial colonization stained by LIVE/DEAD bacterial viability kit. Red: dead bacteria; blue: vital bacteria; green: algae; white: cell membrane. The colors red, blue and green indicate the fluorophores SYTO 9, propidium iodide, respectively. The green color stems from the autofluorescence of chlorophyll. Arrows in A indicate the chain-forming bacteria. Encircled bacteria in C indicate a cluster formed by life and dead bacteria. Scale bar: 10 µm.

When observing the samples on non-coated objective slides, non-encapsulated *H. pluvialis* cells were detectable (Figure 12). The pink color of the algae cells is a result of staining with LIVE/DEAD bacterial viability kit. Both fluorophores seemed to permeate the cell wall of non-encapsulated cells. The oval-shape is typical for motile *H. pluvialis* cells. A high abundance of chain-forming rod-shaped bacteria was detected.

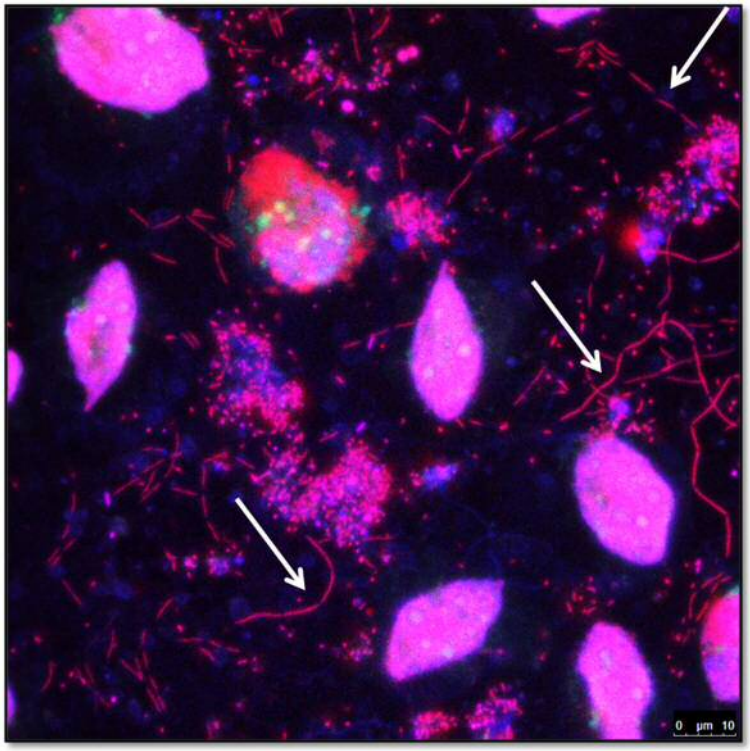

Figure 12: CLSM observation of LIVE/DEAD stained algae suspension. The oval-shaped form of the algae cells is typical for non-encapsulated *H. pluvialis* cells. Arrows indicate chain-forming rod-shaped bacteria. Scale bar: 10 µm.

3.2.2 Epifluorescence microscopy was used to visualize active flagellated cells and co-occurring eukaryotes

Sample “DEMO 10100 17.03.2016” of photobioreaction C was observed after LIVE/DEAD staining using an epifluorescence microscope. Samples were excited at 488 nm and 532 nm. Bacteria and algae were stained with SYTO 9, indicating living organisms (Figure 13.C). Propidium iodide nucleic-acid red fluorescent dyed cells were considered to be dead (Figure 13.B).

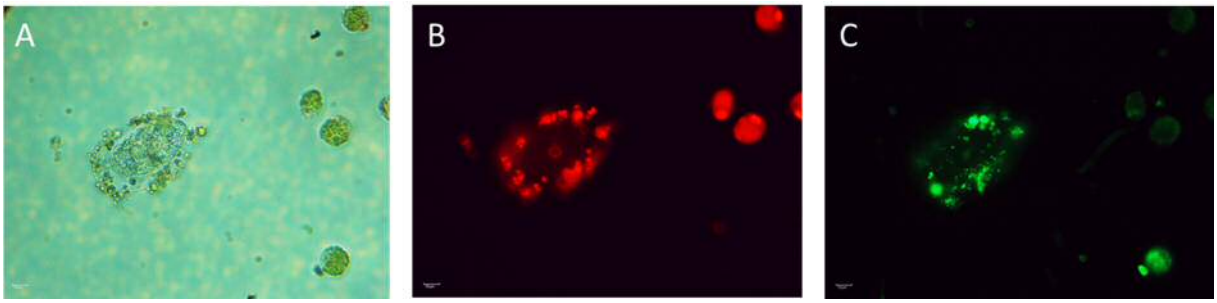

Figure 13: Observation of sample "DEMO 17.03.16" under the epifluorescent microscope after staining the cells using LIVE/DEAD staining kit. A: bright field, B: excitation at 532 nm, C: Excitation at 488 nm. Scale bar: 10 µm.

Under excitation at 488 nm bacterial cell clusters were detected (Figure 14.A). Rod-shaped living bacteria formed chains and were observable under the epifluorescence microscope (Figure 14.B)

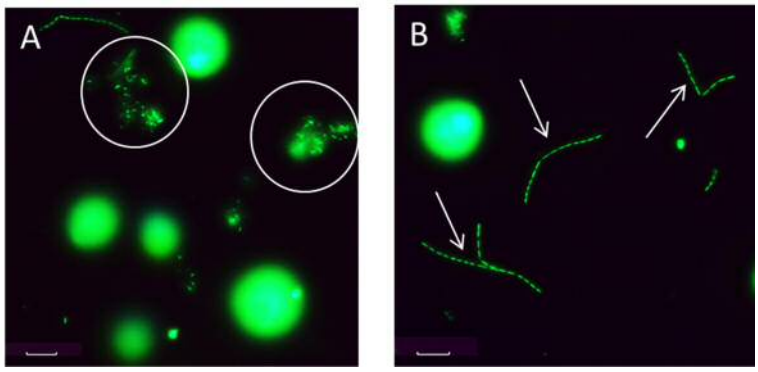

Figure 14: Algae suspension was observed at 488 nm using an epifluorescence microscope. Circles indicate bacteria clusters (A). Arrows point to the chains formed by bacteria (B). Scale bar: 10 µm.

When observing the sample under bright field, two different algae species were detectable due to phenotypical differences. *H. pluvialis* was identified by its characteristic size and by their two flagella indicated by the arrows in Figure 15.A. While *H. pluvialis* is distributed discretely among single cells, the co-cultivated algae distribution is clustered. Also *H. pluvialis* is clearly distinguishable from the co-cultivated algae due to the bigger size of its cells (Figure 15).

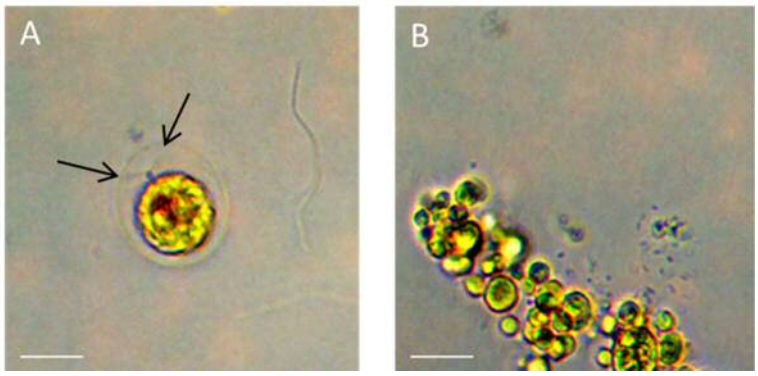

Figure 15: Observation of algae suspension using bright field. A: *H. pluvialis* with its characteristic flagella (indicated by arrows). B: Cluster-forming co-cultivated algae. The spherical-shaped algae species differ in size and distribution. Scale bar: 20 µm.

3.3 Cultivation-independent analyzes

3.3.1 Structural analysis of algae-associated microorganisms by SSCP showed heterogeneous microbial community assembly between the different reactors.

The bacterial and eukaryotic community patterns in industrial-scale algae cultivation were analyzed by SSCP. Respective bands were excised from the polyacrylamide gel and subsequently sequenced and identified by aligning them against the NCBI nucleotide database. Furthermore the differences of microbial diversity in two separately processed photobioreactors were investigated (photobioreaction B, photobioreaction C).

3.3.1.1 Co-cultured organisms within the *H. pluvialis* mass-cultivation

16S rRNA genes, 18S rRNA genes and ITS regions were partially amplified and analyzed by single-strand conformation polymorphism to obtain bacterial and eukaryotic community patterns. Detailed results obtained from Sanger-sequencing 16S rRNA gene sequences are shown in Table 8. No significant difference of the community pattern was found when comparing the results of the two used DNA extraction methods. SSCP fingerprints of the bacterial communities revealed the first insight into the high diversity among the cultivation processes as well as among different reactor sizes. A high bacterial diversity was already detected in the *H. pluvialis* preculture, which originally was considered to be a pure culture (Figure 16). Patterns which occur in the 5 L photobioreactor persist over the whole cultivation process.

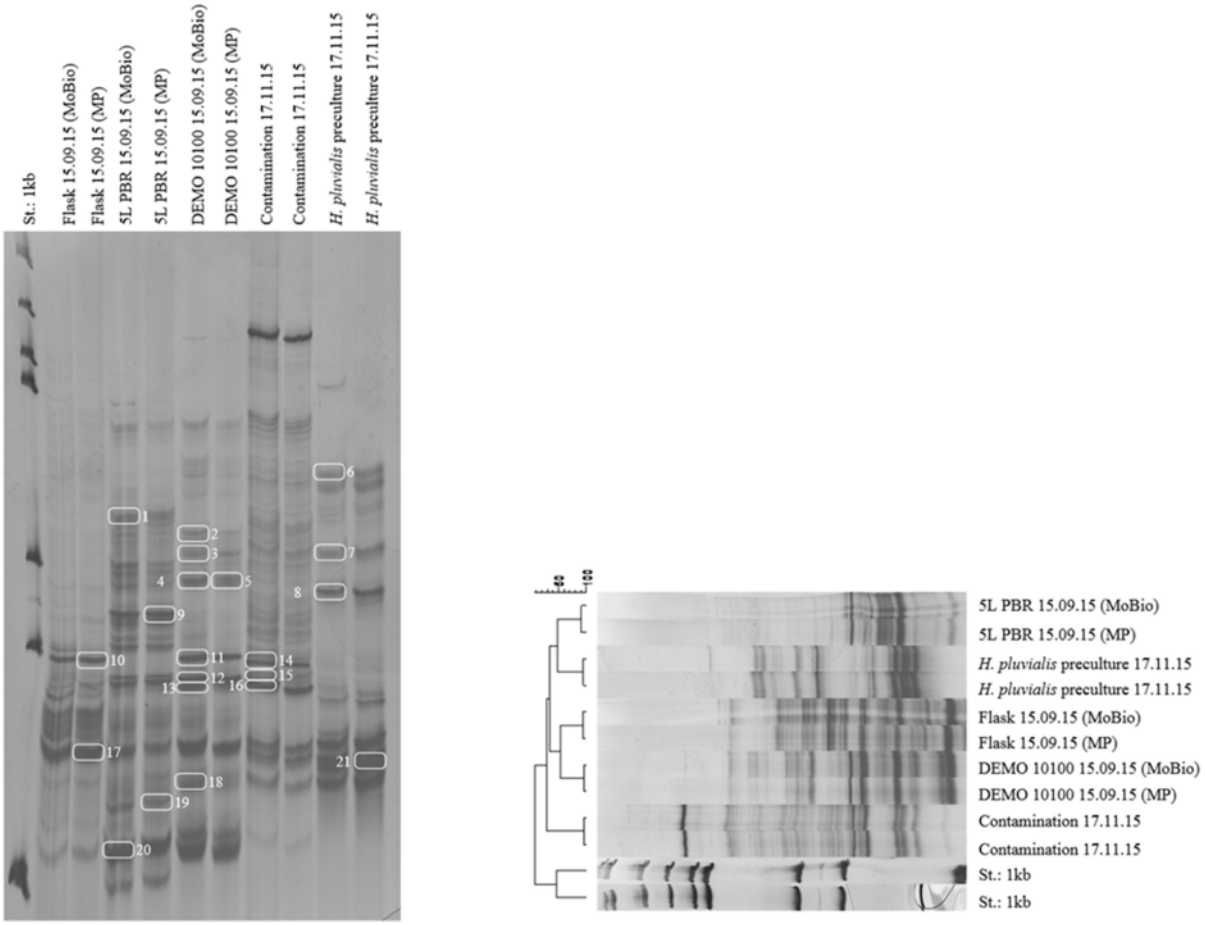

Figure 16: SSCP profile showing the bacterial communities of the differently contaminated samples and the references (left). Analysis was done in double determination; two different DNA extraction methods (MoBio PowerSoil isolation kit and MP FastDNA SPIN kit for soil) were compared. **Computer-assisted representation of bacterial SSCP profile (right).** Standard: Gene ruler 1kb ladder (Thermo Fisher Scientific, Massachusetts, USA; St.: 1kb).

Table 8: 16S taxons present at different stages of the cultivation.

ID	*Taxon*	*Class*	Identity	Occurrence
1	*Acidovorax avenae*	*Gammaproteobacteria*	93%	5 L PBR 15.09.16
2	*Curvibacter delicatus*	*Betaproteobacteria*	99%	DEMO 10100 15.09.15
3	*Curvibacter delicatus*	*Betaproteobacteria*	97%	DEMO 10100 15.09.15
4	*Caldimonas manganoxidans*	*Betaproteobacteria*	92%	DEMO 10100 15.09.15
5	*Brachymonas denitrificans*	*Betaproteobacteria*	91%	DEMO 10100 15.09.15
6	*Pelomonas aquatica*	*Betaproteobacteria*	99%	*H. pluvialis* preculture 17.11.15
7	*Pelomonas aquatica*	*Betaproteobacteria*	99%	*H. pluvialis* preculture 17.11.1 5
8	*Pelomonas aquatica*	*Betaproteobacteria*	98%	*H. pluvialis* preculture 17.11.15
9	*Prosthecobacter fluviatilis*	*Verrucomicrobia*	98%	5 L PBR 15.09.16
10	*Rhizobium selenitireducens*	*Alphaproteobacteria*	96%	Flask 15.09.16
11	*Cytophaga hutchinsonii*	*Cytophagia*	87%	DEMO 10100 15.09.15
12	*Fimbriimonas ginsengisoli*	*Fimbriimonadia*	89%	DEMO 10100 15.09.15
13	*Fimbriimonas ginsengisoli*	*Fimbriimonadia*	89%	DEMO 10100 15.09.15
14	*Dyadobacter beijingensis*	*Cytophagia*	96%	Contamination 17.11.15
15	*Sutterella wadsworthensis*	*Betaproteobacteria*	91%	Contamination 17.11.15
16	*Methylotenera versatilis*	*Betaproteobacteria*	99%	Contamination 17.11.15
17	*Runella limosa*	*Cytophagia*	96%	Flask 15.09.16
18	*Runella limosa*	*Cytophagia*	97%	DEMO 10100 15.09.15
19	*Hyphomicrobium hollandicum*	*Alphaproteobacteria*	89%	5 L PBR 15.09.16
20	*Flectobacillus roseus*	*Cytophagia*	99%	5 L PBR 15.09.16
21	*Sediminibacterium goheungense*	*Sphingobacteria*	93%	*H. pluvialis* preculture 17.11.15

The most dominant phylum during the whole cultivation process turned out to be *Proteobacteria (Alphaproteobacteria, Betaproteobacteria, Gammaproteobacteria)* followed by *Bacteriodetes (Cytophagia,Sphingobacteria*; Table 8).

Eukaryotes were identified by partial 18S rRNA gene sequencing and subsequent alignment using the BLAST algorithm (Altschul *et al.*, 1997) against the NCBI nucleotide collection database (excluding uncultured and environmental sample sequences). Detailed results are shown in Table 9. The patterns of the eukaryotic communities showed little differences comparing the two DNA extraction methods. Microbial fingerprints based on separation by single-strand conformation

polymorphism analysis revealed a highly stable community structure over the cultivation process (Figure 17).

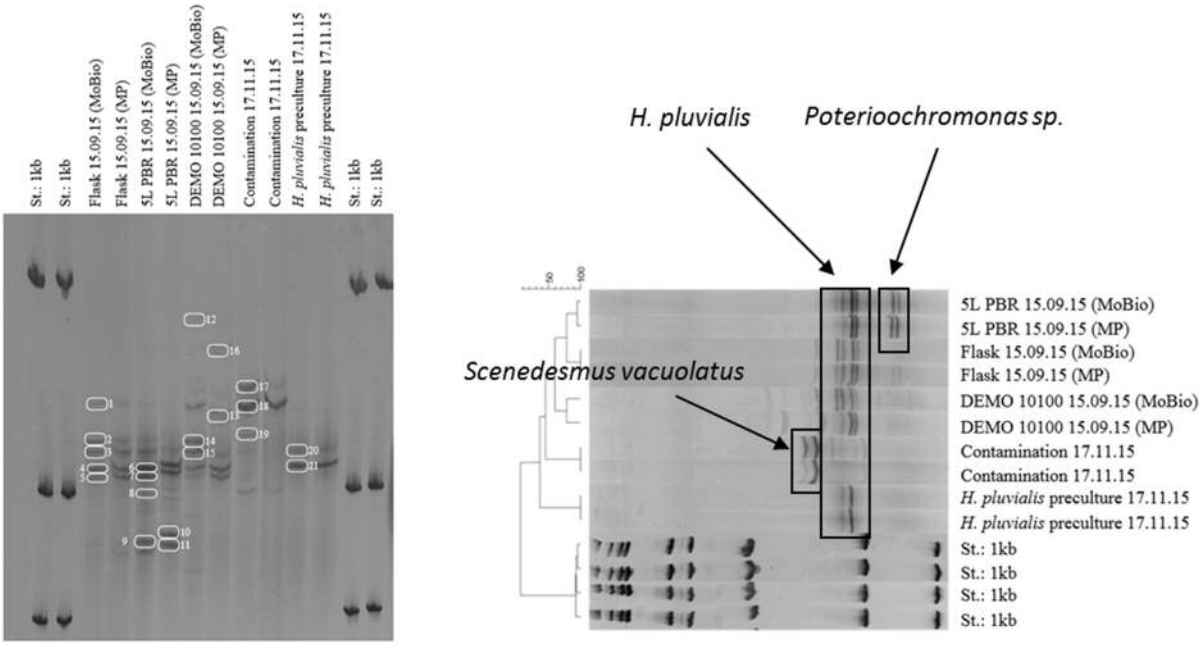

Figure 17: SSCP profile showing the eukaryotic communities of the differently contaminated samples and the references (left). Analyzes were done in double determination; two different DNA extraction methods (MoBio PowerSoil isolation kit and MP FastDNA SPIN kit for soil) were compared. **Computer-assisted representation of eukaryotic SSCP profile (right).** Standard: Gene ruler 1kb ladder (Thermo Fisher Scientific, Massachusetts, USA; St.: 1kb).

Table 9: Eukaryotic taxons in the reaction process.

ID	*Taxon*	*Class*	Identity	Occurrence
1	*Haematococcus pluvialis*	*Chlorophyceae*	98%	Flask 15.09.15
2	*Haematococcus pluvialis*	*Chlorophyceae*	98%	Flask 15.09.15
3	*Haematococcus pluvialis*	*Chlorophyceae*	98%	Flask 15.09.15
4	*Haematococcus pluvialis*	*Chlorophyceae*	98%	Flask 15.09.15
5	*Haematococcus pluvialis*	*Chlorophyceae*	98%	Flask 15.09.15
6	*Haematococcus pluvialis*	*Chlorophyceae*	98%	5 L PBR 19.05.15
7	*Haematococcus pluvialis*	*Chlorophyceae*	98%	5 L PBR 19.05.15
9	*Poterioochromonas sp.*	*Chrysophyceae*	97%	5 L PBR 19.05.15
10	*Poterioochromonas sp.*	*Chrysophyceae*	100%	5 L PBR 19.05.15
11	*Poterioochromonas sp.*	*Chrysophyceae*	100%	5 L PBR 19.05.15
12	*Trichotria tetractis*	*Eurotatoria*	99%	DEMO 10100 15.09.15
13	*Trichosporon japonicum*	*Tremellomycetes*	99%	DEMO 10100 15.09.15
14	*Haematococcus pluvialis*	*Chlorophyceae*	98%	DEMO 10100 15.09.15
15	*Haematococcus pluvialis*	*Chlorophyceae*	98%	DEMO 10100 15.09.15
16	*Brachionus angularis*	*Monogonota*	98%	DEMO 10100 15.09.15
17	*Scenedesmus vacuolatus*	*Chlorophyceae*	100%	Contamination 17.11.15
18	*Scenedesmus vacuolatus*	*Chlorophyceae*	100%	Contamination 17.11.15
19	*Scenedesmus vacuolatus*	*Chlorophyceae*	99%	Contamination 17.11.15
20	*Haematococcus pluvialis*	*Chlorophyceae*	98%	*H. pluvialis* preculture 17.11.15
21	*Haematococcus pluvialis*	*Chlorophyceae*	98%	*H. pluvialis* preculture 17.11.15

Performing single-strand conformation polymorphism analysis using universal eukaryotic primers allowed insights into the distribution of Eukaryotes over the cultivation process. *Haematococcus pluvialis* preculture was considered to be pure with respect to eukaryotic communities (Figure 18). The 18S rRNA gene sequence of the putative contamination was identified as *Scenedesmus vacuolatus*. Besides *H. pluvialis* and *S. vacuolatus*, algae from the class *Chrysophyceae* (*Poterioochromonas sp*.) grew during the cultivation. First occurrence of the potential contamination was reported in the 5 L photobioreactor. In the DEMO 10100 samples, no algae species were found besides *H. pluvialis* but the rotifers *Trichotria tetractis* and *Brachionus angularis* and the fungus *Trichosporon japonicum.*

Fungal communities were identified by sequencing the amplified ITS region and subsequent alignment using the BLAST algorithm (Altschul *et al.*, 1997). Detailed results are shown in Table 9. When blasting against the NCBI nucleotide collection database (excluding uncultured and environmental sample sequences) no fungi were under the best hits as algae contain ITS regions where primers can align.

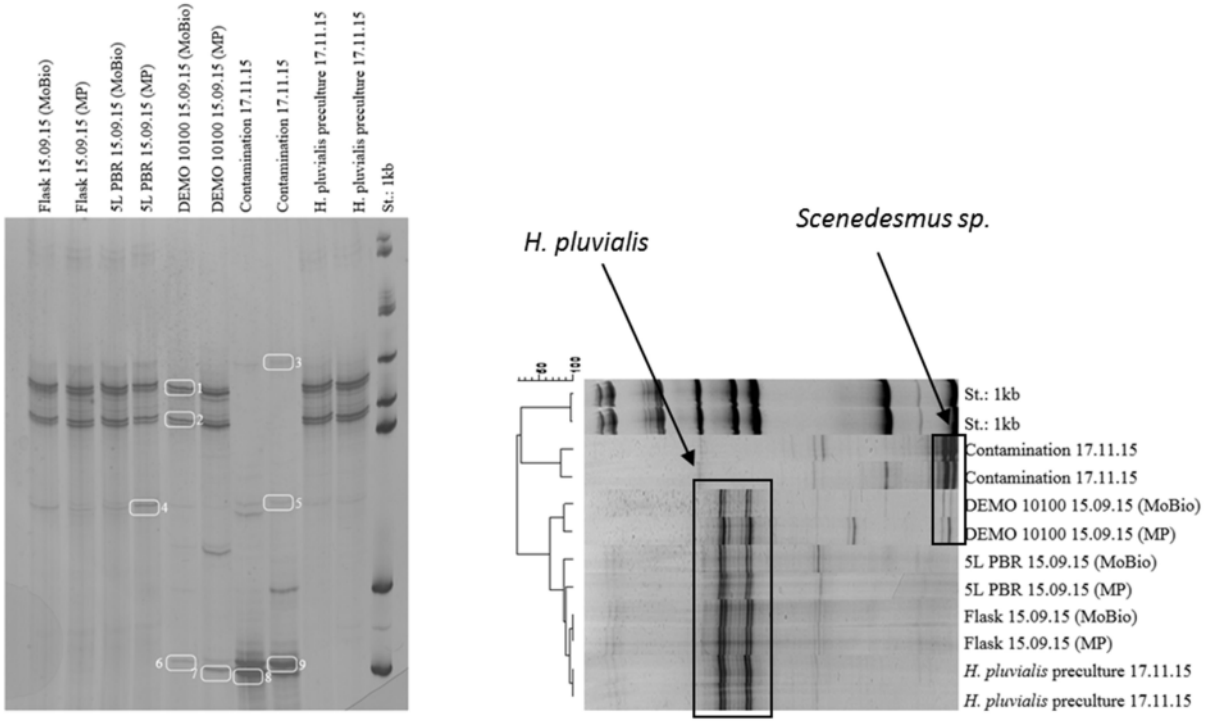

Figure 18: SSCP profile showing the eukaryotic communities amplified with ITS specific primers of the differently contaminated samples and the references (left). Analyzes were done in double determination to compare different DNA extraction methods (MoBioPowerSoil isolation kit and MP FastDNA SPIN kit for soil). **Computer-assisted representation of SSCP profile (right).** Standard: Gene ruler 1kb ladder (Thermo Fisher Scientific, Massachusetts, USA; St.: 1kb).

Comparing the two DNA extraction methods no significant differences were observed (Figure 18). The band representing *H. pluvialis* was abundant in each respective sample. The putative contaminations were again identified to be *Scenedesmus sp.* (Table 10). Furthermore the patterns indicating *Scenedesmus sp*. were found in the DEMO reactor. Amplification with ITS specific primer showed similar results as with 18S rRNA gene specific primer.

Table 10: Taxons in the reaction process based on ITS aplificates.

ID	*Taxon*	*Class*	Identity	Occurrence
1	*Haematococcus pluvialis*	*Chlorophyceae*	99%	DEMO 10100 15.09.15
2	*Haematococcus pluvialis*	*Chlorophyceae*	98%	DEMO 10100 15.09.15
3	*Scenedesmus sp.*	*Chlorophyceae*	96%	Contamination 17.11.15
4	*Haematococcus pluvialis*	*Chlorophyceae*	99%	5 L PBR 15.09.15
5	*Scenedesmus sp.*	*Chlorophyceae*	99%	Contamination 17.11.15
6	*Scenedesmus sp.*	*Chlorophyceae*	99%	DEMO 10100 15.09.15
7	*Scenedesmus sp.*	*Chlorophyceae*	99%	DEMO 10100 15.09.15
8	*Scenedesmus sp.*	*Chlorophyceae*	99%	Contamination 17.11.15
9	*Scenedesmus sp.*	*Chlorophyceae*	99%	Contamination 17.11.15

3.3.1.2 Comparison of two individual cultivation processes showed a general highly restructured microbiota but similar potential eukaryotic contaminants

In order to compare two cultivation processes (photobioreaction B, photobioreaction C) with respect to the bacterial and eukaryotic communities at different process-stages, single-strand conformation polymorphism fingerprints were obtained. All samples were treated with MP FastDNA SPIN kit for soil except the references (putative contamination and *H. pluvialis* strain 34-1e) were treated with ethanol to extract the DNA.

When comparing the bacterial community of the two photobioreactors, the diversity in the photobioreaction B was higher already at the beginning. Whereas only two bands were detected in the flask of photobioreaction C (Flask 05.05.16), more bands could be traced in the sample of photobioreaction B. Furthermore the bands of the two respective flask-samples were not at the same height which indicated that the bacterial community within the two samples differed. The same is to say when comparing the diversity in the respective 5 L photobioreactor. During cultivation the bacterial diversity increased with the reactor size. In the DEMO reactor no differences between photobioreaction B and photobioreaction C regarding the number of different bacterial communities were detected. SAG *H. pluvialis* seemed to be nearly bacteria free, only one light band was visible (Figure 19).

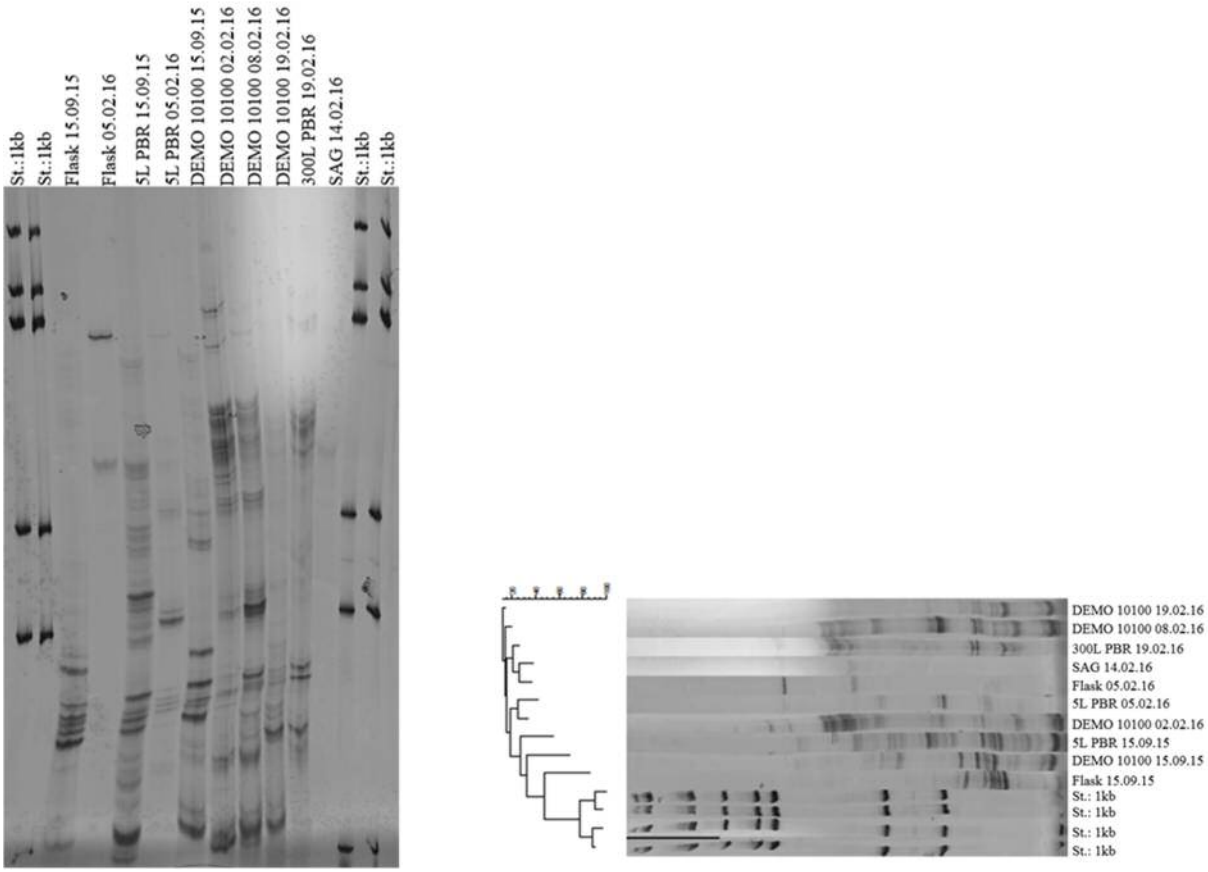

Figure 19: SSCP patterns obtained from single-stranded DNA products amplified by eubacterial PCR from different stages of the cultivation process (left). Computer-assisted representation of the bacterial community (right). Two cultivation processes were compared. Standard: Gene ruler 1kb ladder (Thermo Fisher Scientific, Massachusetts, USA; St.: 1kb).

For comparing the eukaryotic communities within the two cultivation approaches, universal eukaryotic primers were used, covering the V4 region of the 18S rRNA gene. Eukaryotes were identified by partial 18S rRNA gene sequencing and subsequent alignment using the BLAST algorithm (Altschul *et al.*, 1997) against the NCBI nucleotide collection database excluding uncultured and environmental sample sequences. Detailed results are shown in Table 11. With sequencing, *Poterioochromonas malhamensis* was first detected in the flask in photobioreaction B. *Chlorella vulgaris,* another co-cultivated alga was detected in the sample "DEMO 10100 15.09.15." The pattern of *P. malhamensis* (ID: 2, 3, 10, 14) persisted over the whole cultivation approach B, while it first occurred in the sample "DEMO 10100 02.02.16" within photobioreaction C; two days after inoculation). In cultivation approach C, *C. vulgaris* was first identified in "DEMO 10100 17.03.16" (Figure 20). According to BDI rating, samples were considered to be strongly contaminated when *Poterioochromonas sp.* and *Chlorella vulgaris* were co-cultivated. *Scenedesmus sp*. was identified in the reference sample (ID 17) when analyzing the partial 18S rRNA genes amplified by primers covering the V4 region.

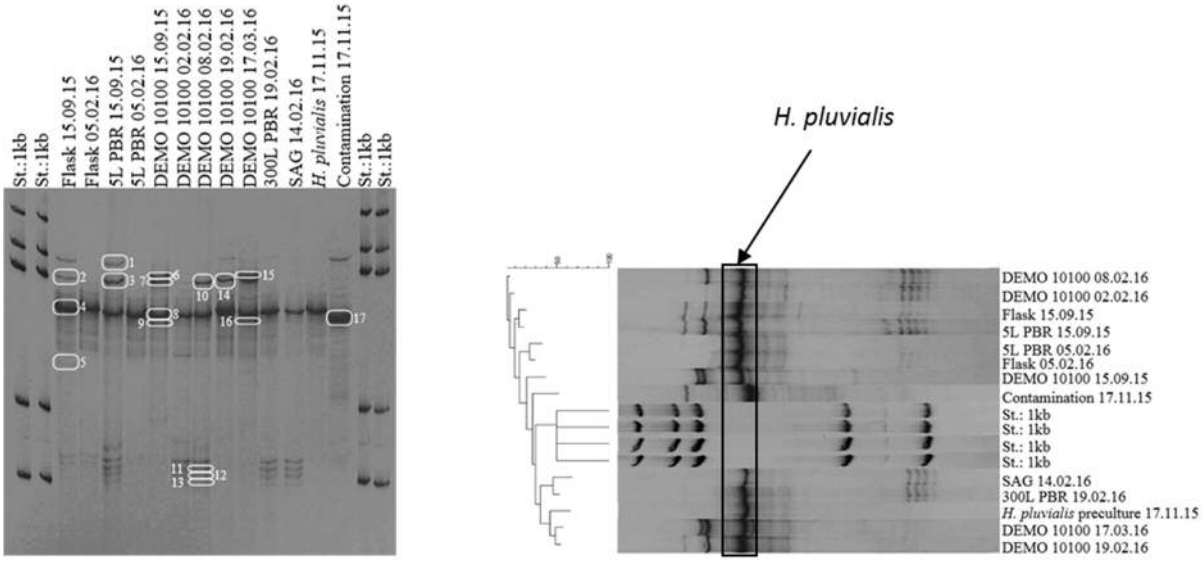

Figure 20: SSCP profile showing the eukaryotic diversity within photobioreaction B and photobioreaction C. 18S rRNA genes were amplified by using primers (TAReuk454FWD1 and TAReukREV3P) covering the variable region 4 (V4; left) for the comparison of two photobioreactions. **Representation of SSCP results by using GelComparII software (right).** Standard: Gene ruler 1kb ladder (Thermo Fisher Scientific, Massachusetts, USA; St.: 1kb).

Table 11: Results of partial 18S rRNA gene alignment amplified with primers covering the V4 region.

ID	*Taxon*	*Class*	Identity	Occurrence	
1	*Nucleocercomonas sp.*	*Cercozoa*	99%	5 L PBR 15.09.15	
2	*Poterioochromonas malhamensis*	*Chrysophyceae*	99%	Flask 15.09.15	
3	*Poterioochromonas malhamensis*	*Chrysophyceae*	99%	5 L PBR 15.09.15	
4	*Haematococcus pluvialis*	*Chlorophyceae*	100%	Flask 15.09.15	Photobioreaction B
5	*Haematococcus pluvialis*	*Chlorophyceae*	99%	Flask 15.09.15	
6	*Chlorella vulgaris*	*Trebouxiophyceae*	100%	DEMO 10100 15.09.15	
7	*Chlorella vulgaris*	*Trebouxiophyceae*	99%	DEMO 10100 15.09.15	
8	*Haematococcus pluvialis*	*Chlorophyceae*	100%	DEMO 10100 15.09.15	
9	*Haematococcus pluvialis*	*Chlorophyceae*	100%	DEMO 10100 15.09.15	
17	*Scenedesmus sp.*	*Chlorophyceae*	100%	Contamination 14.11.15	
10	*Poterioochromonas malhamensis*	*Chrysophyceae*	100%	DEMO 10100 08.02.16	
11	*Haematococcus pluvialis*	*Chlorophyceae*	99%	DEMO 10100 08.02.16	
12	*Dunaliella sp.*	*Chlorophyceae*	100%	DEMO 10100 08.02.16	Photobioreaction C
13	*Gungnir neglectum*	*Chlorophyceae*	100%	DEMO 10100 08.02.16	
14	*Poterioochromonas malhamensis*	*Chrysophyceae*	100%	DEMO 10100 19.02.16	
15	*Chlorella vulgaris*	*Trebouxiophyceae*	99%	DEMO 10100 17.03.16	
16	*Haematococcus pluvialis*	*Chlorophyceae*	100%	DEMO 10100 17.03.16	

In a second approach, the differences of the two photobioreactions based on 18S rRNA gene sequencing were revealed by using primers, covering the V9 region of the 18S rRNA gene. Again, 18S rRNA genes were sequenced and subsequently aligned against the NCBI nucleotide collection database (excluding uncultured and environmental sample sequences) using the BLAST algorithm (Altschul *et al.*, 1997). Results are displayed in Table 12. Little differences were detected when comparing the flasks of the respective cultivation processes. The diversity in the 5 L PBR from photobioreaction B differed from that in photobioreaction C, as an additional band in the lower region of the gel was formed (Figure 21). Sample “DEMO 10100 05.02.16” showed an uncommon pattern which may be caused by incorrect storage after sampling. Therefore this sample was excluded from further analyzes.

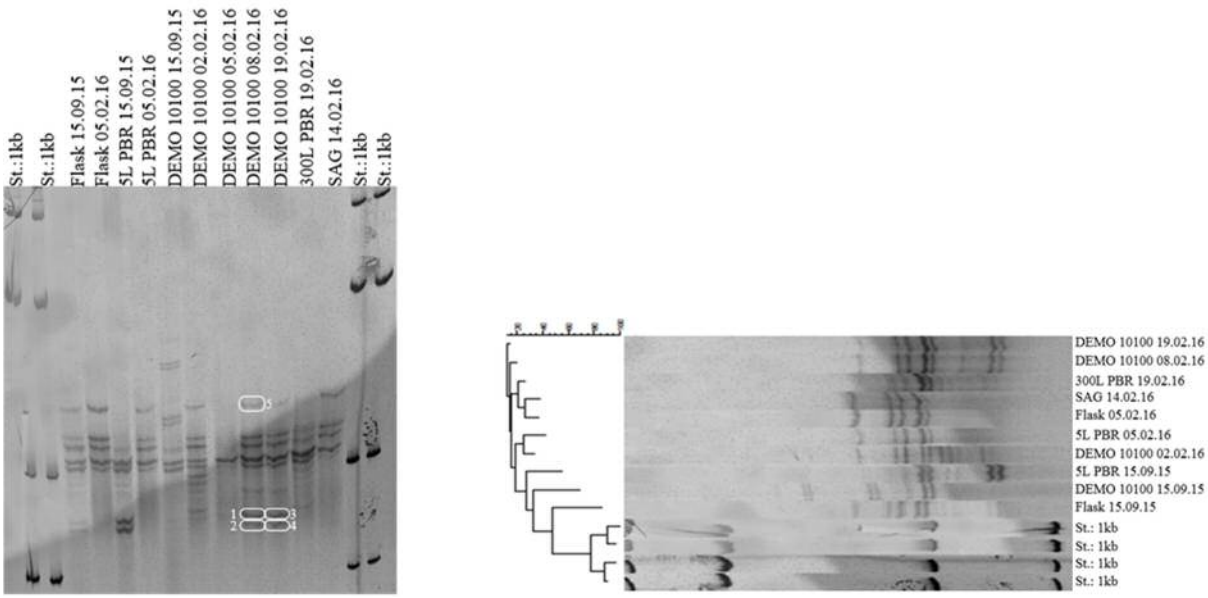

Figure 21: SSCP-profile showing the eukaryotic diversity in photobioreaction B (2015) and photobioreaction C (2016). 18S rRNA fragments were amplified by using primers (1391f/EukBrP) covering the variable region 9 (left) for comparison of two photobioreactors. **Representation of the eukaryotic community pattern using GelComparII software (right).** Standard: Gene ruler 1kb ladder (Thermo Fisher Scientific, Massachusetts, USA; St.: 1kb).

Table 12: Results of partial 18S rRNA gene alignment amplified with primers covering the V9 region.

ID	*Taxon*	*Class*	Identity	Occurrence
1	*Biddulphia sp.*	*Mediophyceae*	100%	DEMO 10100 08.02.16
2	*Poterioochromonas sp.*	*Chrysophyceae*	100%	DEMO 10100 08.02.16
3	*Poterioochromonas sp.*	*Chrysophyceae*	100%	DEMO 10100 08.02.16
4	*Poterioochromonas sp.*	*Chrysophyceae*	100%	DEMO 10100 19.02.16
5	*Haematococcus pluvialis*	*Chlorophyceae*	98%	DEMO 10100 19.02.16

When analyzing the V4 region of the 18S rRNA gene, similar results as in the first approach were obtained. *Poterioochromonas sp*. was identified in the DEMO 10100 reactor of photobioreaction B in samples taken at different time points (08.02.16, 19.02.16).

In a third approach, eukaryotic communities were analyzed with ITS-specific primers. Different patterns between the two photobioreactors were observed

(Figure 22). Reason for that may be the usage of different *H. pluvialis* strains. In photobioreaction B*, H. pluvialis* strain 34-1e was used, while photobioreaction C was inoculated with *H. pluvialis* strain 192.80.

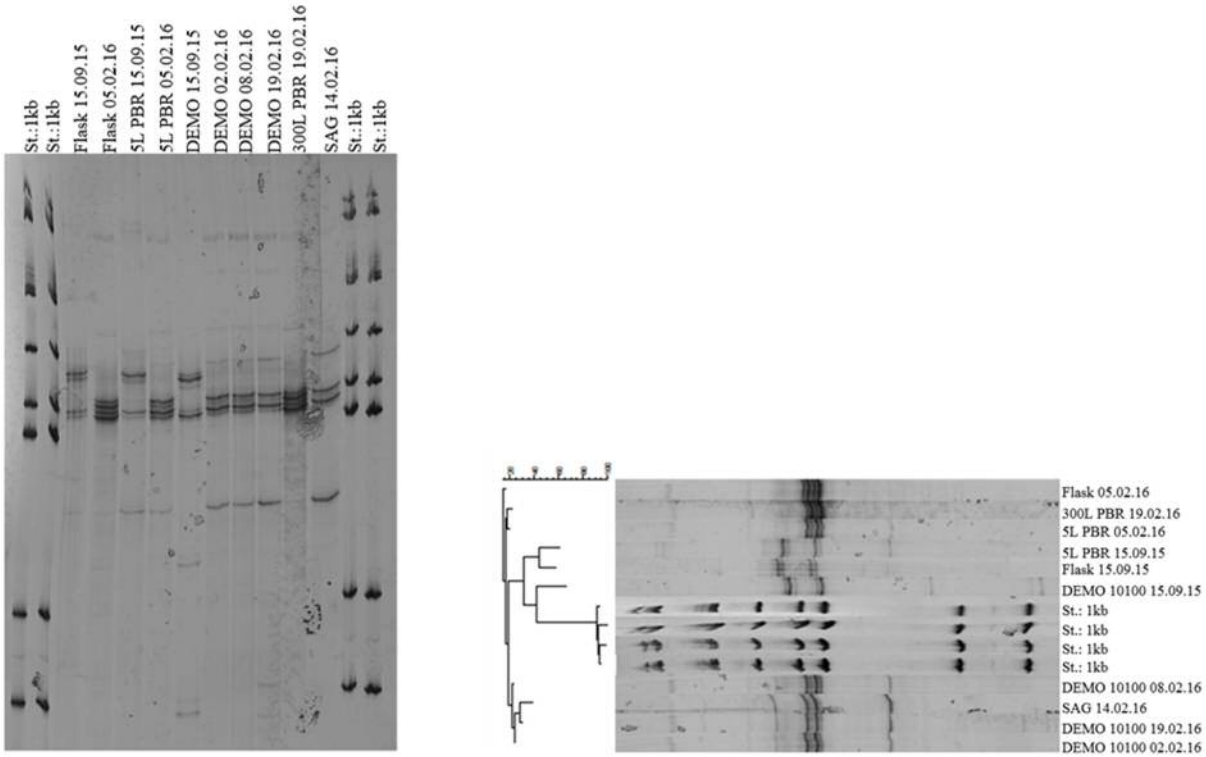

Figure 22: SSCP profile showing the eukaryotic communities after amplification with ITS specific primers (left). Analysis was done in double determination to compare different DNA extraction methods (MoBioPowerSoil isolation kit and MP FastDNA SPIN kit for soil). **Computer-assisted representation of the SSCP profile (right).** Standard: Gene ruler 1kb ladder (Thermo Fisher Scientific, Massachusetts, USA; St.: 1kb).

3.3.2 Illumina MiSeq/HiSeq sequencing revealed potential contaminants already in first stages of the microalgae production

An Illumina sequencing-based analysis of the 16S rRNA gene, 18S rRNA gene and ITS region was done to gain insight into the community composition and diversity over the scale-up process of the industrial algae cultivation. As the two different DNA-extraction methods (PowerSoil DNA isolation kit and FastDNA SPIN kit for soil) showed no significant difference in the abundance and the occurrence of bacterial, eukaryotic and fungal communities, the mean abundance is displayed in the graphs.

3.3.2.1 Comparison of two different barcode constructs for 16S rRNA gene amplicon sequencing

To unravel the bacterial communities in the algae cultivation two different approaches for 16S rRNA gene amplification were executed. OTUs with a high relative abundance were observable with both primer designs. 37 OTUs with a relative abundance above 1 % in all samples were only observed when using barcoded primer (barcode construct 1) but not when amplifying with barcode construct 2. Conversely six OTUs were only detectable when using barcode design 2. The relative abundance of non-observed OTUs when using barcode design 2 never exceeded 5 % except one (*Salinibacterium*), which had a relative abundance of 11 % in the 5 L PBR-sample (Figure 23). The respective OTU was filtered from the OTU table of the golay barcodes, when all OTUs with a relative abundance beneath 1 % in total were excluded from further analyzes.

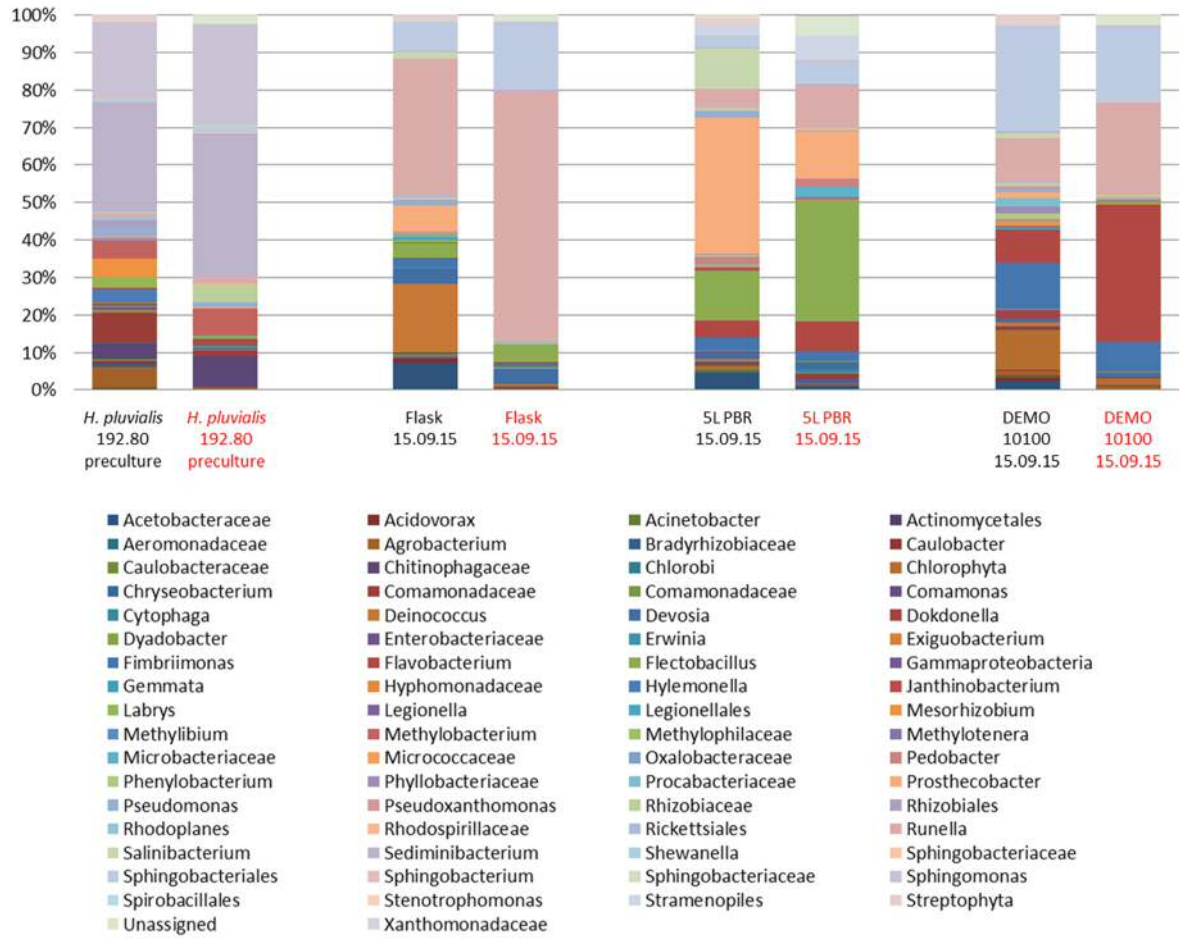

Figure 23: Comparison of two differently barcoded primer for amplification for Illumina MiSeq sequencing. Black: Primer and Barcode are one construct (barcode construct 1). Red: Golay barcodes are aligned on the primer using a linker sequence (barcode construct 2).

Alpha rarefaction indicates differences in the sequence depth when using two different barcode constructs. Direct barcodes (barcode construct 1) reveal orders of magnitude higher sequencing depth than barcode construct 2 (nested barcode approach; Figure 24). The number of sequences when using barcode construct 1 reached 30,000, while the number of amplifications is only 4,000 when using barcode construct 2. These results reflect the number of observed OTUs. When using barcode construct 1, a maximum of 1,200 OTUs were observable while when amplifying with barcode construct 2, the highest number of observed OTUs was 500. If not mentioned otherwise the dataset received by using barcode construct 1 was used for further analyzes.

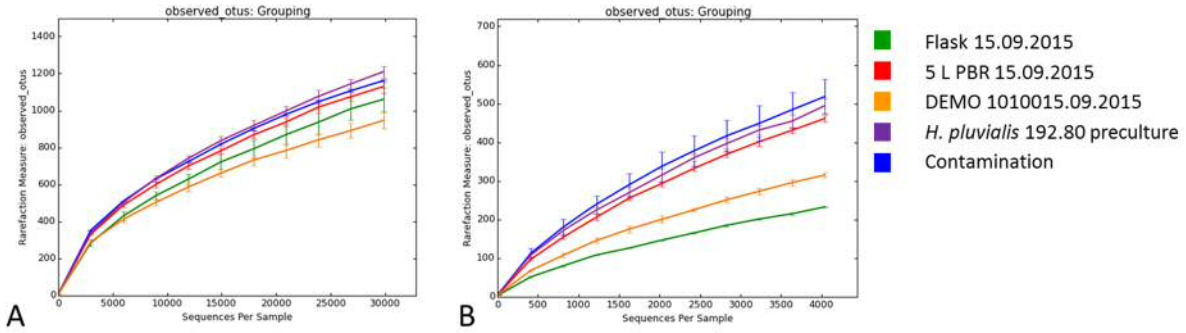

Figure 24: Comparison of rarefaction analyzes when using two different barcode constructs for amplicon sequencing. A: barcode construct where barcode is part of the primer (barcode construct 1). B: Barcode had to be amplified on the primer by using a 2 base long linker-sequence (barcode construct 2).

3.3.2.2 Comparison of two separately proceeded algae-cultivations

Co-cultured organisms of two separately proceeded cultivation approaches (photobioreaction B and C) were identified by partial amplification of 16S rRNA genes and subsequent sequencing and alignment.

16S rRNA gene sequences obtained from photobioreaction B were analyzed by doing Illumina MiSeq amplicon sequencing. A high bacterial diversity was revealed over the whole cultivation process which starts already in the *H. pluvialis* preculture. The most abundant bacterial genus in the *H. pluvialis* 192.80 preculture was *Sphingomonas* within the phylum *Proteobacteria* with a relative abundance of 29 % followed by *Sediminibacterium* within the phylum *Bacteriodetes* (20 %). The composition of the bacterial communities changed when algae culture was transferred for inoculation. Therefore the dominating bacterial genus in the flask (15.09.2015) was *Runella* sp. belonging to the phylum *Bacteriodetes* with 36 % relative abundance. *Deinococcus* was the second most common bacterial genus in the flask (15.09.2015; 18 %). Again the most abundant bacterial communities were completely different in the 5 L photobioreactor (15.09.2015). The most abundant bacterial genus was *Prosthecobacter* (*Verrucomicrobia*) with a relative abundance of 36 % followed by *Flectobacillus* within the phylum *Bacteriodetes* (13 %). The three most abundant bacterial communities in the DEMO were *Sphingobacteriales* (27 %), *Fimbriimonas* (12 %) and *Cyanobacteria* (10 %; Figure 26).

Additionally, samples from photobioreaction C were investigated. No PCR products were received when amplifying the 16S rRNA genes from the SAG *H. pluvialis* 34-1e, the flask (05.02.2016) and the 5 L photobioreactor (05.02.2016). Illumina HiSeq amplicon sequencing of 16S rRNA genes was performed on DEMO reactor samples taken at different points in time (02.02.2016, 08.02.2016, 19.02.2016, 17.03.2016) and on one 300 L photobioreactor sample (19.02.2016). The most abundant bacterial family in the 300 L photobioreactor was *Comamonadaceae* within the phylum *Proteobacteria* with a mean relative abundance of 42 %. Additionally the genus *Roseateles* within the family *Comamonadaceae* is observable in a high number (15 %). In total a relative abundance of Betaproteobacteria of 57 % was determined. The bacterial community patterns in the 300 L persist over the scale-up process since the algae suspension from the 300 L photobioreactor serves as inoculate for the DEMO reactor. The relative abundance of *Comamonadaceae* decreased over time while the amount of *Flavobacteriales* increased. In the strongly contaminated sample “DEMO 17.03.16” *Cyanobacteria* became the second most abundant (16 %) followed by *Flavobacteria* (13 %; Figure 25).

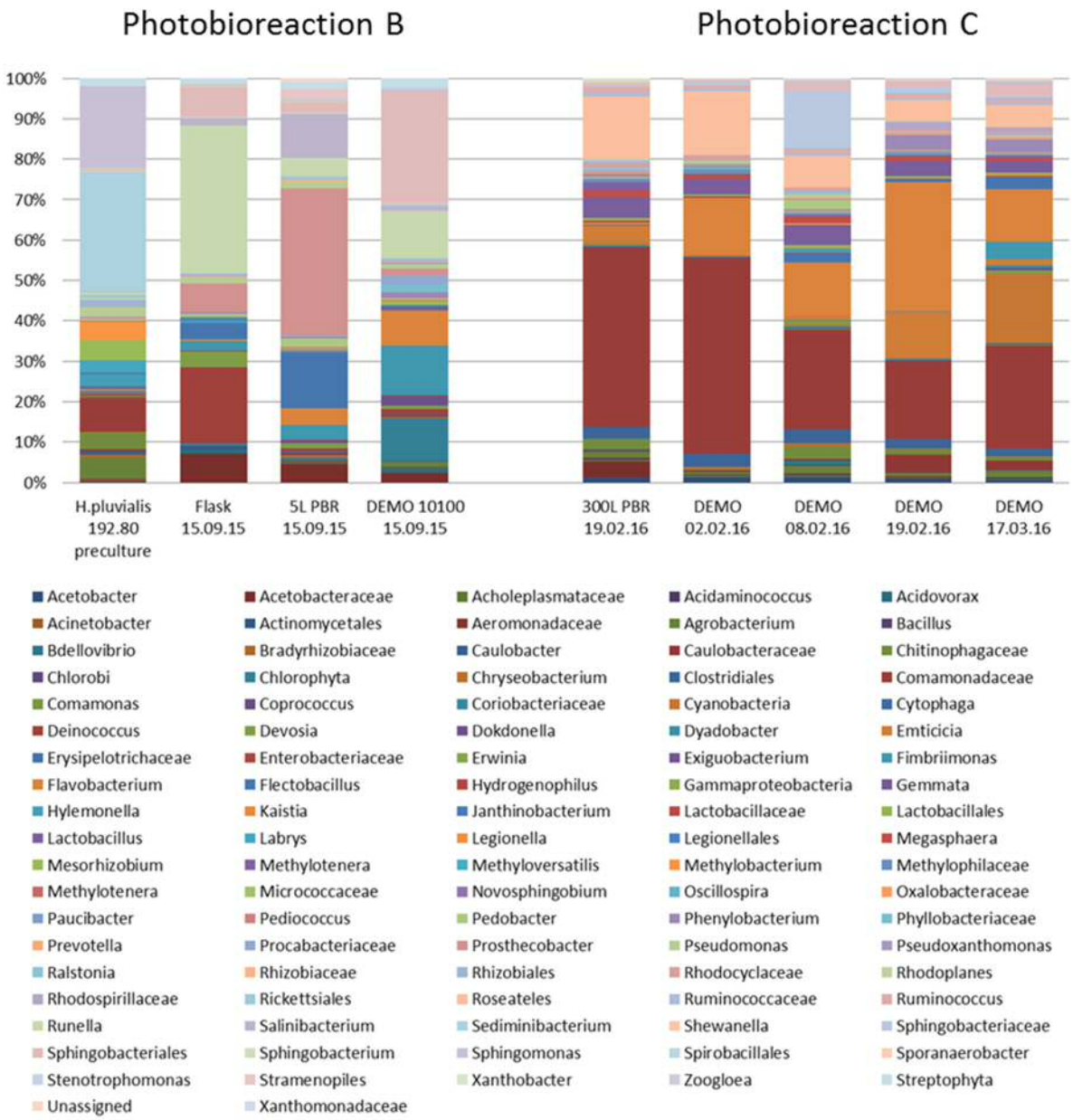

Figure 25: Comparison of bacterial communities in two microalgae cultivation approaches. The bacterial composition in the photobioreaction B over the scale-up was mainly stochastic, as no continuous presence of a specific bacterial genus was detected. In cultivation approach C the change of bacterial communities over the time in one DEMO photobioreactor was observed. The bacterial pattern of the inoculum (300 L photobioreactor) persisted in the DEMO reactor with slight shifts in the abundance of respective taxa.

In addition co-cultured organisms of two separately run algae cultivation approaches (photobioreaction B and photobioreaction C) were identified by partial amplification of 18S rRNA genes and subsequent sequencing and alignment.

In photobioreaction B the dominating eukaryotic taxon was *H. pluvialis* but with reactor-size the abundance of co-cultivated algae raised. The relative abundance of the genus *Poterioochromonas* (*Ochrophyta*) in the preculture, the flask, the 5 L photobioreactor and in the DEMO reactor is 0.2 %, 2.5 %, 19 % and 1 %, respectively. While the number of *Poterioochromonas* decreased in the DEMO reactor, the relative abundance of *Cholrella* raised up to 25 %. The relative abundance of the rotifer *Brachionus* increased with the scale-up process to reach up to 4 % in the DEMO reactor (Figure 26).

Poterioochromonas is the second most abundant algae in the DEMO photobioreactor of photobioreaction C. Differently to photobioreaction B *Vannellida* sp. (*Amoebozoa*) was present in a high relative abundance (28 %) in the DEMO reactor shortly after inoculation (02.02.2016), while its abundance decreased rapidly until the next sampling (08.02.2016). In the strongly contaminated sample the relative abundance of *Chlorella* was higher (12 %) compared to not-contaminated samples (<1 %). In total a number of 15 eukaryotic communities were observed in both cultivation approaches. Six of them were part of the core microbiome of both processes (*Haematococcus pluvialis, Brachionus, Chlorella, Poterioochromonas, Scenedesmaceae, Vannella* sp.), three were specific for process B (*Bosea, Paracercomonas, Ripella*) and six could only be detected in the core microbiome of photobioreaction C (*Bodo saltans, Bresslaua vorax, Cercomonas* sp*., Cochliopodium minus, Dictyosphaerium ehrenbergianum, Hartmannella vermiformis;* Figure 26).

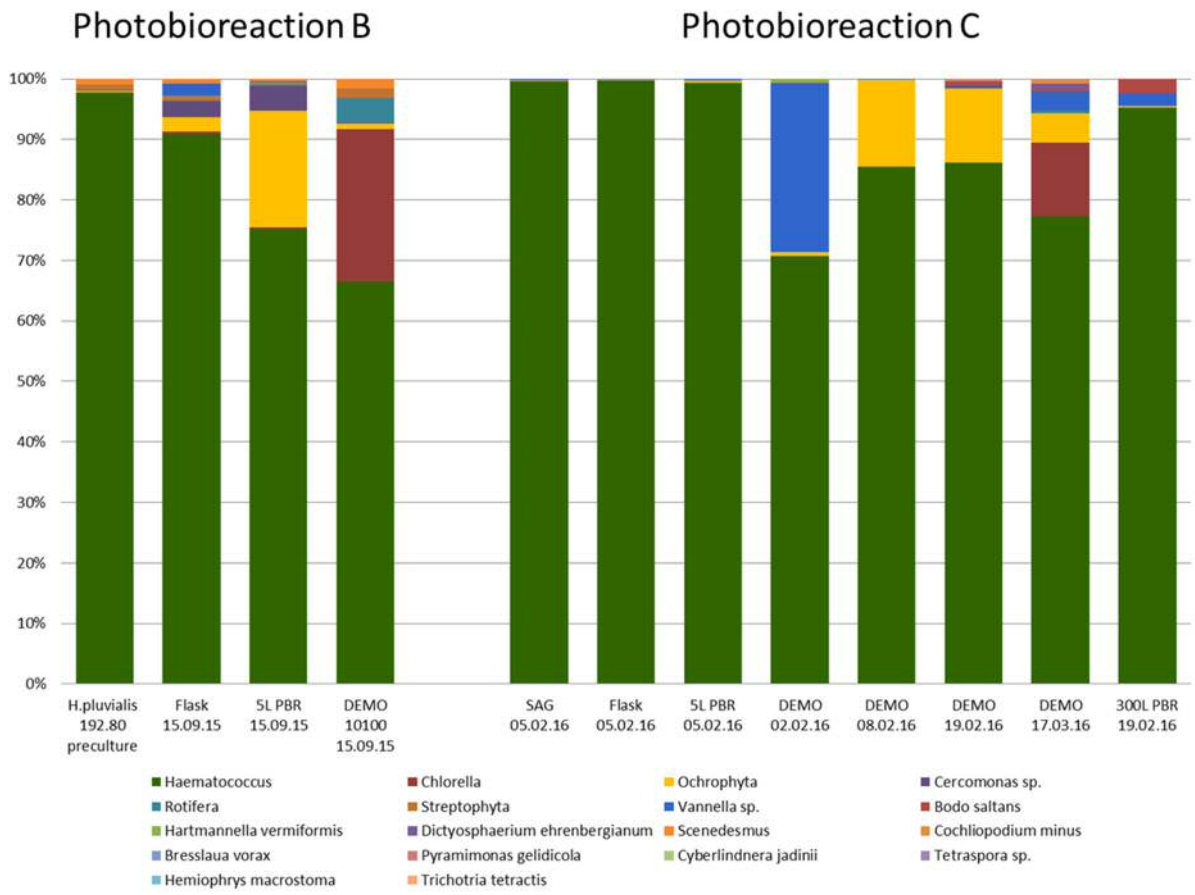

Figure 26: Core microbiome analysis of the 18S rRNA gene sequences from two microalgae cultivation approaches. Sequences were aligned against the nucleotide collection database excluding uncultured and environmental sample sequences using the BLAST algorithm (Altschul *et al*., 1997).

Investigation of ITS regions revealed similar results as 18S rRNA gene analysis. *Chorella* and *Scenedesmus* occurred in a high abundance (up to more than 40 %) in photobioreactors where reduction of *H. pluvialis* biomass yield was reported ("DEMO 10100 15.09.15" from photobioreaction B and "DEMO 10100 17.03.16" from photobioreaction C). *Poterioochromonas* was not detected using ITS specific primers (Figure 27).

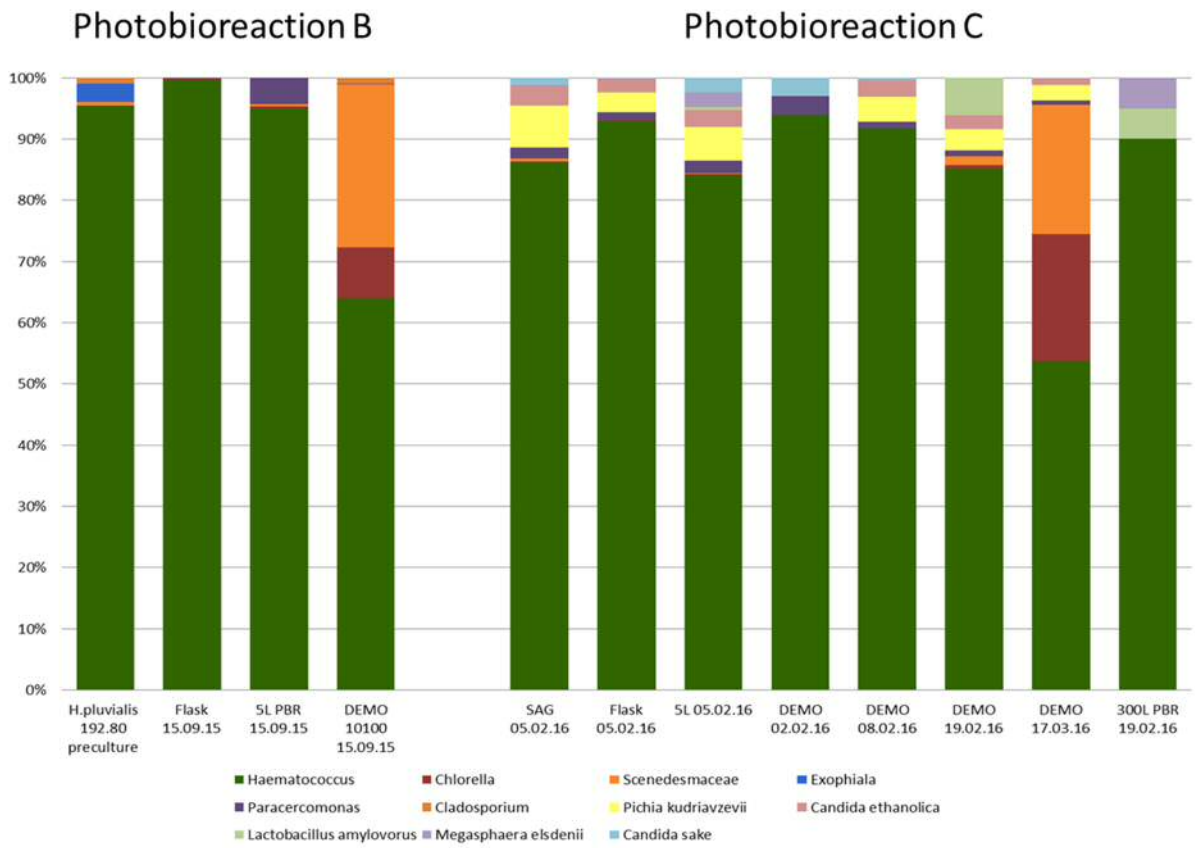

Figure 27: Microbiome analysis based on ITS region amplicon sequencing. Sequences were aligned against the nucleotide collection database excluding uncultured and environmental sample sequences using the BLAST algorithm (Altschul *et al*., 1997).

3.3.2.3 Co-occurrence network analysis revealed reactor specific clustering where positive correlations prevail

The co-occurrence network forms four clusters of dense interaction (Figure 28). Three of them are dominated by positive interactions (A, B, D), while cluster C comprised more negative correlations.

Comamonadaceae within the phylum *Proteobacteria* have the highest number of interactions – 15 considered to be positive, 5 negative. Whereas bacteria from the order *Rhizobiales* (*Proteobacteria*) shows 18 positive interactions, mostly with other *Alphaproteobacteria* (*Proteobacteria*) and *Saprospirae* (*Bacteriodetes*) (Figure 28.C), Proteobacterium *Acetobacteraceae* is with 10 negative interactions, mostly with *Gammaprotebacteria* leading the negative influence group.

Bacteria of the phylum *Verrucomicrobia* and *Thermi-Deinococci* influence each other in a positive way (Figure 28.D) No negative influence of *Actinobacteria* was detected (Figure 28.A).

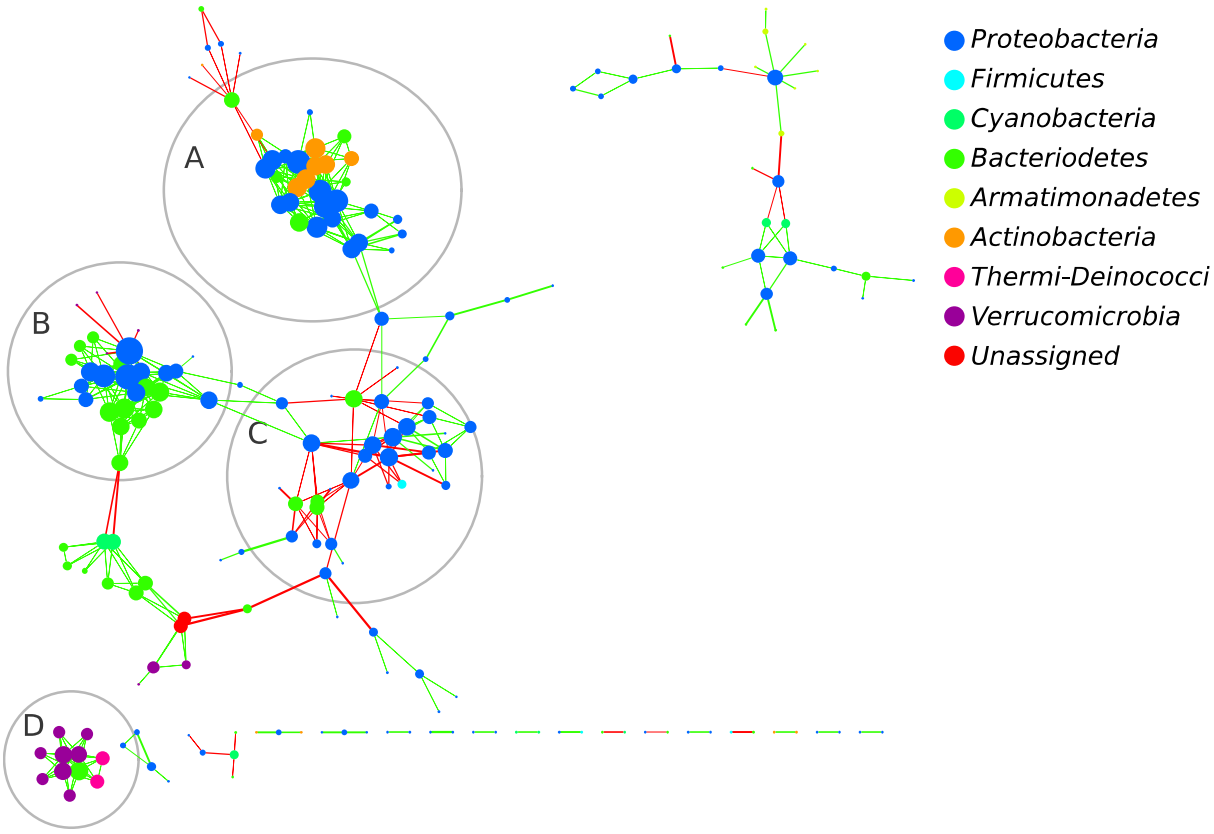

Figure 28: A co-occurrence network of the bacterial OUTs computed from the core-microbiome over the cultivation process was built using Cytoscape add-on "CoNet" (Co-occurrence Network inference). The color of the edges represent the interaction type (green = co-presence, red = mutual exclusion). Thickness of edges represents the significance of the interaction (based on q-value). Node size corresponds to the number of interactions of the respective taxa.

3.3.2.4 OTU-network analysis confirmed random community assembly with low shared proportions of microorganisms

Bacterial OTU network was computed with the OTU table based on amplification of samples within photobioreaction B using golay barcodes (barcode construct 2). The dataset received from QIIME was not reduced for this analysis. From a total number of 2,538 operational taxonomic units only 42 are shared by all four reactors, independent from DNA extraction method (1.65 %). The highest number of individual OTUs was computed for the *H. pluvialis* 192.80 preculture (31.25 %). The number of

OTUs occurring only in the flask, the 5 L photobioreactor and the DEMO reactor are 159 (6.26 %), (389 %), 389 (15.68 %) and 165 (6.50 %), respectively. More than 60 % of the abundant bacteria are individually distributed in the photobioreactors, independent from reactor-size and level of contamination (Figure 29).

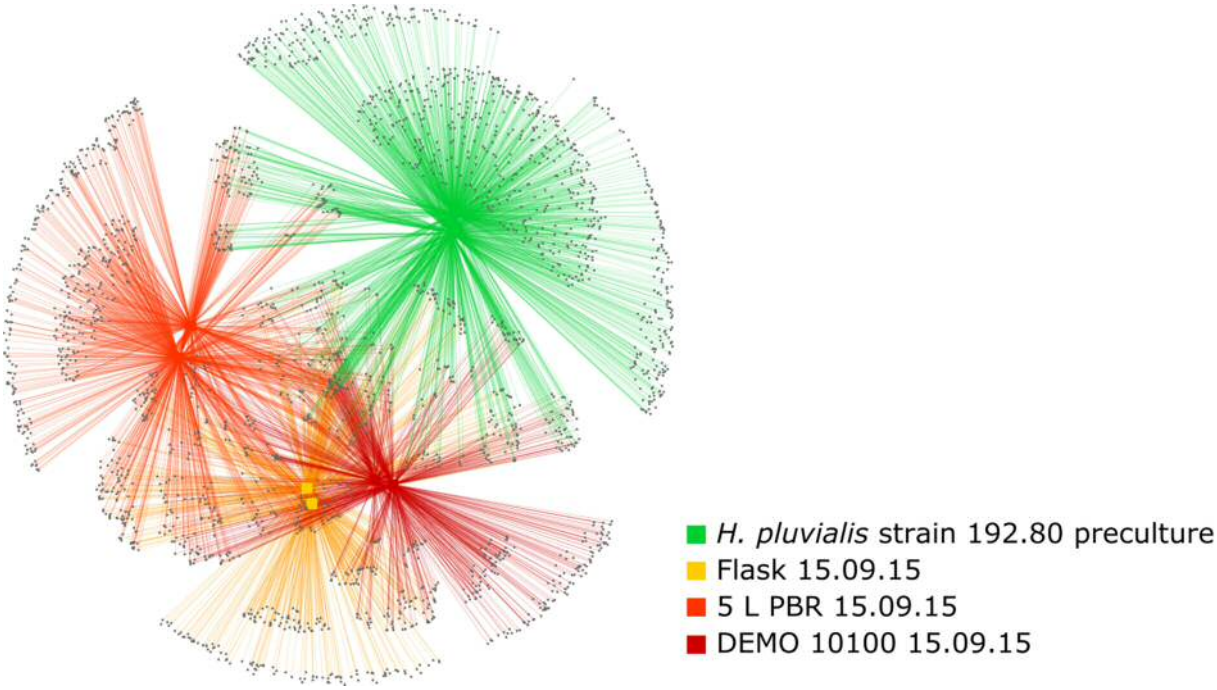

Figure 29: Operational taxonomic units of bacteria in photobioreaction B were analyzed using Cytoscape software. OTUs are spring embedded eweighted. The color of the edges equals their source.

Eukaryotic OTU-network of photobioreaction B showed that most taxa were shared by all samples of photobioreaction B. The flask, the 5 L PBR and the DEMO reactor had eight specific OTUs occurring only in the respective vessel. The algae preculture had seven individual OTUs. In total, 13 OTUs were shared by all photobioreactors, independent from the DNA extraction method (Figure 30).

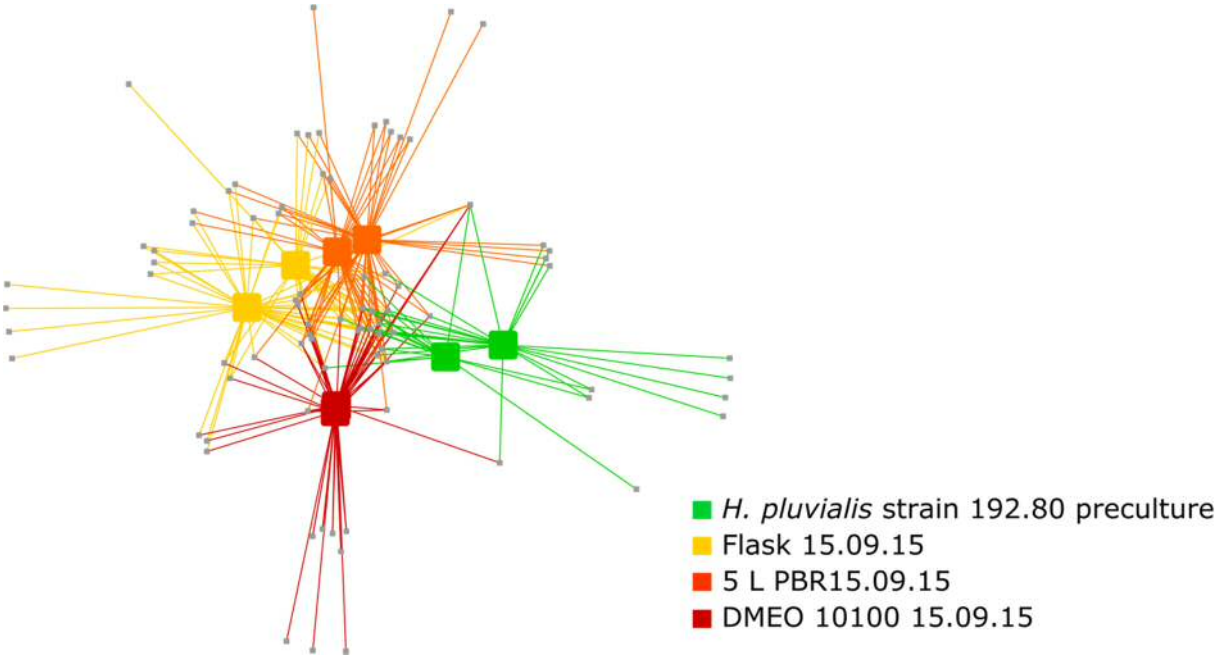

Figure 30: OTUs based 18S rRNA gene sequencing of photobioreaction B were analyzed using Cytoscape software. OTUs are spring embedded eweighted. Two spots of the same color indicate the same sample treated with two different extraction kits (MoBio PowerSoil isolation kit and MP Fast DNA SPIN kit for soil) respectively two separately treated preculture samples (EtOH).

Eukaryotic OTU-network analysis of photobioreaction C showed that even in the same photobioreactor (DEMO) the eukaryotic diversity changed over time. A total number of 554 OTUs was established in the network. The pink and red colored edges and nodes in Figure 31 display the DEMO 10100 reactor at four different time points. This algae suspension showed the highest number of not shared OTUs (178; 32 %). The sample “DEMO 10100 17.03.2016” was considered to be strongly contaminated according to microscopic analyzes. The number of OTUs shared by all photobioreactors is 19 (3 %; Figure 31).

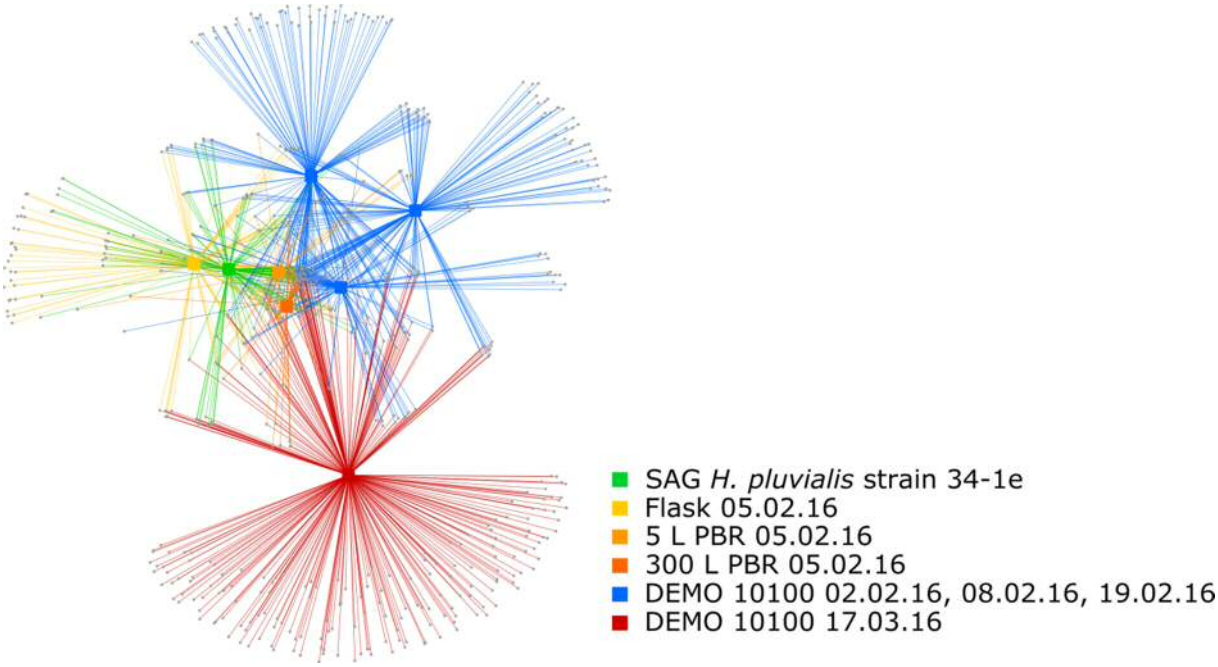

Figure 31: OTU-network based on 18S rRNA gene sequencing of samples within photobioreaction C were analyzed using Cytoscape software. OTUs are spring embedded eweighted.

IV. Discussion

This study provided first insights in the co-occurring microbiome of industrial-scale microalgae cultivation process. The bacterial and eukaryotic communities were investigated. The cultivation of microalgae starts usually in sterile closed system until high cell density (0.4 to 0.6 g cell dry weight per liter) is reached. Subsequently the preculture serves as inoculum for upscaling. Based on the sequencing data from the 16S rRNA genes, the 18S rRNA genes and the ITS regions a high diversity of bacterial taxa was found over the scale-up process. Considering the eukaryotic communities, the starter inoculum contained unwanted contaminations.

4.1 Random assembly of associated microbiota in artificial algae cultivation approaches

Based on the results the general assembly and formation of co-occurring microorganisms followed random patterns. Especially the formation of the bacterial fraction did not follow strict rules, as the diversity in two independent processes showed high heterogeneity. Hardly any differences were found by comparing DNA extraction methods. Similar results were obtained for both, the taxonomic structure and abundances for dominant OTUs. Although most OTUs were shared by the two DNA extraction methods, particular OTUs with a relative abundance under five percent were specific for one extraction method.

In comparison to the extraction kit approaches, EtOH extraction resulted in a diversity loss. A dual extraction of the same sample revealed a heterogeneous diversity, where only some taxa were identified in both samples, while others were specific. Hence, to test statistical significances, especially by using simplified extraction methods, further analyses should include a higher number of replications.

By using a complementary approach, namely single-strand conformation polymorphism and MiSeq/HiSeq Illumina amplicon sequencing, the bacterial communities within the microalgae cultivation were revealed. The bacterial diversity explored in this study is partially similar to those observed in a previous study by Krohn-Molt *et al.* (2013). Krohn-Molts research group investigated the abundance of

associated microbial communities with *Chlorella vulgaris* and *Scenedesmus obliquus*. The most abundant bacteria were mainly members of the classes *Alphaproteobacteria, Betaproteobacteria, Gammaproteobacteria*, and *Bacteriodetes.* Some of the most abundant bacterial families found in their study correlates with my results (*Comamonadaceae, Flavobacteriaceae, Sphingobacteriaceae*). Furthermore, they investigated metagenome sequences of the associated bacteria to identify possible gene functions. They could show that most functions are related to the production of B vitamins and esterolytic and lipolytic enzyme activities. Croft *et al.* (2006) reviewed the dependence of some algae species on the occurrence of the three B-vitamins cobalamin (B_{12}), thiamine (B_1) and biotin (B_7). Cobalamin is capable to act as important co-factors for several enzymes that catalyze rearrangement-reduction or methyl transfer reactions. Vitamin B_1 is necessary for enzymes that are involved in the carbon metabolism. Biotin serves as cofactor for carboxylase enzymes. Although all these vitamins are components of the medium, it can be assumed that the algae receive their essential nutrients partly form co-cultivated bacteria. I investigated 16S rRNA genes of two separate industrial-scale microalgae productions, little correlations regarding bacterial taxa were found. In previous studies of Burke *et al.* (2011a), the bacterial communities of the marine green macroalga *Ulva australis* from two different environments was investigated. The working group studied the similarity of the bacterial consortium of the two sampling sites. They revealed that at species level almost no similarity was observable. Also at family level the similarity was minor. In a second study Burke *et al.* (2011b) examined the correlation of different bacterial communities of the algae from different environments with the abundant functional genes. They revealed that the similarity of the bacterial communities associated with two separately sampled algae is only about 15 %, while the similarity of the functional composition is 70 %, indicating that although a high bacterial diversity is present, a core of functional genes exist in two individual samples. It would be interesting in a further study to investigate the whole genome of bacteria associated with the algae-cultivation to proof the existence of such a functional gene system.

The abundance of bacteria in algae-cultivations can have a positive effect on the growth of algae, suggesting bacterial-algae interactions. Cho *et al.* (2015) investigated the effect of *Flavobacterium, Hyphomonas, Rhizobium, Shpingomonas, Microbacterium* and *Exophilia* on the growth of *C. vulgaris* compared to axenic

cultivation. This study revealed that a co-cultivation of the four genera improved the algae-growth. However, co-cultivated algae could also have a negative influence on the algae growth by nutrient competition or direct undesirable effects. Su *et al.* (2016) examined the harmful effect of the denitrifying bacterium *Acinetobacter sp.* (*Gammaproteobacteria*) on the growth of the *Microcyst aeruginosa*. Furthermore the denitrifying algicidal bacterium *Raoultella* (*Gammaproteobacteria*) was identified to have a negative influence on growth behavior of the microcystis (Su *et al*., 2016). When focusing on the harmful bloom forming freshwater diatom *Stephanodiscus hantzschii* and the dinoflagellate *Peridinium bipes*, algicidal bacteria were identified to be *Acidovorax delafieldii, Variovorax paradoxus*, *Hydrogenophaga palleronii* and *Pseudomonas plecoglossicida* by Kang *et al*. (2008).

4.2 Antagonists of *Haematococcus pluvialis* and negative influences on biomass yield

Besides the effect of bacterial communities on the fitness of algae, the presence of co-cultivated algae like *Chlorella, Scenedesmus* and *Poterioochromonas* may result in decreased *H. pluvialis* yield as the algae compete for nutrients. Not only the competition for nutrients may result in a loss of biomass, but *Poterioochromonas sp.* was assumed to have potentially negative effect on the growth of algae as previous studies revealed the production of toxins of *Chrysophyta* which causes fish mortality (Reich and Spiegelstein; 1964) and zooplankton mortality (Boxhorn *et al.*, 1998).

The high abundance of *Scenedesmus* in the large photobioreactor (DEMO) could either result from contaminated inoculates, which according to next generation sequencing already contained unwanted algae species, but also from blind spaces in the reactor concept, which act as reservoir. According verbal communication with BDI, *Scenedesmus* strains were already tested in the existing reactor concept, as they also possess the ability to synthesize astaxanthin (Hanagata and Dubinsky, 1999). This feature also explains the color shift from green to orange of the colonies plated on CMB in the cultivation-dependent approach. The occurrence of *Chlorella* could also be explained by finding them as contaminants already in the SAG *H. pluvialis* pure culture. *Chlorella* is a ubiquitous, distributed and fast-growing alga.

Since large industrial-scale production cannot be carried out under axenic conditions, there is a putative and constant high risk of unwanted co-cultivation.

Besides co-occurring algae I identified the rotifer *Brachionus angularis* in the photobioreactor. Yet there is no evidence based on current literature that rotifer have negative impact on the *H. pluvialis* cultivation and total biomass yield. However, by using the bright field microscopy I observed indications of harmful interactions, and argue that the impact of protists on the algae growth should be further investigated.

Not only presence of co-cultivated and unwanted algae results in a loss of *H. pluvialis* biomass yield, but also the occurrence of parasites. A parasitic chytrid fungus closely related to the plant pathogen *Physoderma* was isolated and characterized by Hoffman *et al.* (2008) and associated to have highly inhibitory effects on *H. pluvialis*.

Besides co-cultivation of unwanted algae, harmful fungi and the presence of parasites which can cause problems in industrial-scale microalgae biomass cultivation, the conceptual design and technical specifications of photobioreactors are of great importance. This includes, amongst others, sufficient light supply, supplementation with CO_2 and low shear stress for unfettered algal growth.

V. Conclusions and Outlook

Monitoring the co-occurring microbiome along the industrial-scale production of the microalgae *H. pluvialis* unraveled more complex associations than originally expected, originating from the phyla bacteria, eukarya and fungi. I argue that the formation is based on both, empirical and stochastic patterns. While the functional role of the bacterial fraction needs to be assessed further, it could be shown that unwanted co-cultivation of other algae than *H. pluvialis* had decisive antagonistic influence. Therefore, to prevent such unwanted co-cultivated microorganisms, the purity of the starter culture has to be ensured. To suppress the unwanted effect of bacterial and eukaryotic communities, or even to enhance the cultivation process, (1) a defined inoculum containing beneficial bacteria should be developed and used as co-inoculum in the first steps of the cultivation process. Such a defined microbiome may prevent the stochastic distribution of bacteria over the process. For further exploration of the algae-associated microbiome it would be interesting to investigate the co-occurring bacterial and eukaryotic communities of *Haematococcus pluvialis* in its natural environment to isolate algae-specific bacteria strains with potential of growth promotion (2). Additionally abiotic factors of biomass production of microalgae and their influence on the growth behavior of *H. pluvialis* should be studied and optimized (3).

VI. References

Allen, A. E., Dupont, C. L., Oborník, M., Horák, A., Nunes-Nesi, A., McCrow, J. P., ...& Bowler, C. (2011). Evolution and metabolic significance of the urea cycle in photosynthetic diatoms. *Nature*, *473*(7346), 203-207.

Altschul, S. F., Madden, T. L., Schäffer, A. A., Zhang, J., Zhang, Z., Miller, W., & Lipman, D. J. (1997). Gapped BLAST and PSI-BLAST: a new generation of protein database search programs. *Nucleic acids research*, *25*(17), 3389-3402.

Amaral-Zettler, L. A., McCliment, E. A., Ducklow, H. W., & Huse, S. M. (2009). A method for studying protistan diversity using massively parallel sequencing of V9 hypervariable regions of small-subunit ribosomal RNA genes. *PLoS One*, *4*(7), e6372.

Anderson, D. G., & Mckay, L. L. (1983). Simple and rapid method for isolating large plasmid DNA from lactic streptococci. *Applied and environmental microbiology*, *46*(3), 549-552.

Banerjee, A., Sharma, R., Chisti, Y., & Banerjee, U. C. (2002).Botryococcus braunii: a renewable source of hydrocarbons and other chemicals. *Critical reviews in biotechnology*, *22*(3), 245-279.

De-Bashan, L. E., Moreno, M., Hernandez, J. P., & Bashan, Y. (2002). Removal of ammonium and phosphorus ions from synthetic wastewater by the microalgae Chlorella vulgaris coimmobilized in alginate beads with the microalgae growth-promoting bacterium Azospirillum brasilense. *Water Research*, *36*(12), 2941-2948.

Bashan, Y., & Holguin, G. (1998). Proposal for the division of plant growth-promoting rhizobacteria into two classifications: biocontrol-PGPB (plant growth-promoting bacteria) and PGPB. *Soil Biology and Biochemistry*, *30*(8), 1225-1228.

Bassam, B. J., Caetano-Anollés, G., &Gresshoff, P. M. (1991). Fast and sensitive silver staining of DNA in polyacrylamide gels. *Analytical biochemistry*, *196*(1), 80-83.

Ben-Amotz, A., Shaish, A., & Avron, M. (1989). Mode of action of the massively accumulated β-carotene of Dunaliella bardawil in protecting the alga against damage by excess irradiation. *Plant Physiology*, *91*(3), 1040-1043.

Bennedsen, M., Wang, X., Willén, R., Wadström, T., & Andersen, L. P. (2000). Treatment of H. pylori infected mice with antioxidant astaxanthin reduces gastric inflammation, bacterial load and modulates cytokine release by splenocytes. *Immunology letters*, *70*(3), 185-189.

Berg, G., Roskot, N., Steidle, A., Eberl, L., Zock, A., & Smalla, K. (2002). Plant-dependent genotypic and phenotypic diversity of antagonistic rhizobacteria isolated from different Verticillium host plants. *Applied and environmental Microbiology*, *68*(7), 3328-3338.

Bloemberg, G. V., & Lugtenberg, B. J. (2001). Molecula rbasis of plant growth promotion and biocontrol by rhizobacteria. *Current opinion in plant biology*, *4*(4), 343-350.

Boussiba, S., & Vonshak, A. (1991). Astaxanthin accumulation in the green alga Haematococcus pluvialis. *Plant and cell Physiology*, *32*(7), 1077-1082.

Boussiba, S., Bing, W., Yuan, J. P., Zarka, A., & Chen, F. (1999). Changes in pigments profile in the green alga Haeamtococcus pluvialis exposed to environmental stresses. *Biotechnology Letters*, *21*(7), 601-604.

Boxhorn, J. E., Holen, D. A., & Boraas, M. E. (1998). Toxicity of the chrysophyte flagellate Poterioochromonas malhamensis to the rotifer Brachionus angularis. In *Rotifera VIII: A Comparative Approach* (pp. 283-287). Springer, Netherlands.

Brembu, T., Winge, P., Tooming-Klunderud, A., Nederbragt, A. J., Jakobsen, K. S., & Bones, A. M. (2014). The chloroplast genome of the diatom Seminavis robusta: new features introduced through multiple mechanisms of horizontal genetransfer. *Marine genomics*, *16*, 17-27.

Burke, C., Thomas, T., Lewis, M., Steinberg, P., & Kjelleberg, S. (2011a). Composition, uniqueness and variability of the epiphytic bacterial community of the green alga Ulva australis. *The ISME journal*, *5*(4), 590-600.

Burke, C., Steinberg, P., Rusch, D., Kjelleberg, S., & Thomas, T. (2011b). Bacterial community assembly based on functional genes rather than species. *Proceedings of the National Academy of Sciences*, *108*(34), 14288-14293.

Caporaso, J. G., Lauber, C. L., Walters, W. A., Berg-Lyons, D., Huntley, J., Fierer, N., ... &GormLey, N. (2012). Ultra-high-throughput microbial community analysis on the IlluminaHiSeq and MiSeq platforms. *The ISME journal*, *6*(8), 1621-1624.

Caporaso, J. G., Kuczynski, J., Stombaugh, J., Bittinger, K., Bushman, F. D., Costello, E. K., ... & Huttley, G. A. (2010). QIIME allows analysis of high-throughput community sequencing data. *Nature methods*, *7*(5), 335-336.

Carmichael, W. W. (2001). Health effects of toxin-producing cyanobacteria:“TheCyanoHABs”. *Human and ecological risk assessment: An International Journal*, *7*(5), 1393-1407.

Carvalho, A. P., Meireles, L. A., & Malcata, F. X. (2006). Microalgal reactors: a review of enclosed system designs and performances. *Biotechnology progress*, *22*(6), 1490-1506.

Chevalier, P.,& de la Noüe, J. (1985). Wastewater nutrient removal with microalgae immobilized in carrageenan.*Enzyme andmicrobialtechnology*, *7*(12), 621-624.

Chisti, Y. (2007). Biodiesel from microalgae.*Biotechnology advances*, *25*(3), 294-306.

Cho, D. H., Ramanan, R., Heo, J., Lee, J., Kim, B. H., Oh, H. M., & Kim, H. S. (2015). Enhancing microalgal biomass productivity by engineering a microalgal–bacterial community. *Bioresource technology*, *175*, 578-585.

Croft, M. T., Warren, M. J., & Smith, A. G. (2006). Algae need their vitamins. *Eukaryotic cell*, *5*(8), 1175-1183.

Fan, L., Vonshak, A., Zarka, A., & Boussiba, S. (1998). Does astaxanthin protect Haematococcus against light damage?. *Zeitschrift für Naturforschung C*, *53*(1-2), 93-100.

Fátima Santos, M., & Mesquita, J. F. (1984). Ultrastructural study of Haematococcus lacustris (Girod.) Rostafinski (Volvocales). I. Some aspects of carotenogenesis. *Cytologia*, *49*(1), 215-228.

feng Su, J., Ma, M., Wei, L., Ma, F., suo Lu, J., & cheng Shao, S. (2016). Algicidal and denitrification characterization of Acinetobacter sp. J25 against Microcystis aeruginosa and microbial community in eutrophic landscape water. *Marine pollution bulletin*, *107*(1), 233-239.

Flotow, J. (1844). Beobachtungen über *Haematococcus pluvialis*. *Verhandlungen der Kaiserlichen Leopoldinisch-Carolinischen Deutschen Akademie der Naturforscher* 12(Abt. 2): 413-606, 3 pls.

Glick, B. R. (1995). The enhancement of plant growth by free-living bacteria. *Canadian Journal of Microbiology*, *41*(2), 109-117.

Gonzalez, L. E., & Bashan, Y. (2000). Increased Growth of the Microalga Chlorella vulgaris when Co immobilized and Co cultured in Alginate Beads with the Plant-Growth-Promoting Bacterium Azospirillum brasilense. *Applied and Environmental Microbiology*, *66*(4), 1527-1531.

Goodwin, T. W., & Jamikorn, M. (1954). Studies in carotenogenesis. 11. Carotenoid synthesis in the alga Haematococcus pluvialis. *Biochemical Journal*, *57*(3), 376.

Grant, M. A., Kazamia, E., Cicuta, P., & Smith, A. G. (2014). Direct exchange of vitamin B12 is demonstrated by modelling the growth dynamics of algal–bacterial cocultures. *ISME J*, *8*(1418), e27.

Hagen, C., Siegmund, S., & Braune, W. (2002). Ultrastructural and chemical changes in the cell wall of Haematococcus pluvialis (Volvocales, Chlorophyta) during aplanospore formation. *European Journal of Phycology*, *37*(2), 217-226.

Hamady, M., Walker, J. J., Harris, J. K., Gold, N. J., & Knight, R. (2008). Error-correcting barcoded primers allow hundreds of samples to be pyrosequenced in multiplex. *Nature methods*, *5*(3), 235.

Hanagata, N., & Dubinsky, Z. (1999). Secondary carotenoid accumulation in Scenedesmus komarekii (Chlorophyceae, Chlorophyta). *Journal of phycology*, *35*(5), 960-966.

Hazen, T. E. (1899). The life history of Sphaerella lacustris (Haematococcus pluvialis). *Memoirs of the Torrey Botanical Club*, *6*(3), 211-246.

Hernandez, J. P., de-Bashan, L. E., Rodriguez, D. J., Rodriguez, Y., & Bashan, Y. (2009). Growth promotion of the freshwater microalga Chlorella vulgaris by the nitrogen-fixing, plant growth-promoting bacterium Bacillus pumilus from arid zone soils. *european journal of soil biology*, *45*(1), 88-93.

Hoffman, Y., Aflalo, C., Zarka, A., Gutman, J., James, T. Y., & Boussiba, S. (2008). Isolation and characterization of a novel chytrid species (phylum Blastocladiomycota), parasitic on the green alga Haematococcus. *mycological research*, *112*(1), 70-81.

Iwamoto, T., Hosoda, K., Hirano, R., Kurata, H., Matsumoto, A., Miki, W., ... & Kondo, K. (2000). Inhibition of low-density lipoprotein oxidation by astaxanthin. *Journal of atherosclerosis and thrombosis*, *7*(4), 216-222.

Kakizono, T., Kobayashi, M., & Nagai, S. (1992). Effect of carbon/nitrogen ratio on encystment accompanied with astaxanthin formation in a green alga, Haematococcus
pluvialis. *Journal of Fermentation and Bioengineering*, *74*(6), 403-405.

Kang, Y. K., Cho, S. Y., Kang, Y. H., Katano, T., Jin, E. S., Kong, D. S., & Han, M. S. (2008). Isolation, identification and characterization of algicidal bacteria against Stephanodiscushantzschii and Peridiniumbipes for the control of freshwater winter algal blooms. *Journal of Applied Phycology*, *20*(4), 375-386.

Kim, B. H., Ramanan, R., Cho, D. H., Oh, H. M., & Kim, H. S. (2014).Role of Rhizobium, a plant growth promoting bacterium, in enhancing algal biomass through mutualistic interaction. *Biomass and bioenergy*, *69*, 95-105.

Kloepper, J. W., Leong, J., Teintze, M., & Schroth, M. N. (1980). Enhanced plant growth by siderophores produced by plant growth-promoting rhizobacteria. *Nature*, *286*(5776), 885-886.

Kobayashi, M., Kakizono, T., Nishio, N., & Nagai, S. (1992). Effects of light intensity, light quality, and illumination cycle on astaxanthin formation in a green alga, Haematococcuspluvialis. *Journal of Fermentation and Bioengineering*, *74*(1), 61-63.

Kobayashi, M., Kurimura, Y., Kakizono, T., Nishio, N., & Tsuji, Y. (1997). Morphological changes in the life cycle of the green alga Haematococcus pluvialis. *Journal of fermentation and bioengineering*, *84*(1), 94-97.

Kouzuma, A., & Watanabe, K. (2015). Exploring the potential of algae/bacteria interactions. *Current opinion in biotechnology*, *33*, 125-129.

Krohn-Molt, I., Wemheuer, B., Alawi, M., Poehlein, A., Güllert, S., Schmeisser, C., ... & Streit, W. R. (2013). Metagenome survey of a multispecies and alga-associated biofilm revealed key elements of bacterial-algal interactions in photobioreactors. *Applied and environmental microbiology*, *79*(20), 6196-6206.

Krinsky, N. I. (1979). Carotenoid protection against oxidation. *Pure and Applied Chemistry*, *51*(3), 649-660.

Lundberg, D. S., Yourstone, S., Mieczkowski, P., Jones, C. D., &Dangl, J. L. (2013). Practical innovations for high-throughput amplicon sequencing. *Nature methods*, *10*(10), 999-1002.

Palozza, P., Torelli, C., Boninsegna, A., Simone, R., Catalano, A., Mele, M. C., & Picci, N. (2009). Growth-inhibitory effects of the astaxanthin-rich alga Haematococcus pluvialis in human colon cancer cells. *Cancer Letters*, *283*(1), 108-117.

Reich, K., & Spiegelstein, M. (1964). Fishtoxins in Ochromonas (Chrysomonadina). *Israel Journal of Zoology*, *13*(3), 141-141.

Sarada, R., Tripathi, U., &Ravishankar, G. A. (2002). Influence of stress on astaxanthin production in Haematococcuspluvialis grown under different culture conditions. *ProcessBiochemistry*, *37*(6), 623-627.

Schwieger, F., & Tebbe, C. C. (1998). A new approach to utilize PCR–single-strand-conformation polymorphism for 16S rRNA gene-based microbial community analysis. *Applied and Environmental Microbiology*, *64*(12), 4870-4876.

Shannon, P., Markiel, A., Ozier, O., Baliga, N. S., Wang, J. T., Ramage, D., ... & Ideker, T. (2003). Cytoscape: a software environment for integrated models of biomolecular interaction networks. *Genome research*, *13*(11), 2498-2504.

Skjånes, K., Rebours, C., &Lindblad, P. (2013).Potential for green microalgae to produce hydrogen, pharmaceuticals and other high value products in a combined process. *Critical reviews in biotechnology*, *33*(2), 172-215.

Stoeck, T., Bass, D., Nebel, M., Christen, R., Jones, M. D., BREINER, H. W., & Richards, T. A. (2010). Multiple marker parallel tag environmental DNA

sequencing reveals a highly complex eukaryotic community in marine anoxic water. *Molecular Ecology*, *19*(s1), 21-31.

Su, J. F., Shao, S. C., Huang, T. L., Ma, F., Zhang, K., Wen, G., & Zheng, S. C. (2016). Isolation, identification, and algicidal activity of aerobic denitrifying bacterium R11 and its effect on Microcystis aeruginosa. *Water Science and Technology*, *73*(11), 2600-2607.

Tanaka, T., Makita, H., Ohnishi, M., Mori, H., Satoh, K., & Hara, A. (1995). Chemoprevention of rat oral carcinogenesis by naturally occurring xanthophylls, astaxanthin and canthaxanthin. *Cancer Research*, *55*(18), 4059-4064.

Tarayre, C., Bauwens, J., Brasseur, C., Mattéotti, C., Destain, J., Vandenbol, M., ... & Thonart, P. (2014). Isolation of an amylolytic chrysophyte, Poterioochromonas sp., from the digestive tract of the termite Reticulitermes santonensis. *Biotechnologie, Agronomie, Société et Environnement*, *18*(1), 19.

Tjahjono, A. E., Hayama, Y., Kakizono, T., Terada, Y., Nishio, N., &Nagai, S. (1994). Hyper-accumulation of astaxanthin in a green alga Haematococcus pluvialis at elevated temperatures.*Biotechnology Letters*, *16*(2), 133-138.

Tominaga, K., Hongo, N., Karato, M., & Yamashita, E. (2012). Cosmetic benefits of astaxanthin on humans subjects. *Acta Biochimica Polonica*, *59*(1), 43.

Triki, A., Maillard, P., & Gudin, C. (1997). Gametogenesis in Haematococcus pluvialis Flotow (Volvocales, Chlorophyta). *Phycologia*, *36*(3), 190-194.

Tso, M. O., & Lam, T. T. (1996). *U.S. Patent No. 5,527,533*. Washington, DC: U.S. Patent and Trademark Office.

Ugwu, C. U., Aoyagi, H., & Uchiyama, H. (2008). Photobioreactors for mass cultivation of algae. *Bioresource technology*, *99*(10), 4021-4028.

Vestheim, H., & Jarman, S. N. (2008). Blocking primers to enhance PCR amplification of rare sequences in mixed samples – a case study on prey DNA in Antarctic krill stomachs. *Frontiers in Zoology*, *5*(1), 1.

Wayama, M., Ota, S., Matsuura, H., Nango, N., Hirata, A., & Kawano, S. (2013). Three-dimensional ultrastructural study of oil and astaxanthin accumulation during encystment in the green alga Haematococcus pluvialis. *PloS one*, *8*(1), e53618.

White TJ, Bruns TD, Lee S, Taylor J. (1990). Analysis of phylogenetic relationship by amplification and direct sequencing of ribosomal RNA genes. Innis MA, Gelfand DH, Sninsky JJ and White TJ (eds). PCR Protocols: A Guide to Methods and Applications. Academic Press: New York, pp 315–322.

VII. Appendix

7.1 Media

- Bold's Basal Medium (BBM)

Per L: 10 mL of the following stock solutions

A1/1	$NaNO_3$ (Carl Roth, Karlsruhe, Germany)	25.0 g × L^{-1}
A1/2	KH_2PO_4 (Carl Roth, Karlsruhe, Germany)	17.5 g × L^{-1}
A1/3	K_2HPO_4 (Carl Roth, Karlsruhe, Germany)	7.5 g × L^{-1}
A1/4	$MgSO_4$ × 7 H_2O (Merck, Darmstadt, Deutschland)	7.5 g × L^{-1}
A1/5	$CaCl_2$ (Carl Roth, Karlsruhe, Germany)	2.5 g × L^{-1}
A1/6	NaCl (Carl Roth, Karlsruhe, Germany)	2.5 g × L^{-1}

Per L: 1 mL of the following stock solutions

A2/1	H_3BO_3(Carl Roth, Karlsruhe, Germany)	2.6 g × L^{-1}
A2/2	$FeSO_4$ × 7 H_2O (Carl Roth, Karlsruhe, Germany)	5.0 g × L^{-1}
	$ZnSO_4$ × 7 H_2O (Merck, Darmstadt, Deutschland)	8.8 g × L^{-1}
	$MnCl_2$ × 4 H_2O (Merck, Darmstadt, Deutschland)	1.4 g × L^{-1}
A2/3	MoO_3 (Carl Roth, Karlsruhe, Germany)	1.4 g × L^{-1}
	$CuSO_4$ × 5 H_2O (Merck, Darmstadt, Deutschland)	1.6 g × L^{-1}
	$Co(NO_3)_3$ × 6 H_2O (Merck, Darmstadt, Deutschland)	0.5 g × L^{-1}
A2/4	EDTA (Carl Roth, Karlsruhe, Germany)	0.5 g × L^{-1}
	KOH (Merck, Darmstadt, Deutschland)	0.3 g × L^{-1}I

For solid media, Agar-Agar (Carl Roth, Karlsruhe, Germany) was added (12 g × L^{-1}) and subsequently sterilized (120 °C, 15 min). For the in in-Agar method 6 g ×$^{-1}$ L Agar-Agar were added. Ampicillin was sterilfiltered (0.20 µm pore size) after autoclaving.

- Bold's Basal Medium (BBM I) – provided by BDI

$NaNO_3$	5.0 × 10^{-1} g × L^{-1}
$MgSO_4$ × 7 H_2O	7.5 × 10^{-2} g × L^{-1}
$CaCl_2$ × 2 H_2O	2.5 × 10^{-2} g × L^{-1}
NaCl	2.5 × 10^{-2} g × L^{-1}
K_2HPO_4 × 3 H_2O	9.3 × 10^{-2} g × L^{-1}

KH_2PO_4	1.8×10^{-1} g × L^{-1}
Na_2EDTA	4.5×10^{-3} g × L^{-1}
$FeSO_4 \times 7\ H_2O$	5.0×10^{-3} g × L^{-1}
$ZnCl_2$	3.3×10^{-5} g × L^{-1}
$MnCl_2 \times 4\ H_2O$	2.5×10^{-4} g × L^{-1}
$CoCl_2 \times 6\ H_20$	1.2×10^{-5} g × L^{-1}
$Na_2MoO_4 \times 2\ H_2O$	2.4×10^{-5} g × L^{-1}
Vitamin B1 (Thiamine)	1.0×10^{-3} g × L^{-1}
Vitamin H (Biotin)	2.5×10^{-4} mg × L^{-1}

For solid media, Agar-Agar (Carl Roth, Karlsruhe, Germany) was added [12g l $\times^{-1}$] and subsequently sterilized (120 °C, 15 min). Ampicillin was sterilfiltered (0.20 µm pore size) after autoclaving.

- Courtney Boyd Myers (CBM) – provided by BDI

$NaNO_3$	8.0×10^{-2} g × L^{-1}
$Ca(NO_3)_2 \times 4H_2O$	2.0×10^{-2} g × L^{-1}
$NaHCO_3$	1.6×10^{-3} g × L^{-1}
$MgSO_4 \times 7H_2O$	5.0×10^{-2} g × L^{-1}
KH_2PO_4	1.2×10^{-2} g × L^{-1}
$NaH_2PO_4 \times H_2O$	1.6×10^{-2} g × L^{-1}
Na_2 EDTA	2.4×10^{-3} g × L^{-1}
FeNa EDTA	2.2×10^{-3} g × L^{-1}
Vitamin H Biotin	1.0×10^{-5} g × L^{-1}
Vitamin B_{12} Cobalamin	1.0×10^{-5} g × L^{-1}
Vitamin B_1 Thiamine	1.0×10^{-5} g × L^{-1}
$MnCl_2 \times 4H_2O$	1.4×10^{-3} g × L^{-1}
$(NH_4)_6Mo_7O_24 \times 4H_2O$	1.0×10^{-3} g × L^{-1}
H_3BO_3	2.5×10^{-3} mg × L^{-1}

For solid media, Agar-Agar (Carl Roth, Karlsruhe, Germany) was added (15 g × L^{-1}) and subsequently sterilized (120 °C, 15 min). Ampicillin was sterilfiltered (0.20 µm pore size) after autoclaving.

- Nutrient Agar (NA)

Nährbouillon 2 (Sifin, Berlin, Germany)	15.0 g × L^{-1}
Agar-Agar (Carl Roth, Karlsruhe, Germany)	20.0 g × L^{-1}

- Plant Agar (Duchefa Biochemie, Haarlem, Netherlands)

- Potato Dextrose Agar (PDA)

Potato -glucose bouillon (Carl Roth, Karlsruhe, Germany)	26.0 g × L^{-1}
Agar-Agar (Carl Roth, Karlsruhe, Germany)	20.0 g × L^{-1}

- Rice Agar

Ca^{2+}	1.1×10^{-1} g × L^{-1}
Mg^{2+}	4.1×10^{-2} g × L^{-1}
Na^{+}	1.5×10^{-2} g × L^{-1}
K^{+}	1.6×10^{-3} g × L^{-1}
SO_4^{2-}	2.2×10^{-1} g × L^{-1}
HCO_3	2.6×10^{-1} g × L^{-1}
Cl	2.0×10^{-2} g × L^{-1}
H_2SiO_3	1.4×10^{-2} g × L^{-1}

For the in-agar method 8 g × L^{-1} Agar-Agar (Carl Roth, Karlsruhe, Germany) were added. S-BUDGET mineral water was used.
Medium for plating was prepared by adding 16 g × L^{-1} Agar-Agar.

- Synthetic Nutrient-Poor Agar (SNA)

Glucose (Carl Roth, Karlsruhe, Germany)	0.2 g × L^{-1}
Sucrose (Carl Roth, Karlsruhe, Germany)	0.2 g × L^{-1}
KH_2PO_4 (Carl Roth, Karlsruhe, Germany)	1.0 g × L^{-1}
KNO_3 (Carl Roth, Karlsruhe, Germany)	1.0 g × L^{-1}
KCl (Carl Roth, Karlsruhe, Germany)	0.5 g × L^{-1}
$MgSO_4 \times 7\ H_2O$ (Merck, Darmstadt, Deutschland)	0.5 g × L^{-1}
Agar-Agar (Carl Roth, Karlsruhe, Germany)	22.0 g × L^{-1}

7.2 Chemicals

- PBS Buffer (Phosphate-Buffered Saline)

KH_2PO_4 (Carl Roth, Karlsruhe, Germany)	3.0 g × L^{-1}
NaCl (Carl Roth, Karlsruhe, Germany)	4.0 g × L^{-1}
Na_2HPO_4 (Carl Roth, Karlsruhe, Germany)	7.0 g × L^{-1}
pH 7.1 ± 0.2	

7.3 Cultivation-dependent analyses of photobioreaction A

Table 13: Viable cell count after different incubation periods for sample "Flask 04.09.2015".

Flask 04.09.2015

Media	Dilution	CFU × 100 µL^{-1} (24h)	CFU × 100 µL^{-1} (48h)	CFU × 100 µL^{-1} (120h)	CFU × 100 µL^{-1} (144h)	CFU × mL^{-1}
NA	10^{-0}	0	15	No data	>400	24h: 0 48h: 130 144h: 363500
	10^{-1}	0	1	No data	>400	
	10^{-2}	0	0	No data	>400	
	10^{-3}	0	0	No data	277	
	10^{-4}	0	0	No data	45	
	10^{-5}	0	0	No data	2	
	10^{-6}	0	0	No data	0	
	10^{-7}	0	0	No data	0	
SNA	10^{-0}	0	0	No data	>400	24h: 0 48h: 0 144h: 100670
	10^{-1}	0	0	No data	>400	
	10^{-2}	0	0	No data	122	
	10^{-3}	0	0	No data	19	
	10^{-4}	0	0	No data	1	
	10^{-5}	0	0	No data	0	
	10^{-6}	0	0	No data	0	
	10^{-7}	0	0	No data	0	
PDA	10^{-0}	0	0	No data	>300	24h: 0 48h: 0 144h: 102000
	10^{-1}	0	0	No data	>300	
	10^{-2}	0	0	No data	>300	
	10^{-3}	0	0	No data	124	
	10^{-4}	0	0	No data	8	
	10^{-5}	0	0	No data	0	
	10^{-6}	0	0	No data	0	
	10^{-7}	0	0	No data	0	
CBM	10^{-0}	0	No data	>300	No data	24h: 0 120h: 470000
	10^{-1}	0	No data	>300	No data	
	10^{-2}	0	No data	>300	No data	
	10^{-3}	0	No data	>300	No data	
	10^{-4}	0	No data	44	No data	
	10^{-5}	0	No data	5	No data	
	10^{-6}	0	No data	0	No data	
	10^{-7}	0	No data	0	No data	
BBM I	10^{-0}	0	No data	>300	No data	24h: 0 120h: 13970
	10^{-1}	0	No data	179	No data	
	10^{-2}	0	No data	14	No data	
	10^{-3}	0	No data	1	No data	
	10^{-4}	0	No data	0	No data	
	10^{-5}	0	No data	0	No data	
	10^{-6}	0	No data	0	No data	

	10^{-7}	0	No data	0	No data

* indicates that colony forming units could not be calculated due to too high or too low colony number on the plates; No data: no observation was carried out.

Table 14: Viable cell count after different incubation periods for sample "5 L BPR 04.09.2015".

5 L PBR 04.09.2015

Media	Dilution	CFU × 100 µL^{-1} (24h)	CFU × 100 µL^{-1} (48h)	CFU × 100 µL^{-1} (120h)	CFU × 100 µL^{-1} (144h)	CFU × mL^{-1}
NA	10^{-0}	26	205	No data	>400	24h: 260 48h: 1330 144h: 450000
	10^{-1}	1	6	No data	>400	
	10^{-2}	0	0	No data	>400	
	10^{-3}	0	0	No data	65	
	10^{-4}	0	0	No data	1	
	10^{-5}	0	0	No data	0	
	10^{-6}	0	0	No data	0	
	10^{-7}	0	0	No data	0	
SNA	10^{-0}	0	0	No data	0	24h: 0 48h: 0 144h: 0
	10^{-1}	0	0	No data	0	
	10^{-2}	0	0	No data	0	
	10^{-3}	0	0	No data	0	
	10^{-4}	0	0	No data	0	
	10^{-5}	0	0	No data	0	
	10^{-6}	0	0	No data	0	
	10^{-7}	0	0	No data	0	
PDA	10^{-0}	60	170	No data	>300	24h: 600 48h: 2745 144h: 27450
	10^{-1}	6	24	No data	129	
	10^{-2}	0	0	No data	42	
	10^{-3}	0	0	No data	0	
	10^{-4}	0	0	No data	0	
	10^{-5}	0	0	No data	0	
	10^{-6}	0	0	No data	0	
	10^{-7}	0	0	No data	0	
CBM	10^{-0}	*	No data	*	No data	24h: * 120h: *
	10^{-1}	*	No data	*	No data	
	10^{-2}	0	No data	*	No data	
	10^{-3}	0	No data	*	No data	
	10^{-4}	0	No data	0	No data	
	10^{-5}	0	No data	0	No data	
	10^{-6}	0	No data	0	No data	
	10^{-7}	0	No data	0	No data	
BBM I	10^{-0}	0	No data	0	No data	24h: 0 120h: 0
	10^{-1}	0	No data	0	No data	
	10^{-2}	0	No data	0	No data	
	10^{-3}	0	No data	0	No data	
	10^{-4}	0	No data	0	No data	
	10^{-5}	0	No data	0	No data	
	10^{-6}	0	No data	0	No data	
	10^{-7}	0	No data	0	No data	

* indicates that colony forming units could not be calculated due to too high or too low colony number on the plates; No data: no observation was carried out.

Table 15: Viable cell count after different incubation periods for sample "DEMO10100 04.09.2015"

DEMO 10100 04.09.2015

Media	Dilution	CFU × 100 µL^{-1} (24h)	CFU × 100 µL^{-1} (48h)	CFU × 100 µL^{-1} (120h)	CFU × 100 µL^{-1} (144h)	CFU × mL^{-1}
NA	10^{-0}	>300	>300	No data	>300	24h: 3750 48h: 13630 144h: 185500
	10^{-1}	20	339	No data	>300	
	10^{-2}	2	50	No data	251	
	10^{-3}	0	2	No data	12	
	10^{-4}	0	0	No data	0	
	10^{-5}	0	0	No data	0	
	10^{-6}	0	0	No data	0	
	10^{-7}	0	0	No data	0	
SNA	10^{-0}	0	>400	No data	>300	24h: 0 48h: >3000 144h: 18050
	10^{-1}	0	6	No data	221	
	10^{-2}	0	0	No data	14	
	10^{-3}	0	0	No data	0	
	10^{-4}	0	0	No data	0	
	10^{-5}	0	0	No data	0	
	10^{-6}	0	0	No data	0	
	10^{-7}	0	0	No data	0	
PDA	10^{-0}	264	>300	No data	>300	24h: 1820 48h: 38250 144h: 530000
	10^{-1}	10	365	No data	>300	
	10^{-2}	1	40	No data	76	
	10^{-3}	0	0	No data	3	
	10^{-4}	0	0	No data	0	
	10^{-5}	0	0	No data	0	
	10^{-6}	0	0	No data	0	
	10^{-7}	0	0	No data	0	
CBM	10^{-0}	>300	No data	>300	0	24h: * 120h: *
	10^{-1}	>300	No data	>300	0	
	10^{-2}	0	No data	>300	0	
	10^{-3}	0	No data	97	0	
	10^{-4}	0	No data	0	0	
	10^{-5}	0	No data	0	0	
	10^{-6}	0	No data	0	0	
	10^{-7}	0	No data	0	0	
BBM I	10^{-0}	0	No data	0	0	24h: 0 120h: 0
	10^{-1}	0	No data	0	0	
	10^{-2}	0	No data	0	0	
	10^{-3}	0	No data	0	0	
	10^{-4}	0	No data	0	0	
	10^{-5}	0	No data	0	0	
	10^{-6}	0	No data	0	0	
	10^{-7}	0	No data	0	0	

* indicates that colony forming units could not be calculated due to too high or too low colony number on the plates; No data: no observation was carried out.

7.4 Primer constructs for amplicon analyzes

Table 16: Primer and barcode-constructs used for amplicon analyzes

Barcode ID forward	Barcode ID reveres	Barcode sequence forward	Barcode sequence reverse	Barcode length
BC85	BC85	ACTATCAGCG	ACTATCAGCG	10
BC86	BC86	CTGTGCGAGT	CTGTGCGAGT	10
BC87	BC87	GCAGCGAGTA	GCAGCGAGTA	10
BC88	BC88	TACTCGCTAT	TACTCGCTAT	10
BC89	BC89	AGCATCGATG	AGCATCGATG	10
BC90	BC90	CATCGCTCGA	CATCGCTCGA	10
BC91	BC91	GTCTCACTGT	GTCTCACTGT	10
BC92	BC92	TGAGACGTAT	TGAGACGTAT	10
BC93	BC93	CACGTAGCGT	CACGTAGCGT	10
BC94	BC94	CAGATAGAGA	CAGATAGAGA	10
BC95	BC95	CATAGCGCAT	CATAGCGCAT	10
BC96	BC96	CGACTATACT	CGACTATACT	10
BC97	BC97	CGCATAGCAG	CGCATAGCAG	10
BC101	BC101	AGTATGTCGT	AGTATGTCGT	10
BC102	BC102	CTACACAGAG	CTACACAGAG	10
BC103	BC103	GAGAGCACTA	GAGAGCACTA	10
BC104	BC104	TAGCTATAGC	TAGCTATAGC	10
BC105	BC105	ACTATGCGTA	ACTATGCGTA	10
BC106	BC106	CTCGAGCATC	CTCGAGCATC	10
BC107	BC107	GATCATCAGC	GATCATCAGC	10
BC108	BC108	TGCGCTCATG	TGCGCTCATG	10
golay_bc_01_for	golay_bc_01_rev	AGCCTTCGTCGC	AGCCTTCGTCGC	12
golay_bc_02_for	golay_bc_02_rev	TCCATACCGGAA	TCCATACCGGAA	12
golay_bc_03_for	golay_bc_03_rev	AGCCCTGCTACA	AGCCCTGCTACA	12
golay_bc_04_for	golay_bc_04_rev	CCTAACGGTCCA	CCTAACGGTCCA	12
golay_bc_05_for	golay_bc_05_rev	CGCGCCTTAAAC	CGCGCCTTAAAC	12
golay_bc_06_for	golay_bc_06_rev	TATGGTACCCAG	TATGGTACCCAG	12
golay_bc_07_for	golay_bc_07_rev	TACAATATCTGT	TACAATATCTGT	12
golay_bc_08_for	golay_bc_08_rev	AATTTAGGTAGG	AATTTAGGTAGG	12

Table 17: Linker sequence and primer pad used for amplification with golay barcode-constructs

Target	Primer	Primer pad	Linker
Eubacteria	515f_primer_pad	TATGGTAATT	GT
Eubacteria	926r_primer_pad	AGTCAGCCAG	GG
Eukaryotes	Euk_1391f_primer_pad	TATGGTAATT	GT
Eukaryotes	EukBr_primer_pad	AGTCAGCCAG	GG

Abbreviations

µ	micro
ATP	adenosine triphosphate
BBM	Bold's basal medium
CBM	Courtney Boyd Myers
CFU	colony forming units
CLSM	confocal laser scanning microscopy
CTAB	cetyltrimethylammonium bromide
EDTA	ethylenediaminetetraacetic acid
et al.	et alia
g	gram
h	hour
ITS	internal transcribed spacer
L	Liter
m	milli
M	mole
min	minute
n	nano
NA	nutrient agar
NADH	nicotinamide adenine dinucleotide
OTU	operational taxonomic unit
PBS	phosphate-buffered saline
PCR	polymerase chain reaction
PDA	potato dextrose agar
pH	pondus hydrogenii
PNA	peptide nucleic acid
QIIME	quantitative insights into microbial ecology
ROS	reactive oxygen species
rpm	revolutions per minute
rRNA	ribosomal ribonucleic acid
SAG	culture collection of algae at Goettingen University

SDS	sodium dodecyl sulfate
sec	second
SNA	synthetic nutrient-poor agar
SSCP	single-strand conformation polymorphism
wt vol^{-1}	weight per volume

List of Figures

List of Tables